To the Graduate Council:

I am submitting herewith a thesis written by Jonathan Troy Adamson entitled "Nonintrusive Mapping of Subsurface Features for Site-Specific Agriculture: Cumberland Plateau and Loess Uplands Physiographic Regions of Tennessee." I have examined the final copy of this thesis for form and content and recommend that it be accepted in partial fulfillment of the requirements for the degree of Master of Science, with a major in Biosystems Engineering Technology.

Robert S. Freeland, Major Professor

We have read this thesis
and recommend its acceptance:

Accepted for the Council:

Associate Vice Chancellor and
Dean of the Graduate School

Nonintrusive Mapping of Subsurface Features for Site-Specific Agriculture: Cumberland Plateau and Loess Uplands Physiographic Regions of Tennessee

A Thesis

Presented for the

Master of Science

Degree

The University of Tennessee, Knoxville

Jonathan Troy Adamson

May, 1999

AG-VET-MED.
Thesis
99
.A343

To:

My father, James T. Adamson, Jr., for his friendship, support, and teaching me how to be a man in all respects. To my mother, Annette B. Ralph, for her support, advice, and always being there for me. And finally to my wife, Amanda B. Adamson, for the love, encouragement, and loyalty that she has shown throughout the time it has taken me to complete my education.

Acknowledgments

The author would like to extend his sincere gratitude to the Department of Agricultural and Biosystems Engineering, and Dr. C. Roland Mote for allowing him the opportunity to be a part of the graduate program. Appreciation and thanks are also extended to Dr. Robert S. Freeland who served as the author's major professor, without his friendship, support, and advice this project would have never been completed.

Thanks are also extended to Dr. John B. Wilkerson and Dr. Donald D. Tyler, committee members, for their time and valuable advice.

Special gratitude is expressed to both of the staffs at the Milan and Plateau Experiment Stations for their extreme patience and gracious hospitality. Technical advice from Dr. Joann Logan and Dr. Arnold M. Saxton was also greatly appreciated.

Special thanks are extended to Mr. Ron Dinwiddie and Dr. Reed Cripps, undergraduate professors at Columbia State Community College and Tennessee Technological University, respectively, for preparing me for the challenges of graduate school and life.

Finally the author would like to thank fellow graduate students John J. Conroy, James W. Bedford, and Leroy L. Leonard for their friendship and enormous contribution of time, effort, and advice.

Abstract

Evaluation studies were conducted to determine if ground-penetrating radar (GPR) could be used to noninvasively map subsurface phenomena that affect the variability of crop yields in two physiographic regions of Tennessee. GPR technology offers great potential to agricultural researchers for noninvasive mapping of the various subsurface features found within these geological regions.

Calibration data were collected at three survey locales containing soils similar to those found in the main research areas. GPR survey methodologies within each region were developed, and optimal system settings were obtained. Primary subsurface features of interest to the study were also mapped and methodologies of interpreting the features from GPR imagery were evaluated using a "blind test". Results of the "blind test" indicated a relatively high degree of accuracy and repeatability.

Geographic information systems (GIS) were used as a tool to geographically join the GPR data to crop yield values from four primary research plots. Statistical analyses were then performed to determine the correlation between the two types of data. Correlation coefficients indicated that interpretations from GPR imagery were capable of describing a great deal of the spatial variability observed in the crop yield trends. Furthermore, results from the Least Squares Means analysis revealed a yield potential pattern of the soils that each GPR interpretation represented.

Recommendations were made concerning survey procedures, equipment, and interpretation methodologies. Difficulties encountered are also discussed along with suggested solutions. Finally, the direction of future research in the area of GPR in site-specific farming (SSF) is discussed, and recommendations for this research are presented.

Table of Contents

Chapter		Page
1	Introduction and Objectives	1
	Trends in Production Agriculture	1
	Technology Overview	3
	Global Positioning System	3
	Basic GPS Operation	5
	Precision and Differential Correction	5
	Geographic Information Systems	8
	Projects	9
	Ground Penetrating Radar	10
	GPR Basics	10
	Justification for Research	14
	Objectives	15
2	Review of Literature	16
	Soil Variability in the Research Areas	16
	GPS in Site-Specific Farming Applications	23
	GIS in Site-Specific Farming Applications	24
	GPR Applications in Agriculture	26
3	Materials and Methods	29
	GPR Equipment Summary	29
	Data Analysis Hardware and Software	32
	Research Plot Design and Layout	33
	GPR Data Collection Summary	36
	Calibration Data Collection	36
	Blind Test Data Collection	39
	Cumberland Plateau Physiographic Region	40
	Loess Uplands Physiographic Region	40
	Main Research Plot Data Collection	41
	Research Plot Image Interpretations	43
	Plateau Experiment Station	43
	Milan Experiment Station	45
	Milan Plot Classifications	47
	Crop Yield Data Collection	53
	Plateau Experiment Station	53
	Milan Experiment Station	55
4	Results and Discussion	57
	Calibration Data Results	57
	Ames Plantation	57
	Plateau Experiment Station	60

Chapter Page

Milan Experiment Station 62
Blind Test Results 65
Plateau Experiment Station 65
Milan Experiment Station 66
Crop Yield Results 69
Statistical Comparison of GPR Interpretations
to Crop Yields 72
Plateau Experiment Station 72
Plot 1 72
Plot 2 72
Milan Experiment Station 73
Plot 1 73
Plot 2 73
Discussion 80
Plateau Experiment Station 80
Milan Experiment Station 81

5 Recommendations 84
Data Collection 84
Environmental Conditions 84
Survey Techniques 85
GPR Data Interpretation 86
Crop Yield Data Collection 87
Future Research 88

6 Summary and Conclusions 89

Bibliography 92

Appendices 96
Appendix A 97
Appendix A1 98
Appendix A2 99
Appendix B 102
Appendix C 104
Appendix D 106
Appendix D1 107
Appendix D2 119

Vita 137

List of Figures

Figure		Page
2.1	Schematic of the Cumberland Plateau and Loess Uplands Physiographic Regions of Tennessee.	19
2.2	Photo taken from within a soil pit of a fragipan horizon occuring below approximately 60-cm depth.	20
2.3	Photo of shallow sandstone bedrock that is typical of the Cumberland Plateau Physiographic Region.	22
3.1	Tractor and trailer configuration used to transport GPR mainframe and power source equipment and tow GPR antenna during data collection.	31
3.2	Corn yield results obtained in fields A6 and A7 at the Milan Experiment Station and locations of the GPR data collection grids (coordinates are in State Plane 1927 projection).	34
3.3	Schematic of GPR survey locales in Tennessee.	37
3.4	Interpreted depth of soil above sandstone bedrock observed on research plot 1 at the Plateau Experiment Station (coordinates are in State Plane 1927 projection).	44
3.5	Interpreted depth of soil above sandstone bedrock observed on research plot 2 at the Plateau Experiment Station (coordinates are in State Plane 1927 projection).	46
3.6	GPR image acquired in research plot 1 at the Milan Experiment Station illustrating interpreted "plot 1 soil codes" 1 and 4.	48
3.7	GPR image acquired in research plot 1 at the Milan Experiment Station illustrating interpreted "plot 1 soil codes" 2, 3, and 5.	49
3.8	GPR image acquired in research plot 2 at the Milan Experiment Station illustrating interpreted "plot 2 soil codes" 2, 5, and 6.	51
3.9	GPR image acquired in research plot 2 at the Milan Experiment Station illustrating interpreted "plot 2 soil codes" 1, 3, 4, and 7.	52
3.10	Tractor and Pixall bean picker used to collect snap bean yields at the Plateau Experiment Station.	54

Figure		Page
4.1	GPR image showing hyperbolic reflection of PVC pipe and depths of the loess/alluvium interface and the coastal plains interface.	58
4.2	Three-Dimensional GPR image of the Centennial Plot (Ames Plantation, Grand Junction, TN).	59
4.3	GPR image collected on the grounds of the Clyde York 4-H Camp, illustrating the variation of depth to the sandstone bedrock interface.	63
4.4	GPR image collected in field N47 of the Milan Experiment Station illustrating the change in lateral characteristics that coincide with the occurrence of a fragipan.	64
4.5	GPR image illustrating "floaters" encountered above the solid sandstone surface during the blind test at the plateau research site.	68
4.6	Snap bean yield trends observed in plot 1 at the Plateau Experiment Station.	70
4.7	Snap bean yield trends observed in plot 2 at the Plateau Experiment Station.	71
4.8	GPR grid from plot 1 (Milan Experiment Station) illustrating the interpretations of each data point.	76
4.9	Corn yield trends observed in plot 1 at the Milan Experiment Station.	77
4.10	GPR grid from plot 2 (Milan Experiment Station) illustrating the interpretations of each data point.	78
4.11	Corn yield trends observed in plot 2 at the Milan Experiment Station.	79

List of Tables

Table		Page
1.1	Approximate dielectric constant (σ) of various-earth materials (GSSI, 1982).	13
4.1	GPR calibration settings for the Plateau Experiment Station data acquisition.	61
4.2	GPR calibration settings for the Milan Experiment Station Data acquisition.	61
4.3	Blind test results from the Plateau Experiment Station Site.	67
4.4	Blind test results from the Milan Experiment Station Site.	67
4.5	Snap bean yield data obtained on plot 1 and plot 2 at the Plateau Experiment Station site.	69
4.6	Statistical significance of Least Squares Means data obtained in plots 1 and 2 at the Plateau Experiment Station site.	74
4.7	Statistical significance of Least Squares Means data obtained in plot 1 at the Milan Experiment Station site.	75
4.8	Statistical significance of Least Squares Means data obtained in plot 2 at the Milan Experiment Station site.	75
4.9	Probable soil series (Barbosa, 1996) and yield potentials of selected soil codes interpreted from GPR data obtained at the Milan Experiment Station.	83

List of Abbreviations and Symbols

λ	Wavelength
σ	Relative Dielectric Constant
AC	Alternating Current
ATV	All Terrain Vehicle
CEP	Circular Error Probable
CDP	Common Depth Point
DGPS	Differential Global Positioning System
ESRI	Environmental Systems Research Institute
GB	Gigabyte
GIS	Geographic Information Systems
GPR	Ground Penetrating Radar
GPS	Global Positioning System
GSSI	Geophysical Survey Systems Inc.
NAVSTAR	NAVigational Satellite Timing and Ranging
ns	Nanosecond
PCs	Personal Computers
S/A	Selective Availability
SIR	Subsurface Interface Radar
SSF	Site-Specific Farming
TT	Two Way Travel Time
USDoD	United States Department of Defense

Chapter 1

Introduction and Objectives

Trends in Production Agriculture

Many of the yield increases obtained in production agriculture over the last several decades have been achieved by identifying and adjusting producer-controlled factors that limit plant growth. In the past, a producer treated large production fields as a single entity. A field was limed at a constant rate, fertilized at a constant rate and herbicides and pesticides were also applied at constant rates throughout an entire production area. One problem exists, however, when treating fields as one homogeneous unit: most production fields consist of two or more soil types with differing crop yield potentials.

Producers are now able to map large production fields into the different soil types or yield potential regions that exist and treat those regions accordingly. These new methods of farming, which include grid-soil sampling, computerized field mapping, variable rate applications, and crop yield monitoring, are collectively called site-specific farming (SSF).

Recent advancements in computer and electronic technologies appear to be a main factor spurring many of the newest trends in production practices. The increase in speed and storage capabilities of computers and the advent of more user-friendly mapping software packages are allowing producers to use personal computers (PCs) in

many areas of the production process that were once thought impossible. Farmers not only use their PCs as farm record keeping devices, but also now have the capabilities of mapping an entire farm into specialized production areas.

The evolution of the Global Positioning System (GPS) as a quick and accurate positioning system has also had a great impact on the direction of today's farming practices. Many of the SSF concepts that are gaining widespread usage implement the GPS system within a latticework of other technologies. One example of this is the variable rate application of fertilizers and pesticides. Variable rate controllers implement GPS to determine precise locations within a field where specified volumes of material should be applied. Another example of GPS technologies in production agriculture is the widespread use of grain yield monitors. Yield monitors use the GPS system to record precise locations within a field as the harvester simultaneously records yield values that correspond with the locations. Once these data are downloaded from the yield monitor, the data can be plotted into color-coded yield maps using a variety of available software packages. These maps may supply spatial information that assists producers in making decisions concerning future production inputs.

Numerous studies have determined that SSF practices may result in lower production inputs and equal or in some cases greater production outputs than conventional farming practices. The focus of future research in these areas is now turning to the development of new methods of determining the factors that influence the usage of SSF practices.

Technology Overview

Environmental concerns and the efficient use of monetary inputs are driving forces toward precision applications in production agricultural operations. To reduce environmental impacts and optimize the use of inputs, SSF practices must utilize today's cutting edge technologies for its implementation. Technologies such as Ground-Penetrating Radar (GPR), GPS, and Geographic Information Systems (GIS) have been made possible by the many advancements in the computer and electronics industries. Each of these technologies have been previously applied and proven in disciplines other than agriculture.

GPR has been used in a variety of disciplines to detect subsurface features or foreign objects. For example, Collins et al., (1989) used GPR technology to detect and map an irregular bedrock surface under glaciated terrain. The GPS has been implemented in areas such as fleet management, air traffic control, and wildlife monitoring. Geographic information systems, a computer based data information system that is capable of managing spatially variable data has been successfully used in urban planning and environmental modeling.

Global Positioning System

The problems associated with navigation and determination of precise positions have been researched throughout time. Ancient peoples used stars as navigational benchmarks; however, meteorological events such as rain or cloud cover prevents that method from being practical. Other navigational systems such as LORAN and DECCA

have become available in recent years. These systems consist of a ground-based network of low-frequency transmitters; however, they have a limited area of coverage and are unable to determine positions as precisely as GPS (Stafford and Ambler, 1994).

The NAVSTAR (NAVigation Satellite Timing And Ranging) GPS is a space based navigational and positioning system developed, operated, and maintained by the US Department of Defense (DoD). Now fully operational, the system is capable of providing an unlimited number of users a means of determining precise position, velocity, and time on a world wide continuous basis in all weather conditions (Rupert and Clark, 1994).

The GPS consists of three primary segments (space, control, and user), all of which work together to make the system function to its fullest capacity. The space segment is comprised of twenty-four satellites orbiting the earth at approximately 20,000 km on six different orbits. The satellites transmit signals on two different frequencies. One signal is known as the L1 (1575.42 MHz), the other signal is called L2 (1227.60 MHz). These two signals are known as carriers and have impressed upon them a course acquisition (C/A) code (on L1) or a precise (P) code (on L2), and a broadcast message which includes ephemeris and satellite health data. Each satellite weighs approximately 860 kg in orbit and is 5.1 m in length with the solar panels extended (Hurn, 1989).

The operational control segment consists of seven different stations throughout the world whose function is to accurately track the satellites. These control stations provide tracking and ephemeris data; they are also capable of correcting errors in the satellite clocks, and monitoring the general health and status of each satellite (Rupert and Clark, 1994). The user segment is composed of the combination of people and their

receivers tracking satellites to receive information required for position determination (Rupert and Clark, 1994).

Basic GPS Operation

Precise locations on earth are calculated by trilateration of the satellites. A synchronized pseudo-random code is generated both by the orbiting satellites and by receivers on the ground. Since the codes are synchronized, the time it takes for the satellite signal to reach the receiver can be computed. From that time, using the speed of light (299792458 m/s), a distance or range to the satellite is calculated. A microprocessor within the GPS receiver then uses these computed distances to satellites to trilaterate a position in either two dimensions (latitude and longitude) or three dimensions (latitude, longitude, and altitude) on earth (Hurn, 1989).

Precision and Differential Correction

Though GPS position locations are more accurate than any previous system offered, there are still rather large errors associated with the system. When used autonomously, or in the stand-alone mode, GPS is accurate to approximately 12-m circular error probable (CEP). When used with a base station and differentially corrected, accuracy may be improved to 2 to 5-m CEP (Johnson et al., 1992). The three factors that are considered to contribute the most to low precision in GPS data are listed below.

1. Satellite Clock and Receiver Errors: Though satellites are equipped with atomic clocks, they may still show small variations. Receivers can also round off mathematical computations or suffer electrical interference that leads to an erroneous determination. Hurn (1989) states that these two factors alone may add up to as much as two meters error in calculated positions.

2. Ionospheric and Atmospheric Errors: The ionosphere, which is a band of negatively charged particles that encompasses the earth at approximately 130 to 200-m altitude, can cause errors in the system by slowing down the pseudo random code generated by the satellites. If the code does not maintain the speed of light, receiver calculations will contain errors. The earth's atmosphere or meteorological events are also capable of delaying the code. According to Hurn (1989), these errors may add up to 3.5 m of error to positions.

3. Selective Availability (S/A): S/A is the intentional addition of errors by the US DoD in the satellite orbit information. This error is added to prevent hostile forces from using the system in times of war. Because of the large amount of civilian use of GPS, S/A is being restricted to reduce the system accuracy to no more than 100 m. Special military GPS receivers are able to decode information on both the L1 and L2 signals even if S/A is turned on.

In agricultural applications such as precision farming, accurate positions are a must. Therefore, due to the positioning errors associated with timing, S/A, and the ionosphere, an alternative way to achieve sufficient accuracy is necessary. The method used to acquire positional data accurate enough for precision farming is the Differential Global Positioning System (DGPS). The Differential Global Positioning System is the technique of using two GPS receivers to collect positional data. One receiver (the base station) is set up at a known point. The second receiver (the rover) is used to move throughout the area to record data points. By comparing the data received by the base station to its known location, the error is estimated and eliminated. The error message is then transmitted to the rover unit, allowing the rover to correct its own location.

Two methods of accomplishing differential correction are:

1. Real Time DGPS: Real Time DGPS refers to correcting the positions as the original data are being collected. When applying real time DGPS, the user has several options on how to receive the correction signal:
    - Having a separate base station and the transmission equipment needed to send the correction signal to the rover unit.
    - Subscribing to a commercially available DGPS service. Several companies offer a subscription of DGPS correction signals valid for a determined area, and charge a fee for this service.

- Use the Coast Guard Beacon signal. The US Coast Guard transmits DGPS signals at no charge to the user. One disadvantage of using the Coast Guard Beacon for differential correction is that the rover unit is restricted to areas where the beacon signal will reach, which are confined to coastal areas and navigable waterways.

2. Post-Processed DGPS: Post processing involves correcting the GPS data after it has been collected. The most common form of post processing data is to contact a local base station and download correction codes that correspond with the time stamp on the uncorrected GPS data that is to be corrected. Post-processed DGPS positions are just as accurate as real-time DGPS data; however, this type of data will often have limitations in agricultural applications because users most often need to know their position while they are in the field and not after they have left.

Geographic Information Systems

A GIS is a computerized system designed to store, process, and analyze spatially varying data. The major components of a GIS include a user interface, system/database management capabilities, database creation/data entry capacity, spatial data manipulation and analysis packages, and display/product generation functions (Evans et al., 1995). A GIS can store, manipulate, and retrieve any data that contain a geographic or location reference. Therefore, data used in a GIS database must contain some reference of its location such as an address or geographical coordinates.

Much of the research involving the use of GIS in SSF practices has used software produced and distributed by the Environmental Systems Research Institute (ESRI)[1]. ESRI, which produces the GIS software ARC/INFO™, PC ARC/INFO™, and ArcView™ define GIS as the only system that permits spatial operations on data. Spatial operations are queries that can only be answered using the geographic coordinates and the listed attributes of the data (ESRI, 1995). Star and Estes (1990) list five aspects of data that a GIS is capable of defining:

1. Location: A location refers to the geographic reference of the data (an address, ZIP Code, or coordinates).
2. Condition: A GIS can be used to find locations that satisfy a certain condition. For example, a yield value range that exists on a soil with a slope lower than 5% and a soil depth less than 50 cm.
3. Trends: A GIS is capable of determining trends in areas by looking at differences in the data over time.
4. Patterns: A GIS is able to reveal patterns in data sets.
5. Modeling: A GIS may be used to answer hypothetical "What if" questions. For example, what happens if a toxic substance seeps into groundwater reservoirs?

Projects

Generally when working with GIS software, each individual data set (i.e., data from a particular production field) is termed a project. A project contains both the geographical reference points of the data and the attribute information that coincides with

[1] The use of brand names does not imply endorsement of these products by The University of Tennessee.

those points. Every GIS project should consist of five essential elements (Star and Estes, 1990):

1. Data acquisition: The process of identifying and collecting the data required for the project.
2. Pre-processing: The manipulation and processing of the data in order that it will conform to the GIS format.
3. Data management: Consistent methods of data entry, update, deletion, and retrieval.
4. Data manipulation and analysis: Allows operators to work with the database and derive new information from the data.
5. Product generation: The generation of thematic maps, graphics, and statistical reports from the information in the database.

Ground-Penetrating Radar

GPR Basics

Ground-penetrating radar is a broadband, impulse radar system that has been specifically designed to penetrate earthen materials (Doolittle, 1987). Images are formed by short electromagnetic pulses emitted from the radar antenna. When the pulse reaches an electrical interface (i.e., a change in electrical properties) in an earthen material, some of the energy is reflected back while the rest proceeds forward. A receiving unit inside the radar antenna detects the reflected signals, and the time difference between transmission and detection is recorded in nanoseconds (nS). A continuous scan of the

electrical interfaces within the medium is then displayed on an output screen as the antenna is simultaneously pulled across the surface.

The relative dielectric constant (σ) of a material is a measure of how well that material stores an electrical charge. Air has a σ of 1 while the σ of water is 81. As listed in table 1.1, other materials have σ that range somewhere in between that of air and water. Since the σ of water is equal to 81, the primary factor affecting the average σ of a soil profile is water content.

There are two separate methods of determining the average σ of soil: the common depth point (CDP) method and the two way travel time (TT) method. The CDP method requires the use of two antennas being operated on a relatively flat surface. One antenna is used as the transmitter and the second is used as the receiver. The two antennas are then pulled away from a common point in equal distance increments. This method allows the velocity of the wave moving through the soil to be calculated by triangulation. When using this method, the antenna separation is set to zero (Ulrikson, 1982).

The TT method of calculating average σ requires that the depth of an object or reflector within the soil column be known. As the antenna passes over the known reflector, the TT is recorded by the receiver in nanoseconds. Using the known depth to the reflector and the TT value, an average σ for the soil can be calculated using equation 1.1.

(eq. 1.1)

$$\sigma = \frac{(ns/m)^2}{43.56}$$

where

σ = overall relative dielectric constant of the medium
ns = two way travel time of radar wave in nanoseconds
m = distance in meters

Overall accuracy and maximum probing depth of GPR are determined by the relative σ of the geologic material over which the unit is being operated, and by the frequency of the antenna being used. Mediums with highly conductive properties such as wet, saline, or high clay content soils produce poor images. However, mediums with lower conductive properties such as sand and other coarse grained materials produce much sharper images (The Finnish Geotechnical Society, 1992).

Maximum probing depth of the antenna is a function of the frequency or wavelength (λ) generated by the antenna. Antennas that transmit high frequencies (500 to 1000 MHz) are capable of resolving very distinct electrical changes within a medium; however, these high frequency models are not able to probe very deep within the medium. Antennas that transmit at lower frequencies (100 to 300 MHz) lack the resolution of the higher frequency models but possess the ability to penetrate to deeper depths.

TABLE 1.1: Approximate dielectric constant (σ) of various-earth materials (GSSI, 1982).

Material	Approximate Dielectric Constant, σ
Air	1
Pure Water	81
Sea Water	81
Granite	8
Sand, dry	4 - 6
Sand, saturated (fresh water)	30
Silt, saturated (fresh water)	10
Clay, saturated (fresh water)	8 - 12
Average soil	12

Justification for Research

In the past, site-specific soil mapping studies (Palmer, 1997; Franzen and Peck, 1995) have used the grid method of sampling to focus primarily on the chemical characteristics of the soil (e.g., pH, N, P, and K concentrations, and Base Saturation) with less attention given to the physical properties of the soil that may limit plant growth such as shallow bedrock and other root-restrictive soil layers. One reason these physical properties have been somewhat overlooked is that previously the soil had to be physically altered for observation, which most often tended to be both a costly and labor intensive venture. Furthermore, extensive disturbance of a naturally occurring soil may limit plant growth by altering the soil structure, porosity, and hydraulic conductivity.

With precision farming and yield monitoring becoming more popular with producers, new and innovative methods are needed to define the subsurface features that affect agricultural production lands. Various types of soil and rock probes are today's standard instruments used for detecting bedrock and layers of high density within a soil profile. Though these instruments can detect the depth to these restrictive layers with a relatively high degree of accuracy, they are only capable of acquiring data at specific points, with subsequent questionable data interpolation between points. Because of the limited amount of non-continuous data that may be taken by these intrusive instruments, this project was devised to evaluate GPR as a means to continuously collect the subsurface data required to correlate crop yields with subsurface phenomena.

Objectives

The primary objective of this project was to evaluate the ability of GPR to nonintrusively detect subsurface features that affect the productive capacities of agricultural production fields. Specific objectives included:

1. Systematically interpret the characteristics of GPR images obtained from research plots, and
2. Statistically compare the interpreted characteristics of GPR images with yield data collected from the research plots.

Chapter 2

Review of Literature

Soil Variability in the Research Areas

As defined by Brady (1990), soil is a "naturally occurring body composed of mineral and organic materials and living forms in which plants grow." Miller (1990) cites five factors that are involved in the soil formation process:

1. Parent material: all soils are developed from weathered rocks, volcanic ash deposits, or accumulated plant residues. Those materials are called parent materials. They influence soil formation by their different rates of weathering, their nutrient content for plant use, and their particle size.
2. Climate: the climate is a dominant factor in soil formation because of the effects of precipitation and temperature.
3. Living organisms: the biota helps soil develop by decomposing organic matter and forming weak acids that dissolve minerals better than pure water.
4. Topography: topography influences soil formation, primarily due to its association with temperature and water.
5. Time: time interrelates the above factors in soil formation. Under ideal conditions for development, a soil profile can develop within 200 years. Under less favorable conditions, it might take several thousand years for this development.

A great amount of variability is often present in soil profiles within a matter of meters (Brady, 1990). One of the more notable variations is the difference in available nutrient levels within the soils. Several different factors are involved in determining the amount of available nutrients that a particular soil may contain. One of those determining factors is the type of parent material that the soil was derived from. For example, a soil formed from limestone sediments will generally have higher residual nutrient levels than that of a soil derived from sandstone sediments. Regional climates also have an effect on the amount and type of nutrients present. Generally regions that are relatively warm and receive a large amount of annual rainfall will incur leaching of nutrients from the topsoil into the subsoil, where they are no longer available for plant uptake due to fixation by other elements.

Numerous studies exist that have concentrated on comparing soil nutrient levels with crop yields. Barbosa (1996) related variably applied nitrogen with yields on corn and found that as the amount of nitrogen applied increased, so did crop yields. Palmer (1997) related yield values of cotton with phosphorus levels and found that the lowest average yields were found in soil mapping units that coincided with low phosphorus levels (between 6 and 9 ppm).

Another form of variability within production fields that is sometimes overlooked is that of the morphological traits found under the surface of the soil. Common variations found in soil morphological properties include differences in soil depth and depths to specific soil horizons. These morphological features often have a large impact on the ability of the soil to produce crops by determining how water and nutrients move through the soil, and ultimately become available for plant uptake.

The morphological feature of key importance in the geographic region of the Loess Uplands of West Tennessee (Figure 2.1) is the fragipan. Figure 2.2 illustrates a fragipan, which is a soil horizon that meets a set of field criteria that include brittleness, tendency to slake in water, evidence of pedogenesis, presence of prisms arranged in a horizontal plane separated by vertical streaks, and high bulk density compared with that of overlying horizons (Rhoton et al., 1996). Rhoton et al. (1996) also state that in terms of plant production, no individual property is more important than the ability of fragipan horizons to restrict the depth of plant root penetration and water movement.

Soils of the Loess Uplands of West Tennessee consist primarily of Alfilsols, and approximately 55% of the highly erosive uplands are underlain by fragipans (Tyler et al., 1991). Accelerated erosion is thought to have been occurring on the highly erosive areas since the first settlers began cultivating the region in the early 1800's. To compound the detrimental effects of erosion, the presence of fragipans makes the accelerated erosion particularly detrimental to the productive capabilities of the soils (Tyler et al., 1991).

For example, in a three-year study of erosion and productivity of soils containing a fragipan, a slightly eroded site (59 cm) stored an average of 30% more water than a moderately eroded site (43 cm) and 72% more water than a severely eroded (20 cm) site. Also, the moderately eroded area stored approximately 58% more water than the severely eroded area (Rhoton et al., 1996). In another study of the relationship between the depth of a fragipan and crop growth, Tyler et al., (1991) found that as the depth to the fragipan layer decreased, rooting depth was restricted and crop yields of soybeans and corn were lowered significantly.

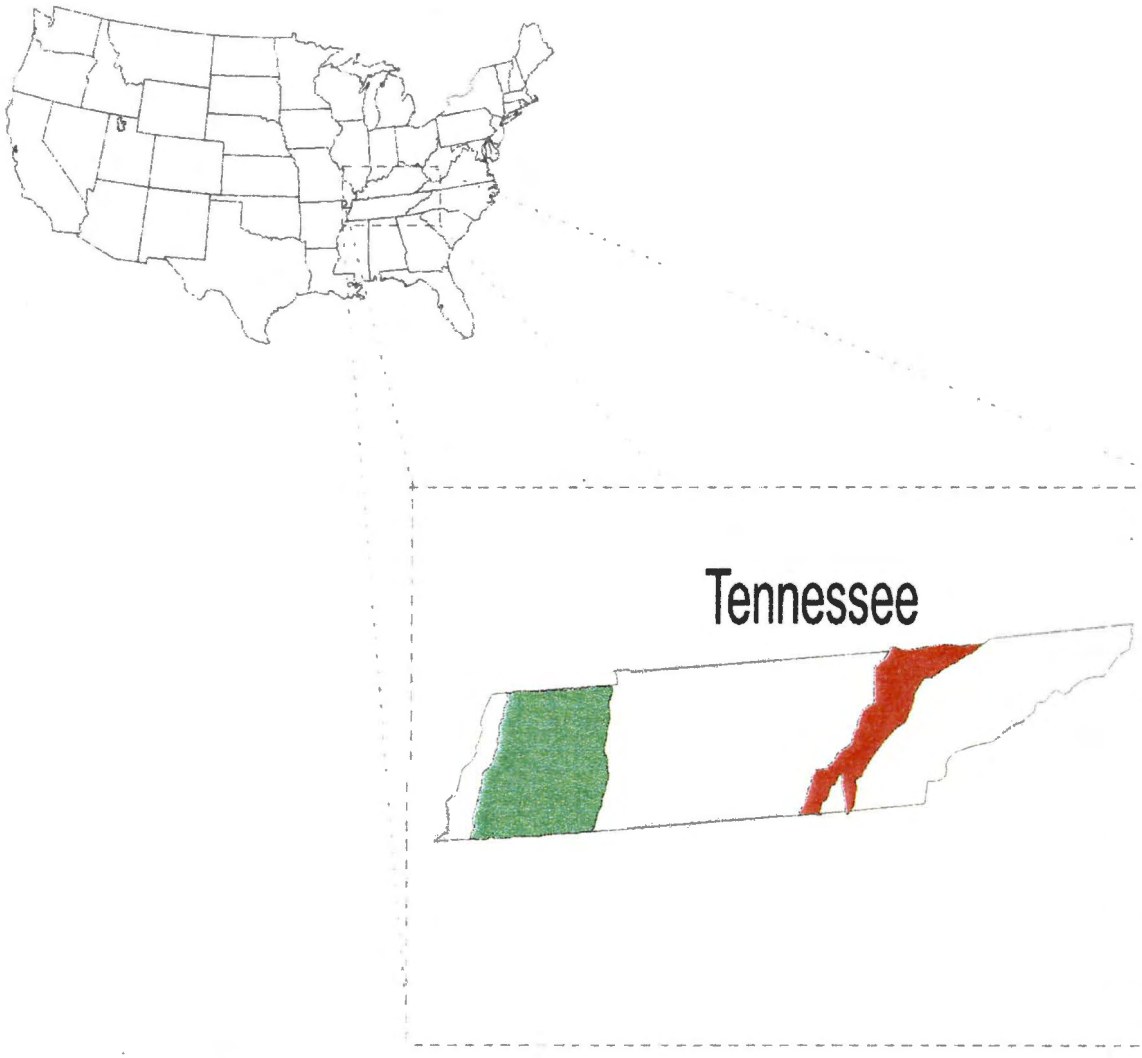


Figure 2.1: Schematic of the Cumberland Plateau and Loess Uplands Physiographic Regions of Tennessee.

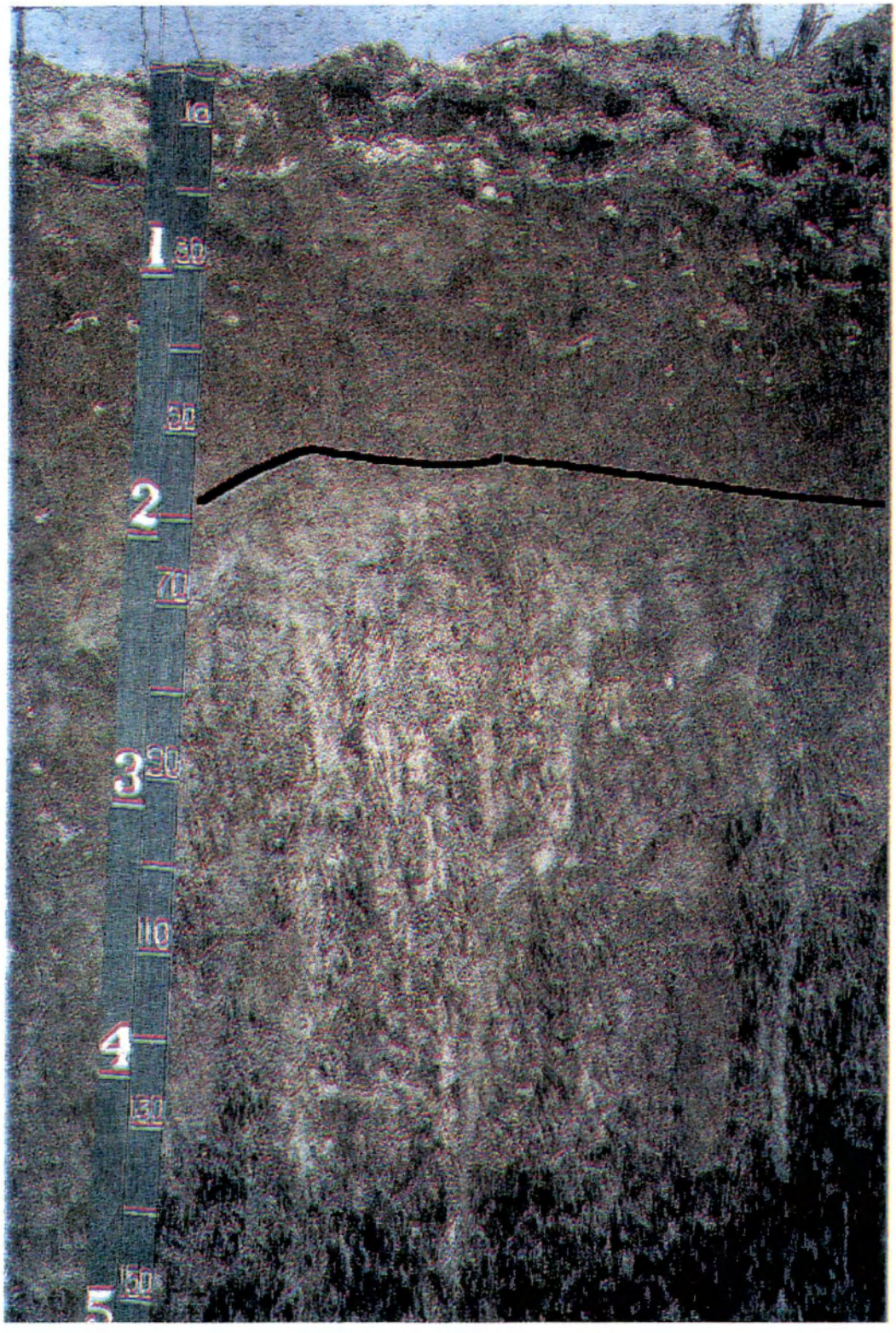


Figure 2.2: Photo taken from within a soil pit of a fragipan horizon occuring below approximately 60-cm depth.

Although erosion has the potential to detrimentally affect soil fertility by removal of nutrients, this problem can often be solved with proper chemical amendments on soils that do not contain a fragipan. However, on soils containing fragipans, erosion and the loss of soil-water storage capacity caused by the decrease in topsoil thickness can be a far more serious problem that cannot be easily ameliorated. In these cases, fragipan horizons generally exert a greater influence on the productivity of the soil, limiting plant-root accessibility to water and nutrients stored above the fragipan. Rhoton et al. (1996) suggests some form of conservation tillage, not as a means to ameliorate the problem, but as a means to control the problem for future production. Furthermore, in addition to reducing the loss of topsoil, the use of conservation tillage practices on shallow fragipan soils may also act as a form of soil-water conservation. However, if erosion is so severe that the fragipan horizon represents the surface, it may be more cost effective for producers to simply take the affected area out of production totally.

Shallow bedrock beneath production areas may also retard plant-rooting depth and reduce the water holding potential of a soil. The morphological feature of key importance in the geographic region of the Cumberland Plateau of Middle Tennessee (Figure 2.1) is shallow soils underlain by sandstone bedrock. Figure 2.3 illustrates the shallow depth at which bedrock can occur on the Cumberland Plateau.

Because precipitation is generally lower during the growing season than for the remainder of the year, and because the soils of the Cumberland Plateau are generally shallow, moisture stresses to plants are frequent. Schumann (1984) determined that the plants most affected by moisture stress on the Cumberland Plateau are those with a limited root system or plants growing where soils are shallow, which is widespread.



Figure 2.3: Photo of shallow sandstone bedrock that is typical of the Cumberland Plateau Physiographic Region.

Although most soils on the Cumberland Plateau exhibit relatively similar textural properties, the agricultural potential of the soils varies greatly. This was found to be primarily due to the differences in depth and stone content, which were closely related to the gradient of slope (Schumann, 1984).

In the past, farmers had a limited amount of information on the variability of soils, and even fewer options in managing this variability. Former methods of planting, fertilizing, and spraying were designed to apply at uniform rates throughout a field. Today, due to the numerous advancements in computer and electronic equipment, agricultural machinery is being designed to take into account the natural variability within a field and treat areas according to recommendations from soil tests. GPS and GIS technologies are now being researched to be used in conjunction with agricultural equipment to allow farmers and agronomists to manage their fields in accordance with the variability and yield potentials of the soils.

GPS in Site-Specific Farming Applications

When using GPS for SSF applications, it is almost a must to differentially correct for positional errors. Researchers and producers alike are using GPS as a tool to determine spatial variability (yield, nutrient, soil type, and pest occurrence) and prescribe treatment according to those specific variables. For this reason, the more accurate the system used to describe the variability, the more practical use it will have for producers.

Many publications exist that have researched GPS technology as related to its use in agricultural operations. Harrison et al. (1992) states that location determination is

arguably the most important data input for SSF management, and that GPS is capable of providing that information. Also, after a series of yield mapping tests using DGPS attached to combines, Auernhammer et al. (1994) concluded that DGPS allows yield mapping with a sufficient precision for current farming practices.

The GPS has also seen widespread usage in the area of spatially variable fertilizer and pesticide applications. When implementing spatially variable applicators, the desired application rate may change often and significantly. Due to these changes in output throughout a field, some method of precise location determination is needed. Schueller and Wang (1994) state that the location methods often used in spatially variable applications include dead reckoning, electromagnetic (radio or microwave) trilateration, or GPS. They also state that discussions with many agronomists and engineers indicate that GPS has the greatest potential for the variable-rate control of fertilizers and pesticides. Furthermore, in a study testing laser, radio, microwave, and GPS positioning techniques, Stafford and Ambler (1994) concluded that GPS had the best potential as an agricultural location system for spatially variable operations.

GIS in Site-Specific Farming Applications

Information that may lead to the maximization of yields and the minimization of inputs is what producers and researchers expect when utilizing GIS technologies in SSF applications. The ability of a GIS to query and manipulate data according to its attributes and geographic location may lead producers to a better understanding of the variability in

yields, nutrients, and soil type, and how to overcome that variability through SSF practices.

Perhaps the most common use of GIS in SSF applications is the production of yield maps that are georeferenced using real-time DGPS coordinate data. Another common application of GIS in agriculture is the map overlay (Evans et al., 1995). For example, soil type maps and nutrient maps are overlaid to generate individual sub-areas with distinguishing soil properties in a field. Crop simulators can then be applied to each unique sub-area to study crop yield distribution.

Some of the more important roles for GIS in agriculture are data base functions used for record keeping and for comparing management decisions (National Research Council, 1997). A GIS is capable of storing data of farm inputs and outputs in a spatial format. For instance, data on crop rotation, yield, soil type, and fertilizer and pesticide applications are capable of being stored and displayed in a GIS. The National Research Council (1997) also states that a GIS has the potential to enhance other components of SSF such as yield monitoring and farm based research (i.e., crop modeling) as well as provide a better record keeping device for producers.

Current research in the agricultural industry is implementing this technology due to the ability of a GIS to map and model spatially varying information of numerous variables associated with SSF practices. Some examples of these variables include: yield potential regions, soil nutrient levels, soil types, crop pest occurrence, subsurface phenomena, plant population, and ground water integrity.

In discussing the capabilities and limitations of GIS technology for SSF, Evans et al. (1995) indicates that GIS is a very useful tool for handling spatial data, but that its role

in precision farming should not be exaggerated. They cite that the main limitations of GIS, as pertaining to precision farming, are its lack of basic analytical tools (e.g., spatial interpolation routines), and the difficulties in linking data with other software packages (e.g., crop simulation models). However, according to the National Research Council (1997), the lack of analytical tools in GIS packages are rapidly changing as several vendors are developing fully functional GIS programs intended for use on PCs. They also state that this should lead to GIS software and hardware systems that are more user friendly and less expensive.

GPR Applications in Agriculture

Computer processing of GPR data can be used to generate economical and detailed two- and three-dimensional maps of subsurface conditions. These maps are capable of showing variations in the depths to soil horizons and summarizing the composition of soils for detailed soil maps. Perhaps the main reasons GPR has been implemented in agricultural soil reconnaissance are its speed of operation and its ability to gather large quantities of continuous, high-resolution subsurface data.

In agricultural applications the cost of inputs are often a major concern to producers and researchers alike. When compared to conventional methods of collecting subsurface data for agricultural research, GPR has proven to be less time consuming and more cost effective. For example, when comparing GPR technologies to conventional soil surveying methods, Doolittle and Collins (1995) found that GPR was more economical and less likely to miss subsurface data than conventional methods. Doolittle

(1982) also compared conventional soil reconnaissance cost with GPR methods and found that GPR could reduce the costs of fieldwork by 70%, while increasing productivity by 210%.

Another advantage GPR possesses over conventional soil reconnaissance methods is its ability to collect subsurface data continuously and noninvasively. Conventional intrusive methods of collecting subsurface data include probes, augers, spades, and often times backhoes. When comparing GPR to each of these intrusive instruments, the intrusive tools require more man-hours and provide less complete data sets. Furthermore, the conventional methods can be less accurate due to obstructions that may be encountered above the feature that is of primary interest. For example, when comparing GPR technology with the use of manual rock probes to determine depths to sandstone bedrock on the Cumberland Plateau of Middle Tennessee, Hamlett (1995) found GPR to be more consistent than the rock probe. This was in large part due to large rock fragments or "floaters" suspended within the soil column that inhibited the probe from reaching solid stone. Hamlett (1995) also concluded that deposits of mudstone were capable of inhibiting the penetration of the rock probe, therefore misrepresenting the actual depth to solid sandstone bedrock.

GPR has also been used to characterize soil map units in conjunction with physical data obtained by soil scientists in the coarse grained soils of Florida (Doolittle, 1982). From these characterizations, Doolittle (1982) found that GPR was capable of detecting, determining the depth, and tracing the lateral extent of subsurface horizons. He found that the compositions of soil horizons could be determined by observing the variations in the strength or intensity of the reflected signals along interfaces.

To date, GPR technologies have also been used to provide the following information to agricultural researchers:

1. Subsurface information used to update and refine existing county soil surveys (Schellentrager et al., 1988).
2. Detection of spatial variability in depth and lateral extent of argillic horizons and water tables (Truman et al., 1988).
3. Determination of microvariability in spodic and argillic horizons in a representative Atlantic Coast Flatwoods area (Collins and Doolittle, 1987).
4. Information used to map soil horizons, permeable zones, clay lenses, organics, water tables, and specific soil types (Benson and Glaccum, 1979).
5. Geotechnical information involving soil cementation (hard pans), soil/rock interfaces, and geological fractures and bedding planes (Benson and Glaccum, 1979).

Chapter 3

Materials and Methods

GPR Equipment Summary

The GPR unit used in this study was the Subsurface Interface Radar (SIR) System-10A designed and manufactured by Geophysical Survey Systems, Inc. (GSSI) of North Salem, NH, USA. The System-10A mainframe consisted of a 486SLC Cyrix motherboard with an 80387 math coprocessor. The coprocessor used a 20-MHz Motorola DSP 56001 digital signal processor for high speed signal processing. To save the data for later analysis in the laboratory, each data file was written to an internal 2.3-GB, 8-mm tape drive, which provided a permanent record for archiving and transport.

Manual inputs to the mainframe were controlled by an industry standard AT keyboard and a hand held file marker switch that could be attached either to the antenna or to the radar mainframe. Inputs from the marker switch placed marks at user determined locations within the GPR data files. These marks were later used to determine the precise location within the field the antenna was located, and they were also used in distance and surface normalization procedures on each data file during lab analysis.

Three antenna models (200, 500, and 900 MHz) were available for this study. Overall, GPR antennas range in center frequencies from 10 to 1000 MHz. Lower frequency antennas such as the 100- or 200-MHz models have a much greater depth of penetration than the higher frequency models. Though the lower frequency antennas

penetrate deeper into a medium, they lack the ability to resolve distinct changes within the mediums that the antennas of the high frequency range are capable of resolving.

The subsurface information pertinent to this project (i.e., soil regions containing restricting layers of high density, parent material or bedrock interfaces) required a moderate penetration depth from the antenna to be used. Furthermore, a high degree of resolution was not needed to distinguish these layers from other layers within the soil profile. Due to this nature of the data required, a 200-MHz center frequency antenna (Model 5106) was chosen for this research project.

For data collection in the field, the radar system was powered by two-deep cycle marine 12-VDC batteries. The batteries were wired in parallel to provide longer life to the system and were converted to alternating current (AC) by a Model PV 1200 FC Tripp-Lite DC/AC Power Inverter that provided a constant 110-VAC. According to Bouldin (1997), this power configuration could allow the system to run for approximately eight hours under optimal field conditions. While collecting the data, a standard VGA color monitor was used to view the radar data files.

Due to the number and overall length of the research transects, a method other than manually dragging the radar antenna was needed. For stability and maximum mobility in the field, the radar mainframe, power system, and VGA monitor were loaded into a trailer that was towed by a small tractor. The radar antenna was connected to the rear of the towed trailer at approximately 1.5-m apart. The length of 1.5 m provided a sufficient distance from the trailer so that the metal in the trailer did not affect the radar signal (Figure 3.1). With the tractor operated in low range,



Figure 3.1: Tractor and trailer configuration used to transport GPR mainframe and power source equipment and tow GPR antenna during data collection.

2nd gear, radar data collection and mobility within the field were accomplished to a satisfactory degree.

Data Analysis Hardware and Software

Once in the lab, the raw GPR data files were downloaded from the 2.3-GB tapes to a 1-GB file server drive using RADAN III software. From that file server the data were then capable of being accessed by a 200-MHz desktop workstation with 32 MB of RAM and 3 GB of hard disk space. RADAN for Windows was the primary software package used to analyze the radar data files. Once the files had been downloaded, each was surface normalized using RADAN for Windows to insure proper file length and file size and also to allow for other processing and filtering techniques.

The crop yield data collected at both research sites were handled by the ArcView™ GIS software package that is manufactured by the Environmental Systems Research Institute (ESRI) of Redlands, CA, USA. ARCVIEW is a Windows based software package that accepts vector based data and is capable of using the entire polygon model. ArcView™ was chosen for this project due to its ability to display data and create thematic maps.

GPR interpretations were statistically compared to crop yield trends using SAS^R for Windows. The SAS^R programs written for these statistical comparisons can be found in Appendix B, and involved the following steps:

Step 1 Calculation of the Pearson Correlation Coefficient for each plot

Step 2 Calculation of the Least Squares Means for each soil code

Research Plot Design and Layout

There were a total of four primary research plots used for GPR data collection in this research project. The location of each plot was determined by the research team for its possible ability to show high degrees of variation in subsurface phenomena. Two research plots were located at the Plateau Experiment Station, on the Cumberland Plateau of Middle Tennessee, and two research plots were located at the Milan Experiment station, which is located in the Loess Uplands of West Tennessee.

The research team selected the specific locations of the research plots located at the Milan Experiment Station by first closely examining corn yield data collected from fields A6 and A7 during the 1997 growing season. The plot locales were then situated within these fields at locations that most exemplified large variations in yield values. Figure 3.2 shows the corn yield data for 1997 and the layout of the research plots within fields A6 and A7.

Since there were no previous yield data to use in determination of plot layout, the specific locations of the research plots located at the Plateau Experiment were selected after several conversations with station personnel who were familiar with the productivity

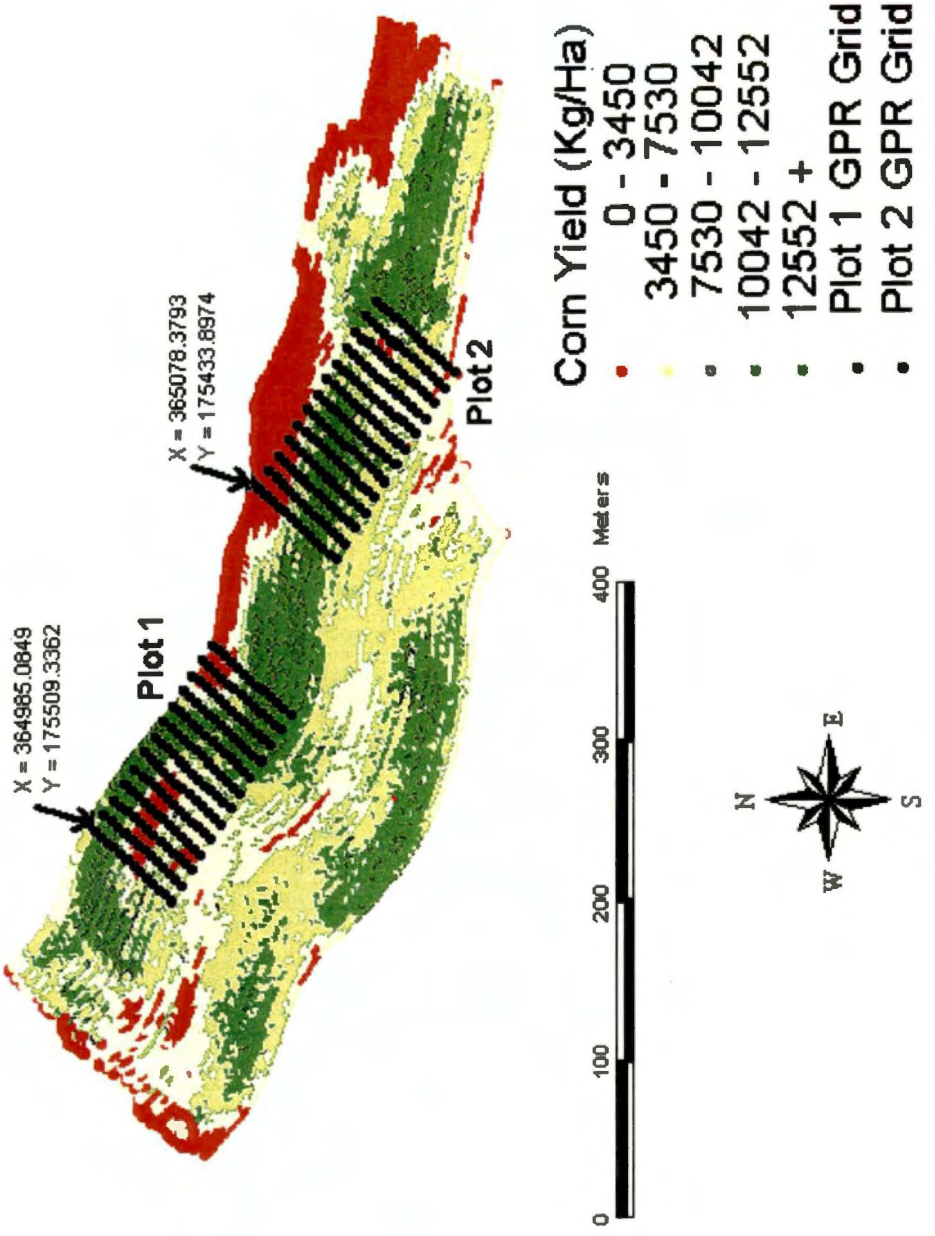


Figure 3.2: Corn yield results obtained in fields A6 and A7 at the Milan Experiment Station and locations of the GPR data collection grids (coordinates are in State Plane 1927 projection).

trends of several sites on the station. Field H13 (plot 2) and field H14 (plot 1) were then chosen as research plots due to the station personnel pointing out these fields as having a high degree of variability in yield and depth to sandstone bedrock in specific areas.

Once the site locales were determined, each plot was laid out using a Pentax Model PTS Total Station electronic surveying device for maximum precision of transect spacing. The data collection transects were marked by placing survey flags every10 m along the length of the plots and every 5 m along the width. The plots located on the Milan Experiment Station had dimensions of 60 m by 120 m; however, due to pre-existing field boundaries, the plots located at the Plateau Experiment Station had to be shortened to dimensions of 40 m by 100 m.

After the transects were completed, topographic data were taken on the two plots located at the Plateau Experiment Station. The topographic data were acquired at each survey flag using the Pentax Model PTS Total Station, which automatically downloaded the data in the field to a Hewlett Packard Calculator. These data were later used in the lab to simulate topographical surface maps of the two plots. No topographical data were acquired at the Milan Experiment Station due to the limited amount of time the research team had on the plots. However, slope data was extracted from a previously developed topographical data set that was generated with a Total Station survey instrument (Barbosa, 1996).

GPR Data Collection Summary

Calibration Data Collection

As shown in Figure 3.3, calibration data sets for this project were collected at three different sites within Tennessee. Two of the sites (The Milan Experiment Station, Milan, TN, and Ames Plantation, Grand Junction, TN) were in the Loess Uplands physiographic region of the state. The third site (The Plateau Experiment Station, Crossville, TN) was located in the Cumberland Plateau physiographic region that runs roughly north and south through Eastern Middle Tennessee. Each of the locales was chosen for its similarity to the soil profiles that would be encountered in the subsequent research plots. The primary goals in collecting the calibration data sets were to identify the reflective characteristics of the targeted soil layers, and to obtain the optimal antenna settings for each of the physiographic regions.

The first calibration data were taken at the Ames Plantation in an area known as the Centennial Field on July 22 and 23, 1997. Two antenna models were used to collect these data sets. A 300-MHz (GSSI Model 3105) and a 200-MHz (GSSI Model 5106) antenna were used to collect data along identical transects. Both antennas were used in an effort by the research team to determine which frequency was best suited to collecting subsurface data in West Tennessee soils.

Calibration processes used at this site consisted of dragging the antenna over a buried PVC pipe that generated a hyperbolic form in the GPR image. From the logged depth to the PVC pipe, a suitable σ for the soil was calculated using equation 1.1. Once

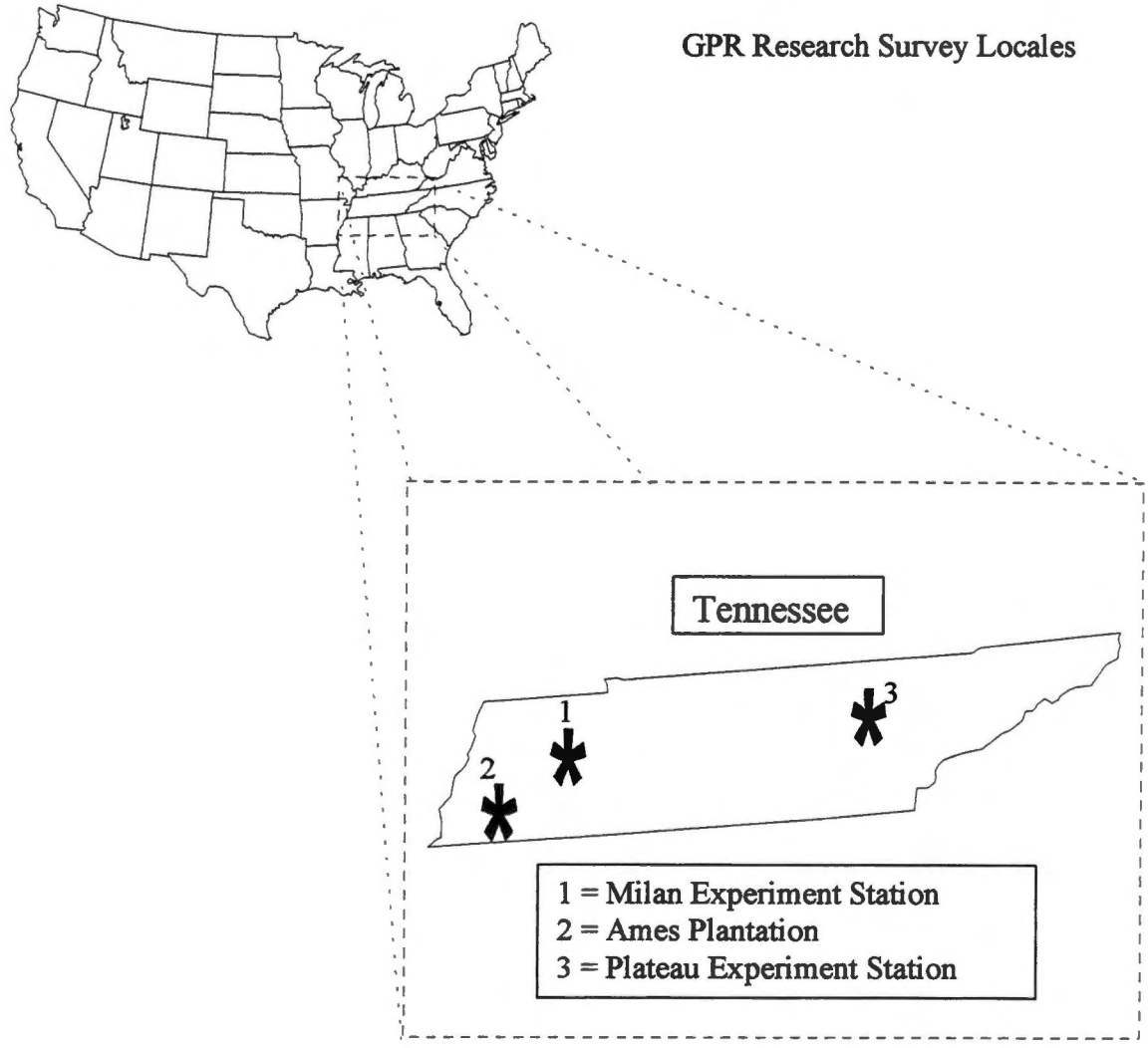


Figure 3.3: Schematic of GPR survey locales in Tennessee.

the σ had been calculated, depths to the Loess/Alluvium interface that underlies the Centennial Plot could be interpreted in the lab using the radar images.

Also of primary interest to the Ames Plantation calibration data set was the generation of 3-D imagery. To accommodate the generation of 3-D GPR images, these data were collected at approximately 1-m intervals throughout the plot. The research team tested this method of data presentation to determine if 3-D imagery would allow for more accurate interpretations of data in subsequent research plots.

Calibration data acquired at the Milan Experiment Station were obtained in field N47. Dr. Donald D. Tyler chose the site locale for these data over an area in the field where a fragipan was present. Not only was a fragipan present, but due to differences in topography, the fragipan was discontinuous. The transect at this location was situated to provide a data set showing soil with no fragipan present, and to provide data showing the presence of a fragipan. The length of the transect line was 45 m, with flags placed every 5 m.

Calibration data acquired on the Cumberland Plateau were obtained on the Clyde York 4-H Camp, which borders the Plateau Experiment Station. These data sets were primarily collected to determine optimal antenna settings and to identify targeted soil layers of the region. However, these data were also used to assist the management of the Clyde York 4-H Camp in determining the feasibility of a proposed site for septic tank fill lines.

Data were collected along a 90-m transect that followed the proposed path of the fill lines. Survey flag spacing were positioned at 10-m intervals along the transect, and the transect was replicated four times using a 200-MHz (GSSI Model 5106) antenna. A

standard rock probe was used for physical calibration purposes. Again, equation 1.1 was used to calculate a suitable σ for the area.

Blind Test Data Collection

Since GPR data can be easily altered, and because interpretation can be very subjective, a blind test was designed by the research team to insure accuracy of GPR interpretations. The blind test that was proposed for this project entailed using the same radar parameter settings that were used in the calibration data sets. The data were collected by someone other than the primary researcher, with the primary researcher having no knowledge of the data files other than which physiographic region the data were obtained in. The primary researcher had to then be able to identify or distinguish whether a particular feature existed in the image (Yes or No), and if the feature did exist, the physical depth to that feature (+/- 5.0 cm to 150-cm depth). Also, to further insure accuracy of the blind test, the primary researcher had to also be able to train another individual to interpret the data in a similar manner. This individual had to have an understanding of and some experience with analyzing GPR imagery. The data were presented to the trained party in the same manner as they were to the primary researcher. Thus, the trained party should have determined relatively the same results.

The length of the blind test transects were 55 m. The interpretation interval within each image was 5 m, marked by the GPR operator using the hand-held switch that places marks within the data file. Physically measured ground truth data points were also gathered at 5-m intervals along each transect.

Cumberland Plateau Physiographic Region

Of the blind test data obtained on the Cumberland Plateau, four different transects were surveyed with the GPR and each transect was replicated four times. Since bedrock usually occurs at or above 150 cm in most areas on the Cumberland Plateau, there were no data files where bedrock was not present. This portion of the blind test primarily focused on the identification of the bedrock interface and the depth to that interface.

Loess Uplands Physiographic Region

Of the blind test data obtained in the Loess Physiographic Region; there were also four separate transects, replicated four times each. Unlike the transects on the Cumberland Plateau; however, this test consisted of three 55-m transects and one 110-m transect. Since no individual soil property is more important than the ability of fragipan horizons to restrict the depth of plant root penetration and water movement (Rhoton et al., 1996), the blind test in the Loess physiographic region focused on the occurrence of a fragipan. Each transect was ground truthed by Dr. Donald D. Tyler, using a standard 5-cm bucket auger.

Initially the ground truth depth measurements were to be used in statistical comparisons of the blind test GPR interpretations. However, upon processing and inspection of the GPR imagery collected at the Milan Experiment Station, this method was found to be unfeasible. Though the GPR operator could discern when he was or was not viewing an image that represented a fragipan, all reflectors in the images were relatively flat. The flat reflectors observed within the GPR images representing the area containing a fragipan disagreed with ground truth interpretations made by Dr. Donald D.

Tyler, which revealed a relatively high degree of variability in depth to the uppermost boundary of the fragipan horizons.

Due to these findings, the blind test design was amended to test the interpreter on his ability to determine, by the characteristics of the image, if a fragipan was present and not take into account the precise depth of the fragipan. The GPR data used for this blind test were the same data collected for the original design. The data were prepared for the blind test by cutting and/or reversing sections of data from each original file and renaming that data under different filenames. The renamed files were then presented to the interpreter. A total of 20 GPR files were presented to the interpreter. Each file contained five markers (100 total points), at which the interpreter made the distinction between:

1 = no fragipan present

2 = transition zone (area of convergence of non-pan and fragipan horizons)

3 = fragipan horizon present

Main Research Plot Data Collection

The main research plots of this project were located at two different University of Tennessee experiment stations. The two research plots located at The Plateau Experiment Station had dimensions of 40 m by 100 m. The two plots located at The Milan Experiment Station had dimensions of 60 m by 120 m. Survey transect spacing for all research plots was 5 m along the 40 and 60-m edges, and 10 m along the 100- and 120-m edges.

The GPR data collected at the Plateau Experiment Station were collected on April 2, 1998 using a 200-MHz (GSSI Model 5106) antenna. These data were collected using a Massey Ferguson Model 290 tractor with a small towed flat bed trailer. The trailer was used to stabilize the GPR mainframe and power source equipment, and also to give the unit mobility within the field. The 200-MHz antenna was attached to the rear of the trailer and was aligned at approximately 0.50 m from the flag markers while being pulled along each transect.

Each transect was sampled twice (along each side of the transect flags) with the GPR unit. The first replication for each transect began at the south end of each plot heading in a northeasterly direction with the second replication starting at the end of the first and heading in the reverse direction on the opposite side of the survey flags. This method of sampling was used for both research plots located at the Plateau Experiment Station.

Data sets were collected at the Milan Experiment Station on June 17 and 18, 1998. These data were also collected using a 200-MHz (GSSI Model 5106) antenna. Data collection techniques were generally identical to those used at the Plateau Experiment Station. Each transect was sampled twice in the method already explained.

Data collection at this site began on the southern most point of the plots heading in a northwesterly direction, with subsequent files reversing direction on the opposite side of the survey flags. Data obtained at this site employed the same mobilization techniques as the data acquired at the Plateau Experiment Station; however, due to differing soil conditions, GPR system settings were not the same.

Research Plot Image Interpretations

Plateau Experiment Station

GPR data were collected on the primary research plots located at the Plateau Experiment Station on April 2, 1998. Interpretations of these GPR data were made using the same methodology implemented while interpreting the blind test data that were also gathered on the Cumberland Plateau. GPR system settings used while collecting these data were also very similar to those used in the blind test data collection. However, due to small changes in soil-water content and site location, gain levels had to be slightly adjusted at each site. As with transects 3 and 4 in the blind test data, the bedrock surface within the research plots was interpreted at the solid interface underlying the broken reflectors.

GPR interpretations of the research plots revealed a high degree of variability in depth to the bedrock interface. Of the two plots, plot 1 contained the largest area of soils that were shallow due to the bedrock surface. An area in the northwest region of plot 1 constituted the majority of shallow soils in that plot; however, the eastern edge of the plot was also shallow at the very ends of the transects (Figure 3.4). Also, prior to the GPR survey, station personnel had pointed out a general area of the plot that coincided with the interpreted shallow region in the northwest section, as having historically low yields as compared to the rest of the field. Low yields were also observed in that section of the field when yield values were recorded as the research team harvested the snap bean crop.

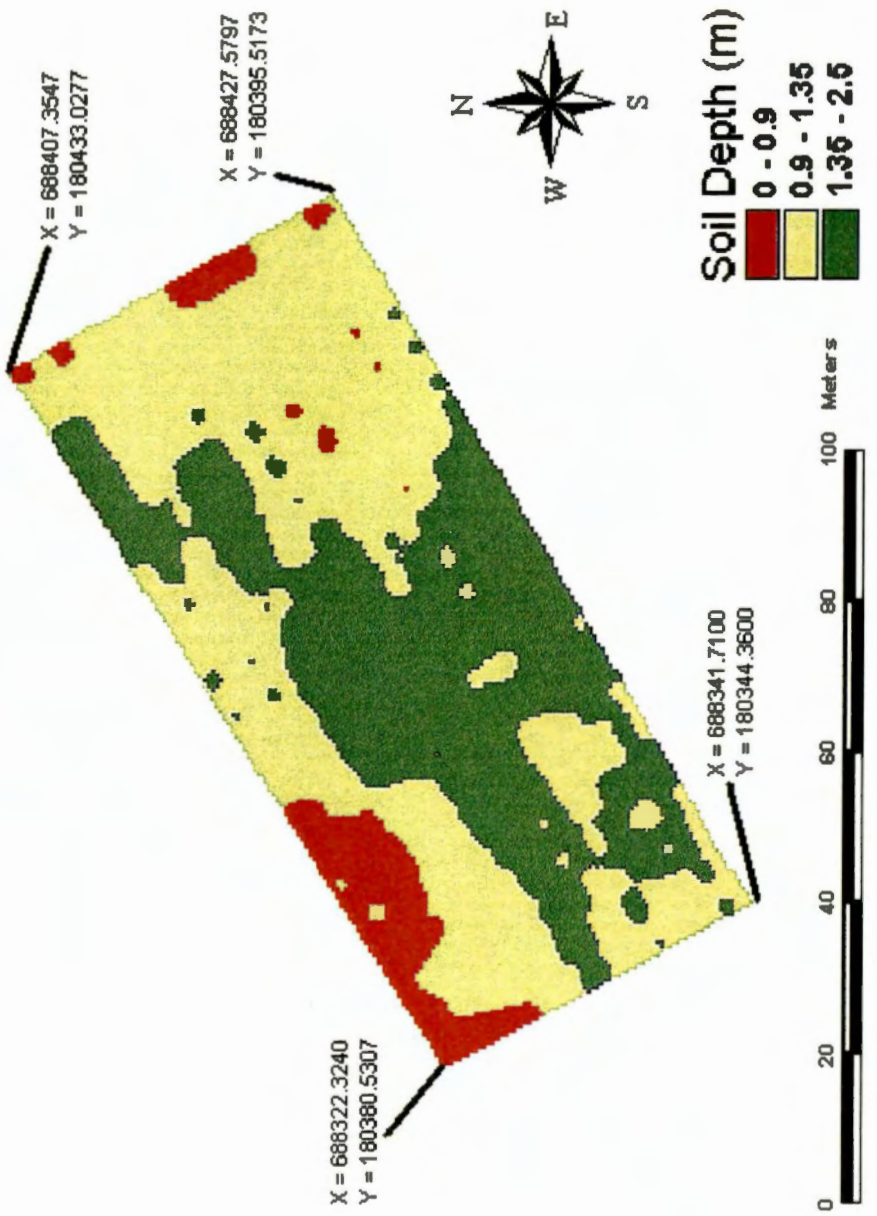


Figure 3.4: Interpreted depth of soil above sandstone bedrock observed on research plot 1 at the Plateau Experiment Station (coordinates are in State Plane 1927 projection).

Interpretations of the bedrock surface-underlying plot 2 also revealed variability in terms of depth to the bedrock interface. Again, these data were interpreted at the solid interface underlying the broken reflectors in the soil. Figure 3.5 illustrates the depth of the bedrock surface-underlying plot 2 as interpreted from GPR imagery.

Milan Experiment Station

GPR data were collected on surveyed research plots located within fields A6 and A7 of the Milan Experiment Station on June 17 and 18, 1998. These data were collected along the survey flag transects using the same methodologies that were implemented while collecting data at the research site located on the Cumberland Plateau.

Two complete data sets were collected from both of the research plots located in fields A6 and A7. One data set was collected with the radar range set to 60-nS depth penetration. In other words, any impulse data were recorded that took 60 nS or less to return to the receiving unit within the antenna. The second data set was collected at 40 nS. The research team varied the range settings in an effort to generate two distinctly different sets of GPR data.

The data collected at the 40-ns setting showed greater detail in the upper portions of the images and gave the research team a means by which to view small discrete changes in the medium. The data collected at the 60-nS setting rendered a less detailed image of the medium, but allowed the research team to view the lateral characteristics of the image with greater ease.

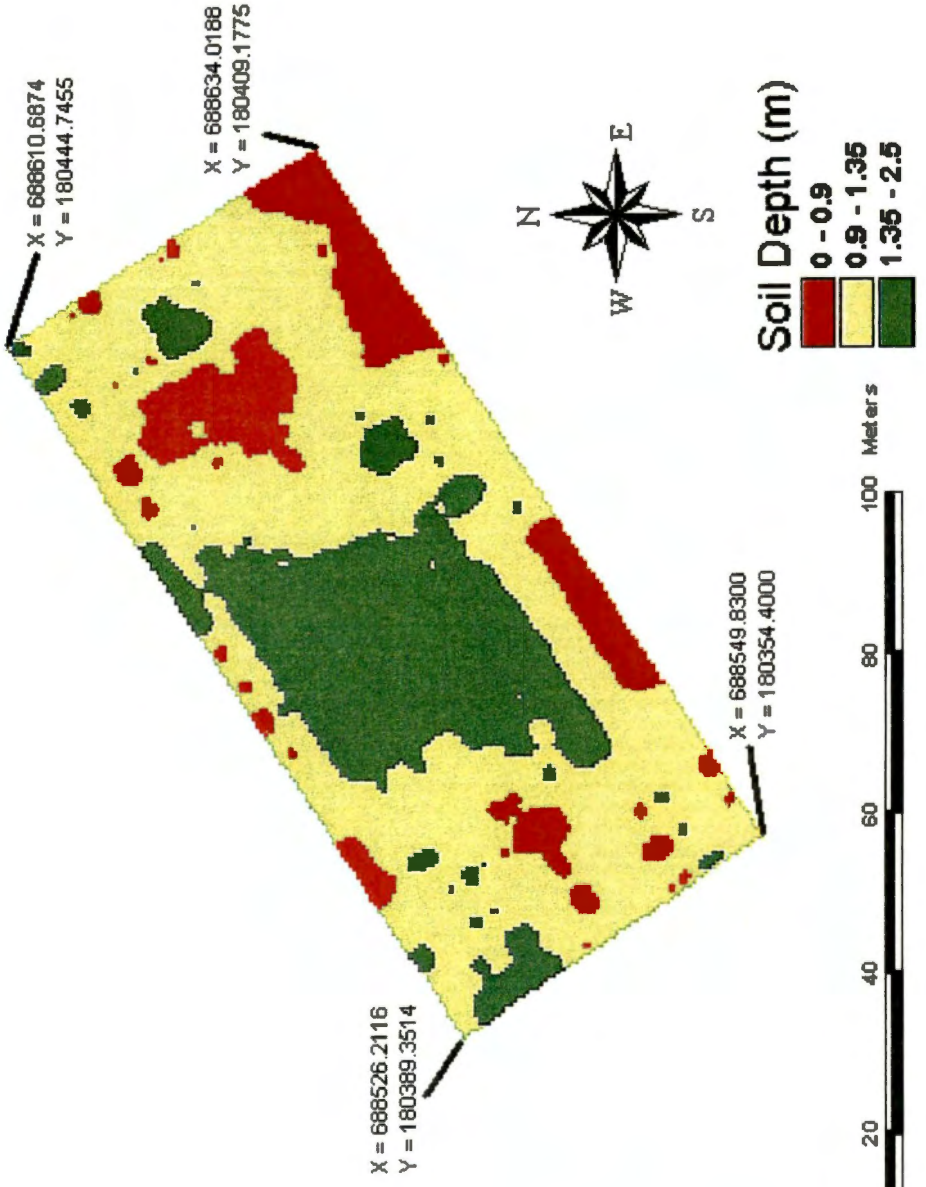


Figure 3.5: Interpreted depth of soil above sandstone bedrock observed on research plot 2 at the Plateau Experiment Station (coordinates are in State Plane 1927 projection).

Further processing (stacking) of the data collected at 60 nS brought the majority of each data file into one viewable screen. This allowed the research team to classify the various patterns that were viewable within the images without having to wait for the data to scroll across the monitor.

Milan Plot Classifications

The GPR imagery collected from fields A6 and A7 were very similar to the blind test data collected from field N47, in that the reflectors were basically flat, and that the characteristics and intensities of the reflectors varied laterally. Therefore, the research team keyed upon the changing characteristics to interpret the data files into classes based upon specific characteristics.

Five different classifications were found within the GPR data collected from plot 1. Each of these classifications was then assigned a value or "soil code", ranging from 1 to 5. The interpretation of each soil code was based first upon the type of primary reflectors present in the image. Since there were only two types of primary reflectors (flat and irregular) observed in plot 1, the other basis for interpretation became the intensity of whichever reflector was present.

Soil codes 1, 4, and 5 all had flat reflectors (Figures 3.6 and 3.7). The reflectors were generally the same width, and occurred at the same depth throughout each file in which they were present. However, the intensities of the reflections in the lower portions of the data files varied laterally across the image. Since the intensity and signal noise found in the lower sections of the image are directly related to what the waveform

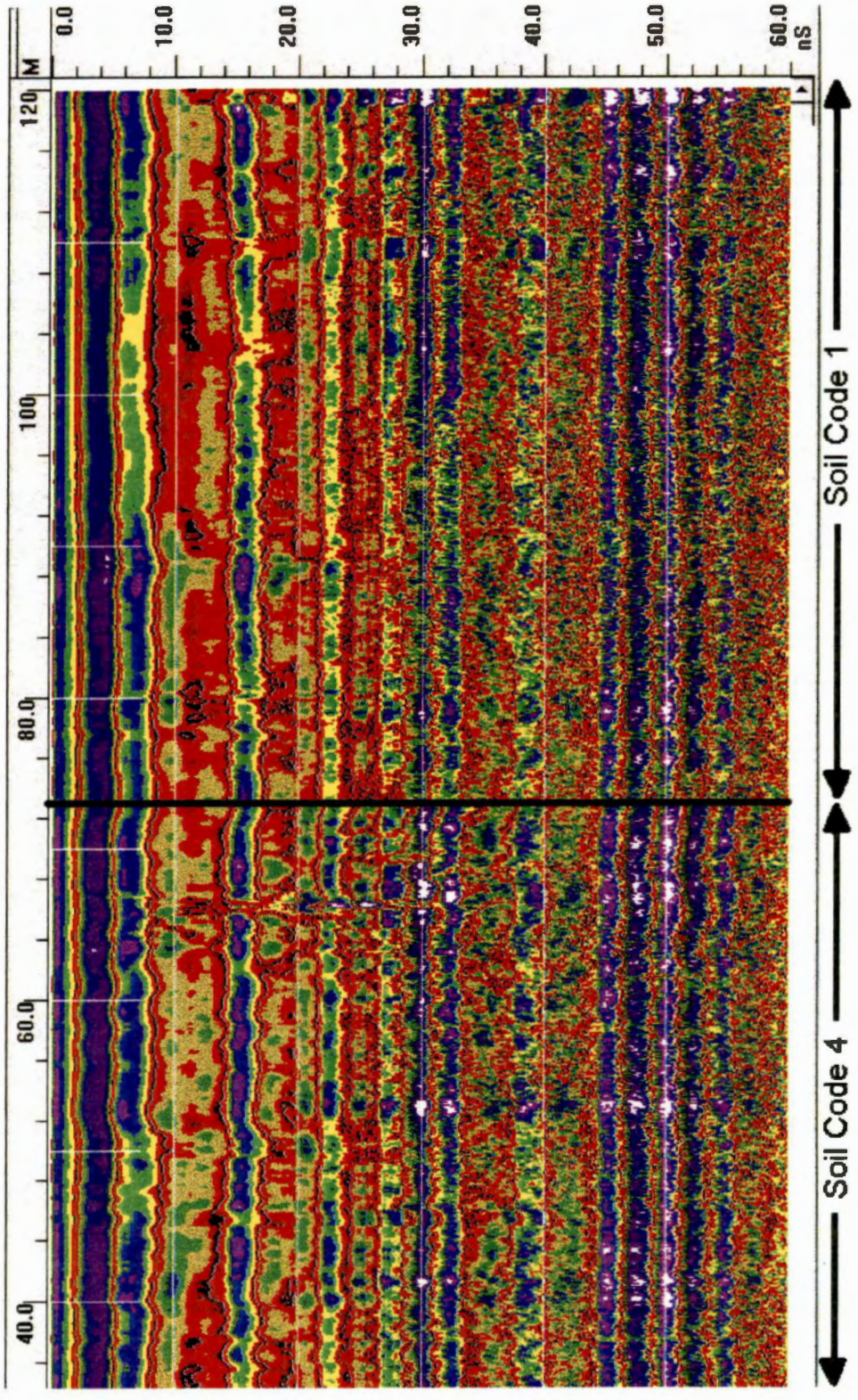


Figure 3.6: GPR image acquired in research plot 1 at the Milan Experiment Station illustrating interpreted "plot 1 soil codes" 1 and 4.

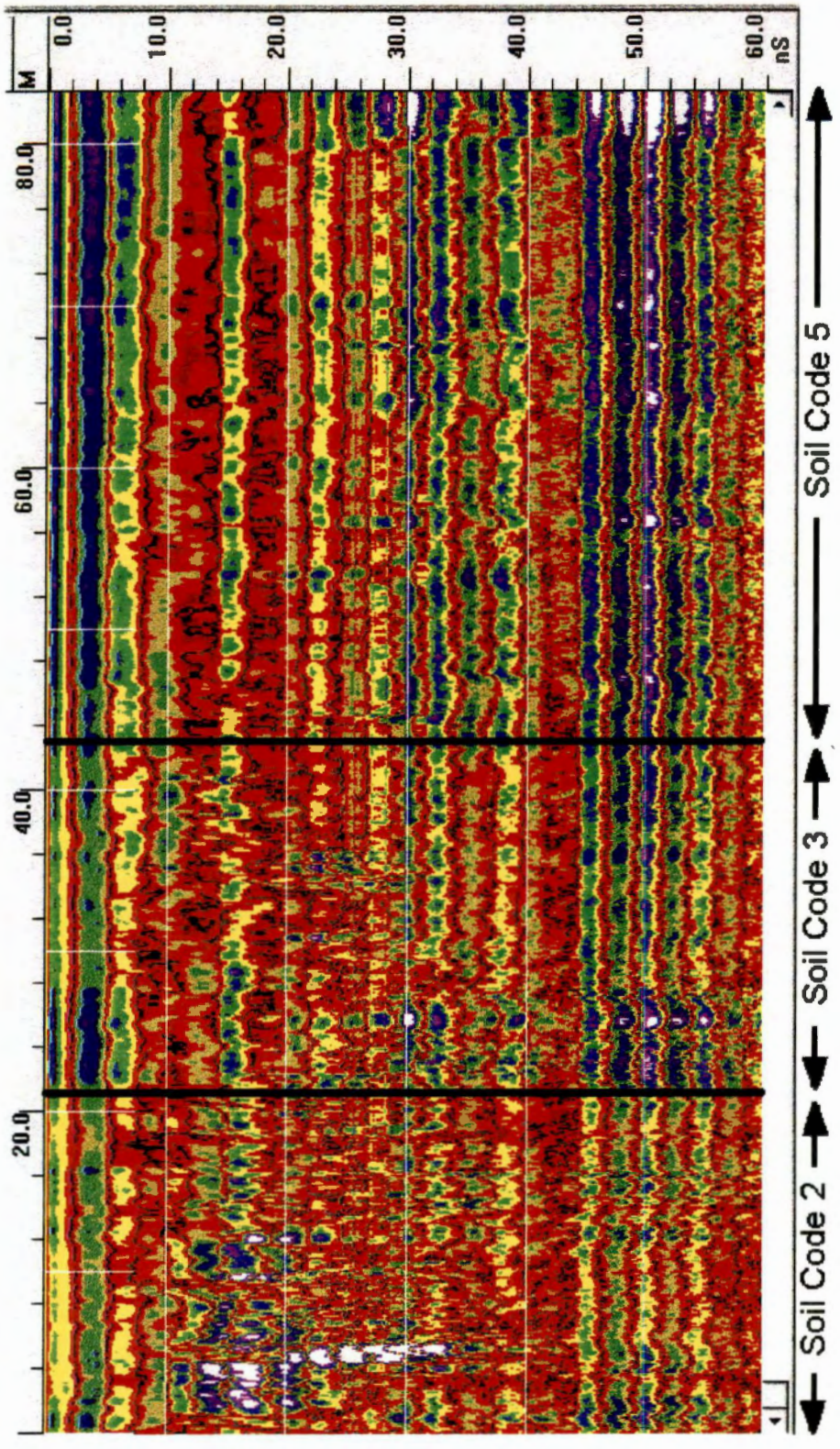


Figure 3.7: GPR image acquired in research plot 1 at the Milan Experiment Station illustrating interpreted "plot 1 soil codes" 2, 3, and 5.

encounters in the upper portion of the image, it was justifiable to classify these intensities separately.

The other type of primary reflector present in plot 1 had characteristics totally unlike that found in soil codes 1, 4, and 5. These reflectors were much more irregular in the upper portions of the images, and did not remain flat throughout the length of the data files. However, like the flat reflectors, this irregular type also contained areas of varying signal intensities. Soil codes 2 and 3, which contained the irregular reflectors, were classified separately due to the differences in intensity of the reflectors found in the upper portions of the images (Figure 3.7).

The GPR data collected from plot 2 were interpreted in the same manner as the data collected from plot 1. However, unlike the imagery obtained in plot 1, these data contained three primary types of reflectors (flat, irregular, and sloping). Therefore, seven different image types (soil codes) were identified from plot 2.

Soil codes 1, 5, 6, and 7 all contained reflectors that were flat, while soil code 2 contained irregular reflectors, and codes 3 and 4 contained sloping reflectors in the upper portions of the images (Figures 3.8 and 3.9). Again, the separations were made within primary reflector types due to the intensity and signal noise observed in the lower portions of the imagery.

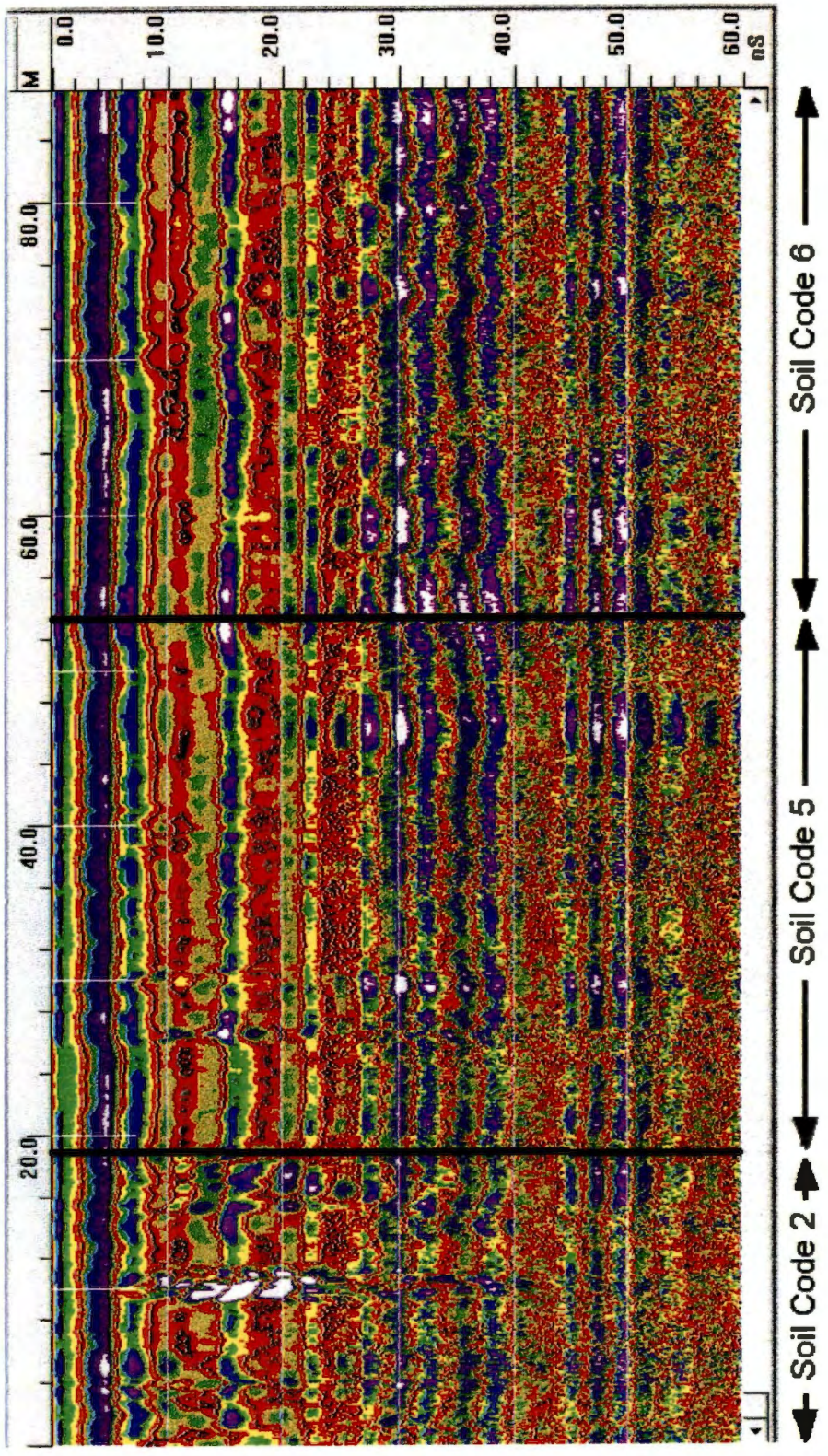


Figure 3.8: GPR image acquired in research plot 2 at the Milan Experiment Station illustrating interpreted "plot 2 soil codes" 2, 5, and 6.

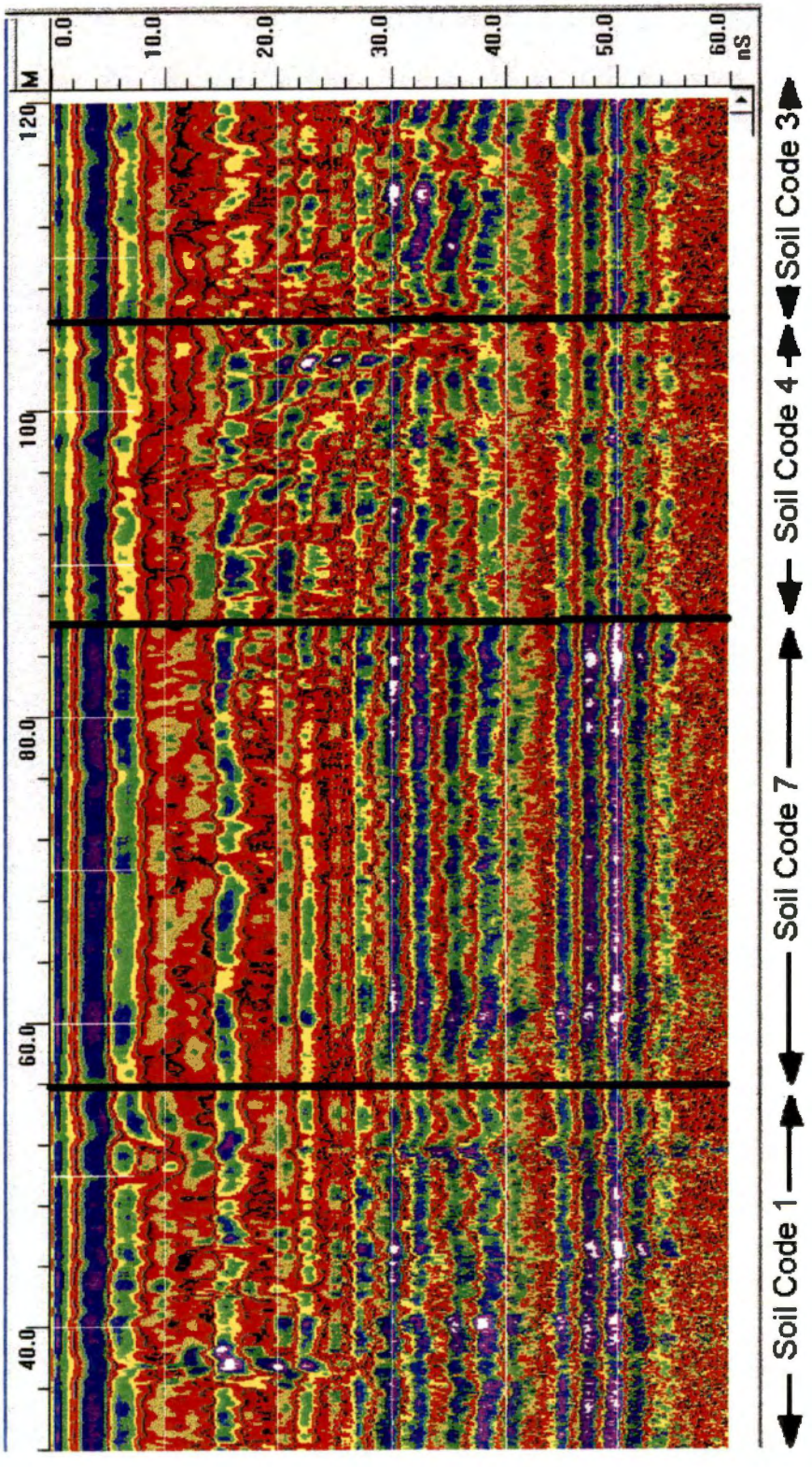


Figure 3.9: GPR image acquired in research plot 2 at the Milan Experiment Station illustrating interpreted "plot 2 soil codes" 1, 3, 4, and 7.

Crop Yield Data Collection

Plateau Experiment Station

Snap bean yield data were collected on plots 2 and 1 at the Plateau Experiment Station on August 10 and 19, 1998 respectively. Vegetable crops and beef cattle productions are the primary areas researched at the Plateau Experiment Station. Therefore, the necessary equipment to conduct on the go yield collection was not available to the research team. To compensate for the lack of "high-tech" equipment, the research team designed a method to collect the yield data using a PixAll one-row bean picker pulled by a Massey Ferguson Model 290 tractor (Figure 3.10).

Since the picker was capable of harvesting only one row at time, the design included collecting the beans in buckets as they fell from the conveyer belt onto the platform. To mark the area represented by one bucket, a member of the research team placed a survey flag in the center of the row when beans began falling in the bucket. When a bucket became full, it was replaced by an empty one, and another flag was placed in the row at that point. When the picker reached the end of a row and beans ceased to fall into the last bucket, a final flag was placed at that point. Each bucket was then weighed using calibrated electronic scales.

The center point of each area within the rows represented by survey flags was georeferenced using a Trimble AgGPS Model 132 receiver. These data were collected in real-time DGPS mode by subscribing to a commercially available base station that automatically corrected errors in the data as it was being collected.



Figure 3.10: Tractor and Pixall bean picker used to collect snap bean yields at the Plateau Experiment Station.

By converting the distances measured between survey flags from latitude and longitude to meters, an area representing the yield weight for each bucket could be calculated in the lab. Once an area and weight were established, yield values were calculated in a spreadsheet to kilograms per hectare.

Once these calculations had been made, the yield values were then matched to the correct latitude and longitude coordinates. These processing steps formatted the data to a sufficient level that the values could then be imported into the GIS software, and be used to generate yield maps of the plots.

Milan Experiment Station

Corn yield data collected on fields A6 and A7 at the Milan Experiment Station were collected on September 16 and 17, 1997. Since much of the research conducted at the Milan Experiment Station involved no-till research on row-crop cultivars, the necessary equipment was available to collect the data using tried and proven yield data collection methods. A John Deere Model 4425 combine implemented with a four-row corn header was used to harvest the crop. The combine was equipped with an AgLeader 2000 yield monitor inside the cab, and a GPS receiver was installed on the combine to transmit positional data to the yield monitor. Data from the GPS receiver and the yield monitor were recorded every second, and were written to a PCMCIA data card for archiving.

The yield monitor used in this study was the AgLeader 2000, which is manufactured by AgLeader Technology Inc. of Ames, IA. To determine yield rates, a load sensor device located just past the top of the clean-grain elevator measured the mass

flow rate of the grain. The mass flow rate was calculated by quantifying the force resulting from the grain impacting the load sensor. In addition, grain moisture was electrically measured during harvest with an on-board moisture sensor.

The GPS equipment used to georeference the yield data for this project was the Trimble AgGPS Model 122 receiver manufactured by Trimble Navigation. All data were collected using real-time DGPS. The correction signal used to correct these data was received from the Coast Guard Beacon located in Memphis, Tennessee (details explained in Chapter 1).

Chapter 4

Results and Discussion

Calibration Data Results

Ames Plantation

Results of the calibration data acquired at the Ames Plantation site included:

1. Determination of the average σ for the soil using equation 1.1.
2. Analysis of 3-D GPR imagery.
3. Analysis of the CDP method of calculating average σ.

Calibration processes used at the Ames Plantation site consisted of dragging the antenna over a buried PVC pipe that generated a hyperbolic form in the GPR image (Figure 4.1). From the known depth of the PVC pipe, a σ of 13 was calculated for the soil using equation 1.1. Once the σ had been calculated, depths to targeted soil horizons that occurred beneath the surface of the Centennial Plot were interpreted in the lab using the radar images (Figure 4.1).

The research team tested the 3-D method of data presentation at the Ames Plantation site in an effort to determine if 3-D imagery would allow for more accurate interpretations of data in subsequent research plots. Figure 4.2 is a 3-D GPR image of the Centennial Plot generated in the RADAN for Windows software.

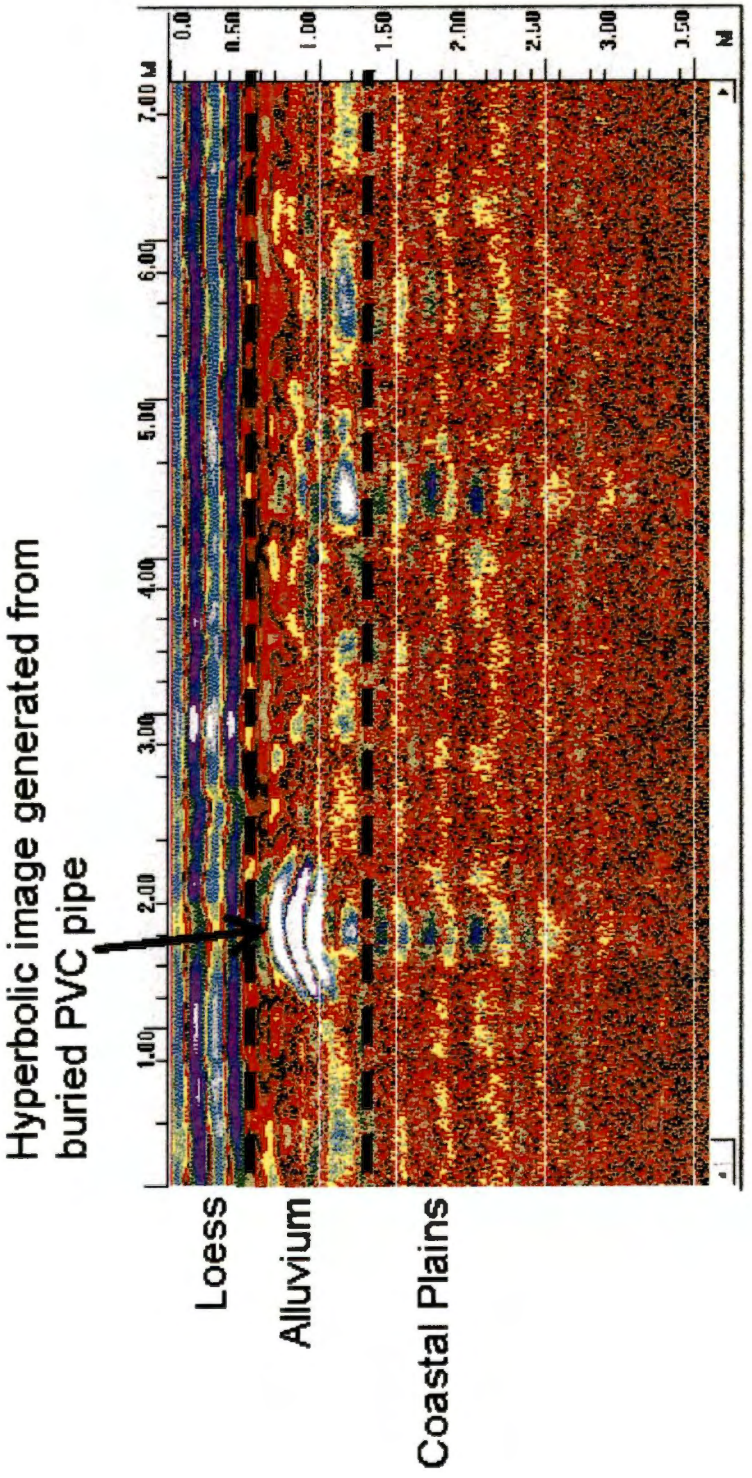


Figure 4.1: GPR image showing hyperbolic reflection of PVC pipe and depths of the loess/alluvium interface and the coastal plains interface.

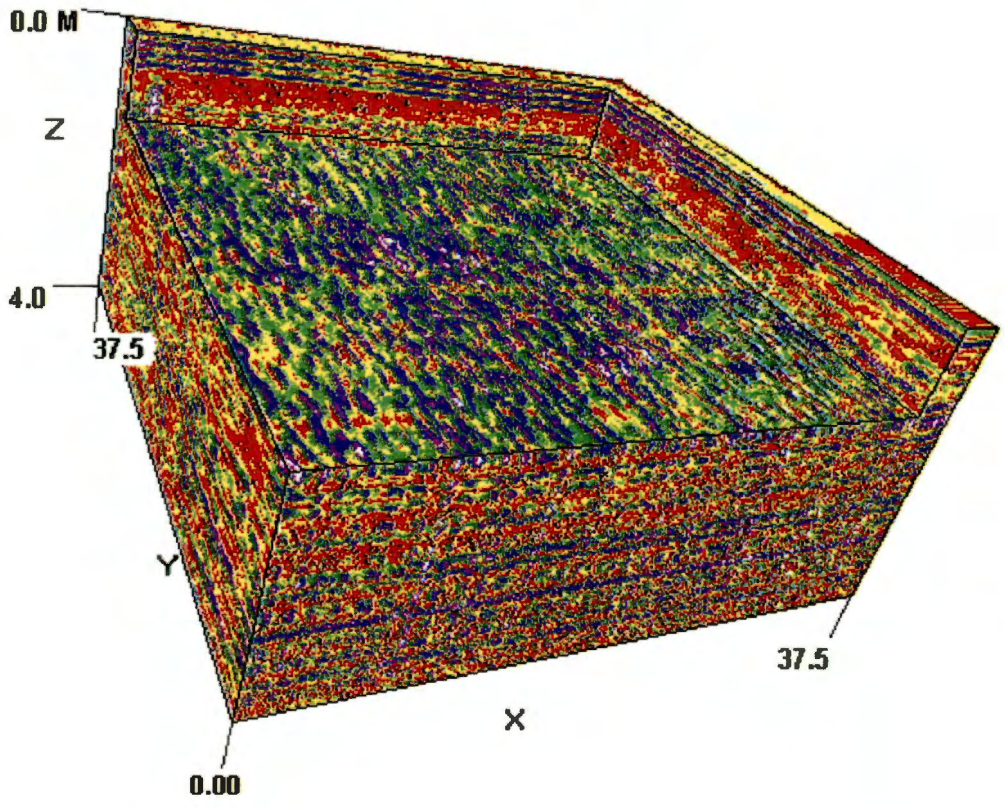


Figure 4.2: Three-dimensional GPR image of the Centennial Plot (Ames Plantation, Grand Junction, TN).

Analysis of this imagery revealed the 3-D method of displaying data using the RADAN for Windows software to be difficult to interpret. These difficulties were primarily due to file size. To convert the 2-D files to 3-D images, the file size had to be drastically reduced to conform to the maximum number of scans allowed per 3-D file by the software. When the images were shortened to conform to the size required, the image characteristics became distorted and difficult to see. Another problem associated with interpreting the data was the inability of the software to rotate or zoom in and out while displaying the image. Due to these inefficiencies, the research team focused on 2-D imagery throughout the remainder of the study.

The Common Depth Point (CDP) method of determining the average σ of the soil was also tested at the Ames Plantation site. Results of these data indicated the CDP method of determining average σ to be just as accurate as using equation 1.1. However, since ground truth measurements were acquired in most cases and because the research team didn't have access to a second antenna at all times, equation 1.1 was used to determine the average σ when the depth of a specific interface within the GPR imagery was required.

Plateau Experiment Station

Calibration data taken at the Plateau Experiment Station were acquired on the grounds of the Clyde York 4-H Camp. These data sets were primarily collected to determine optimal antenna settings (Table 4.1) and to identify targeted soil features of the Cumberland Plateau physiographic region.

TABLE 4.1: GPR calibration settings for Plateau Experiment Station data acquisition.

200 MHz Antenna Model #5106	
Settings	**Value**
Range	40 nS
Number of Gain Settings	5
Gain Settings	15.0
	32.0
	45.0
	53.0
	54.0
Samples per scan	512
Vertical IIR Low Pass Filter	
	N = 2
	F = 1000 MHz
Vertical IIR High Pass Filter	
	N = 2
	F = 100 MHz

TABLE 4.2: GPR calibration settings for Milan Experiment Station data acquisition.

200 MHz Antenna Model #5106	
Settings	**Value**
Range	60 nS
Number of Gain Settings	5
Gain Settings	11.0
	43.0
	60.0
	63.0
	66.1
Samples per scan	512
Vertical IIR Low Pass Filter	
	N = 2
	F = 1000 MHz
Vertical IIR High Pass Filter	
	N = 2
	F = 100 MHz

From the GPR data files collected at the Clyde York 4-H Camp, the research team was able to view GPR imagery of a sandstone bedrock surface. At many of the points within these files, the bedrock surface exemplified a high degree of variation in physical depth. Figure 4.3 is a GPR image collected at the Clyde York 4-H Camp that illustrates the variation of depth to the sandstone bedrock surface observed in these data. Again, equation 1.1 was used to calculate the average σ of the soil.

Milan Experiment Station

Calibration data collected at the Milan Experiment Station were collected in field N47 on October 1, 1997. Prior soil pits located in field N47 confirmed that no fragipan was present on an upland Memphis soil series but that a fragipan was present on a side-slope Grenada soil series. The GPR transect was laid out over an area that covered both the Memphis and Grenada soils. GPR data were acquired along this transect that allowed the research team to view an image that could be associated with fragipan characteristics. Observation of these data files revealed that the characteristics of the images changed dramatically at a point that coincided with the transition between the two soil series (Figure 4.4).

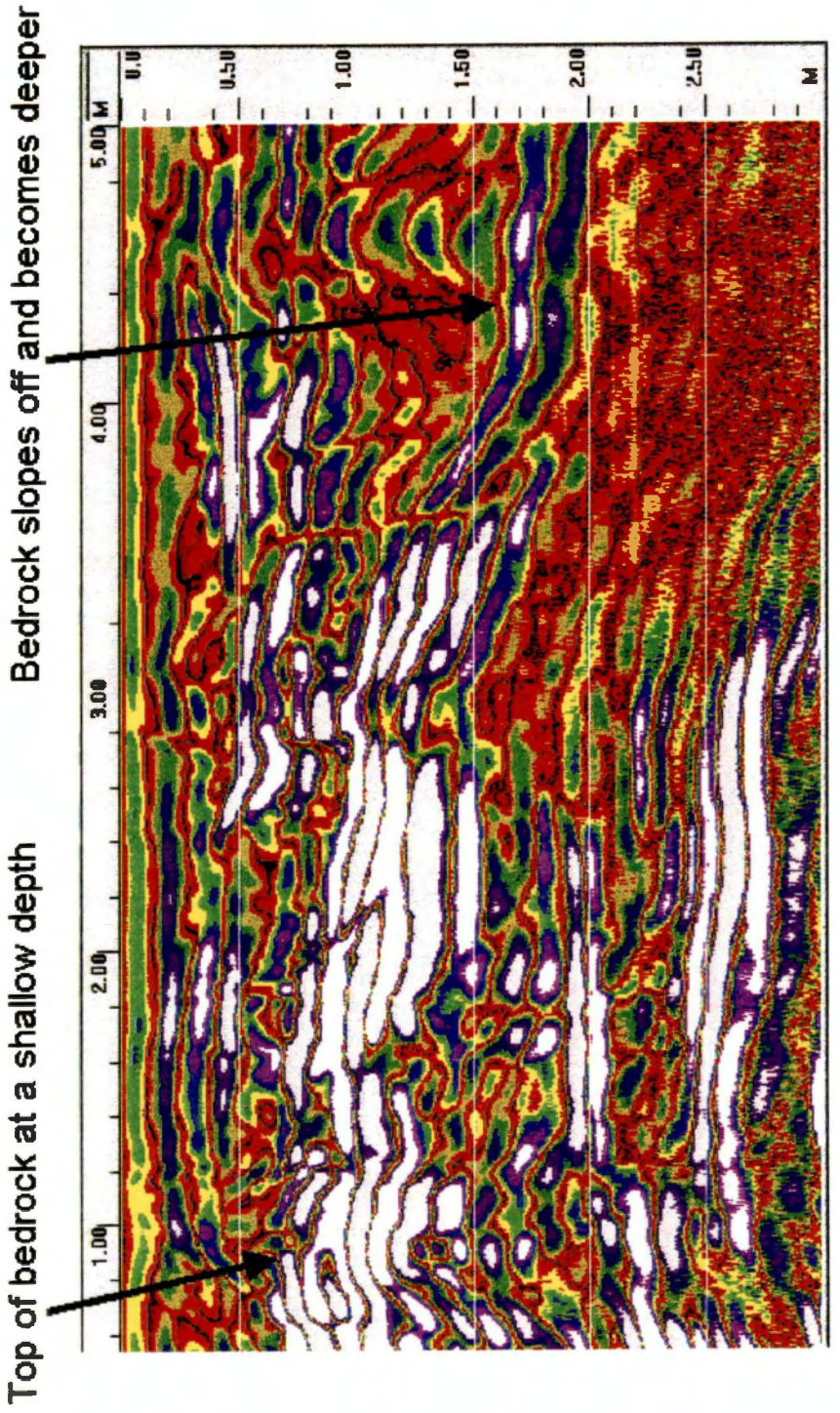


Figure 4.3: GPR image collected on the grounds of the Clyde York 4-H Camp, illustrating the variation of depth to the sandstone bedrock interface.

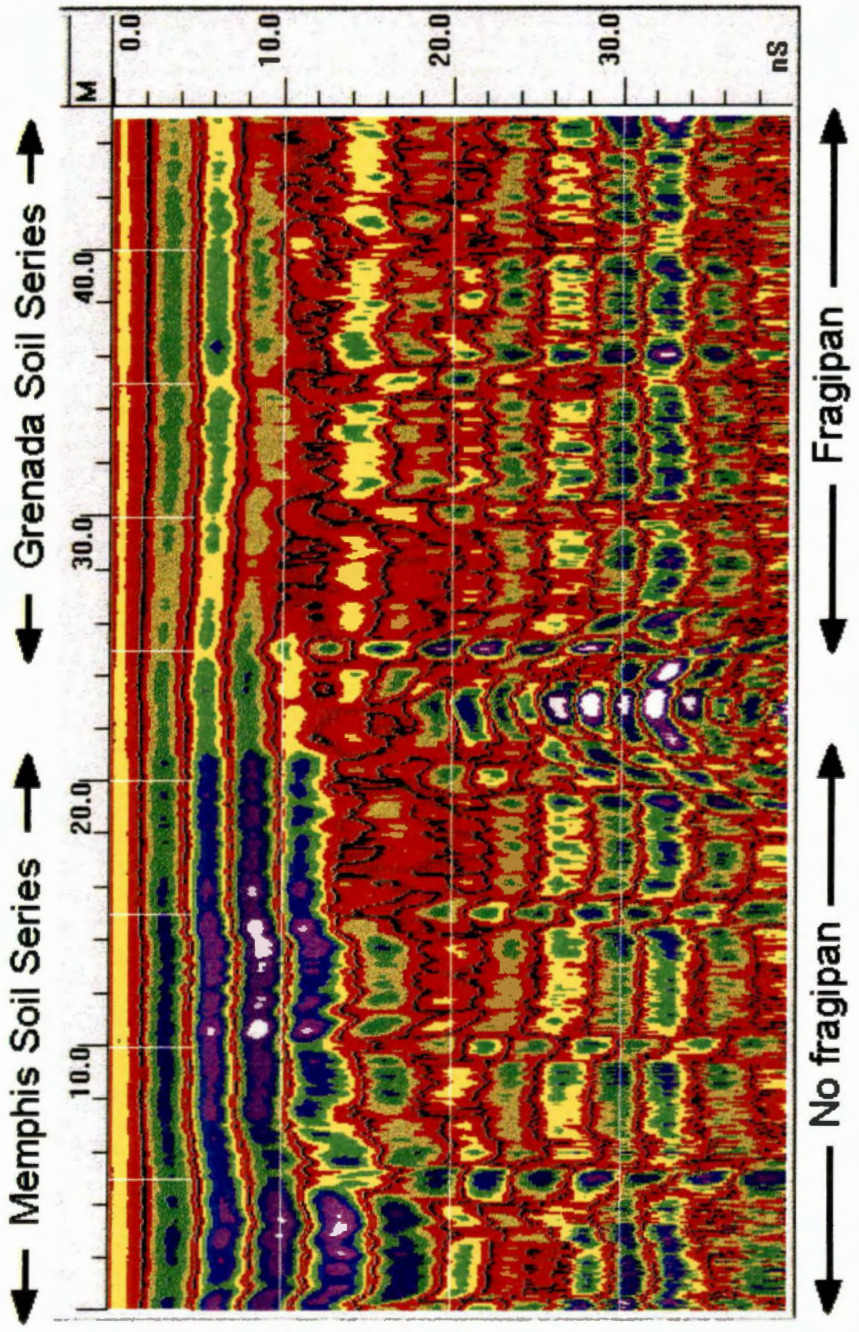


Figure 4.4: GPR image collected in field N47 of the Milan Experiment Station illustrating the change in lateral characteristics that coincide with the occurrence of a fragipan.

Blind Test Results

Plateau Experiment Station

The ground truth measurements and the GPR interpretations that were logged for each blind test transect located at the Plateau Experiment Station are listed in Appendix A1. Out of the four transects surveyed, the bedrock surface in transects 1 and 2 proved to be more difficult to interpret. These images contained reflections in the upper portions of the imagery that were discontinuous and broken. The depth interpretations of the bedrock surface were often made at these discontinuous reflectors in transects 1 and 2 due to their similarity to the reflections that represented bedrock in the calibration data sets.

The bedrock interface in transects 3 and 4; however, were more continuous and thus were interpreted more accurately from GPR imagery. Results from a linear regression model (Table 4.3) illustrate that the continuous reflection within the GPR images represents the actual bedrock surface. The broken reflections observed in the upper portions of the GPR images from transects 1 and 2, that did not agree with ground truth measurements, appear to be pieces of weathered rock suspended in the soil profile (Figure 4.5). Though these pieces of rock or "floaters" were detectable with GPR imagery, they did not impede the penetration of the rock probe used to ground truth the data.

Transect 3 ground truth measurements agreed to +/- 5 cm with GPR interpretations at seven out of the ten observation points (70%), while transect 4 ground truth measurements agreed to +/- 5 cm with GPR interpretations at eight out the ten

observation points (80%). Linear regression results indicated an r^2 value equal to 0.93 for transect 3, while the r^2 value of transect 4 was equal to 0.97 (Table 4.3).

To further insure accuracy and to determine if interpretation results were repeatable, a second individual was also required to interpret the blind test data. The interpretations made by the second individual were then compared to those of the primary interpreter. Results of that comparison were similar to those determined by the primary interpreter. Out of 40 observation points, the second individual's interpretations agreed to within +/- 5 cm of the primary interpreters' interpretations 33 times (82.5%).

Milan Experiment Station

Results of the blind test conducted at the Milan Experiment Station revealed that the primary interpreter was capable of determining, by the lateral characteristics of the images, the difference between an upland Memphis soil series, a Grenada soil series, and an area of transition between those two series. Ground truth data revealed that no fragipan was present on the Memphis soils, but that in most cases a fragipan or fragic characteristics were found on the Grenada soils.

Table 4.4 lists the results of the statistical comparison of the ground truth data and the primary interpreters' results. These data revealed that the GPR interpretations agreed with ground truth data at 95 out of the 100 data points (95%). As illustrated by the bold numbers in Appendix A2, each data point where the data did not agree, represented a disagreement in the location of the transition zone. Though the areas representing the transition zones in the GPR files generated very similar images, ground truth

measurements did not agree with GPR imagery in areas of the transition zone at all times, which explained the errors in interpretations.

These data were also tested for accuracy and repeatability by presenting the GPR data files to a second individual for interpretation. Comparisons of the primary interpreters' results and the results obtained by the second individual showed that they agreed at 97 out of the 100 points (97%) (Table 4.4). A list of all of these interpretations can be found in Appendix A2.

TABLE 4.3: Blind test results from the Plateau Experiment Station Site.

	Linear Regression Output	
Transect #	**Primary Interpreter r^2**	**% Agreement of Secondary Interpreter**
1	0.139	100%
2	0.523	80%
3	0.934	90%
4	0.975	60%

TABLE 4.4: Blind test results from the Milan Experiment Station Site.

	Linear Regression Output	
Transect #	**Primary Interpreter r^2**	**% Agreement of Secondary Interpreter**
1 - 20	0.925	97%

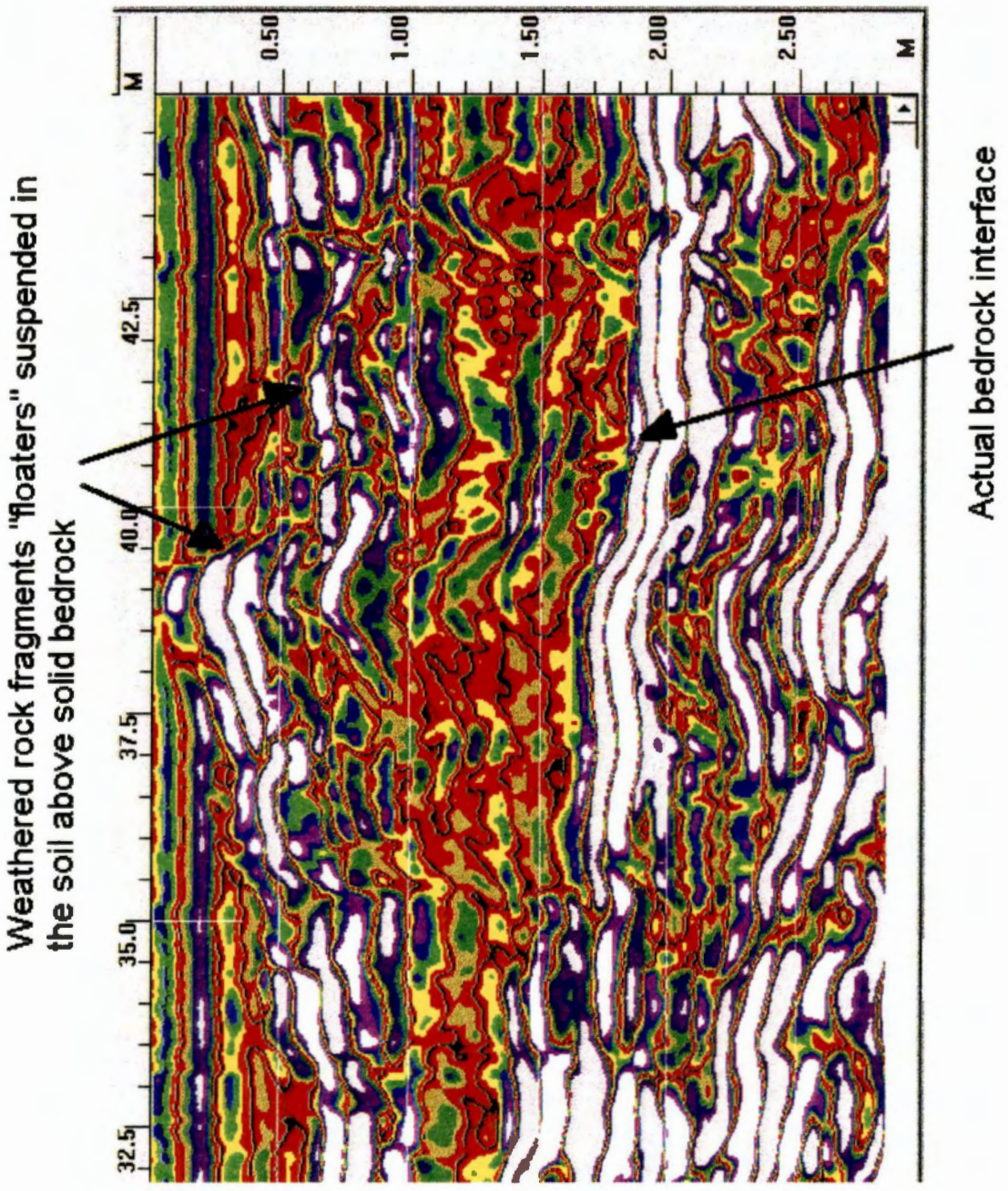


Figure 4.5: GPR image illustrating "floaters" encountered above the solid sandstone surface during the blind test at the plateau research site.

Crop Yield Results

The average bean yields obtained in each plot located at the Plateau Experiment Station are listed in Table 4.5. The overall yield trend observed in plot 1 at the Plateau Experiment Station is illustrated in Figure 4.6, while the overall yield trend observed in plot 2 is illustrated in Figure 4.7.

The overall yield result of fields A6 and A7 at the Milan Experiment Station and the relative locations of research plots 1 and 2 are shown in Figure 3.2. The average corn yield obtained in these fields was 8221 kilograms per hectare.

TABLE 4.5: Snap bean yield data obtained on plot 1 and plot 2 at the Plateau Experiment Station Site.

Plots 1 and 2, Plateau Experiment Station

Plot No.	No. of observations	CV%	Average Yield
1	409	29.12	9209 kg/ha
2	387	19.14	9165 kg/ha

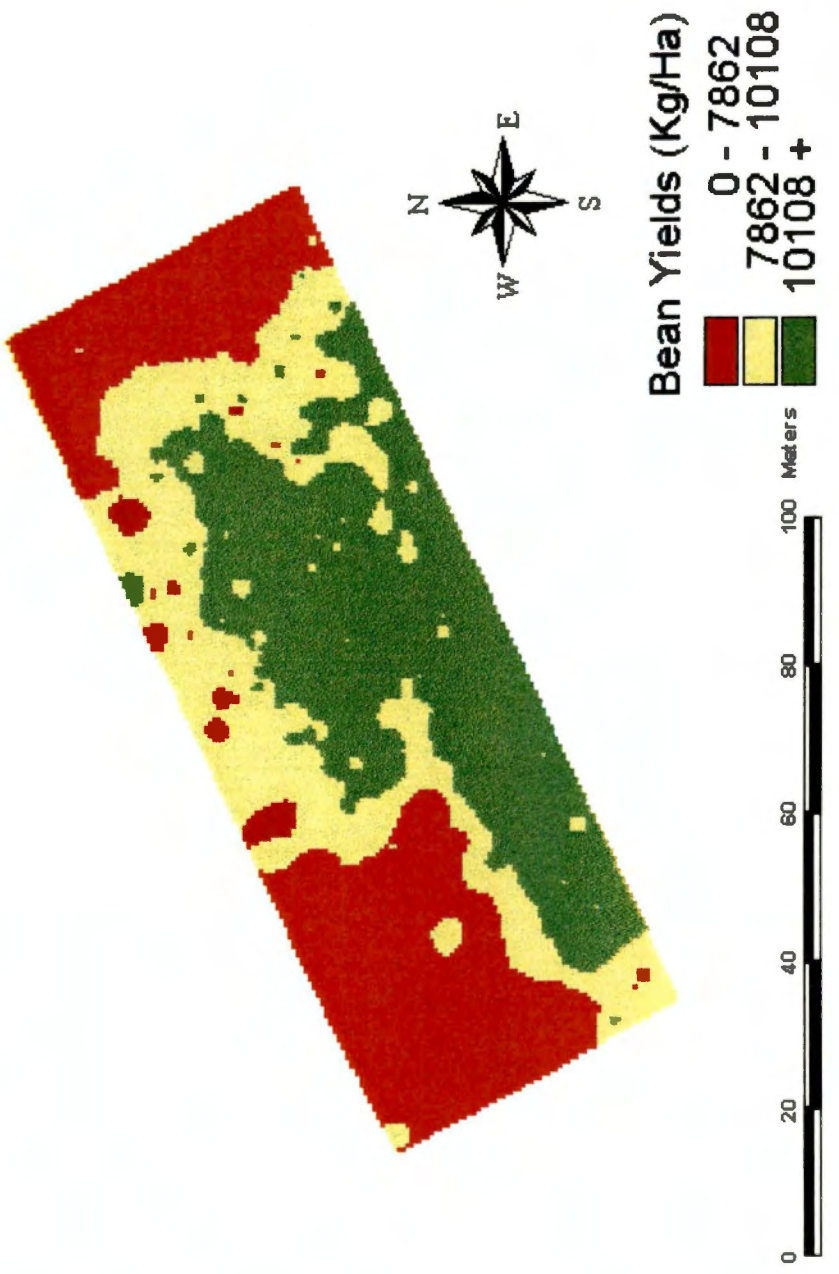


Figure 4.6: Snap bean yield trends observed in plot 1 at the Plateau Experiment Station.

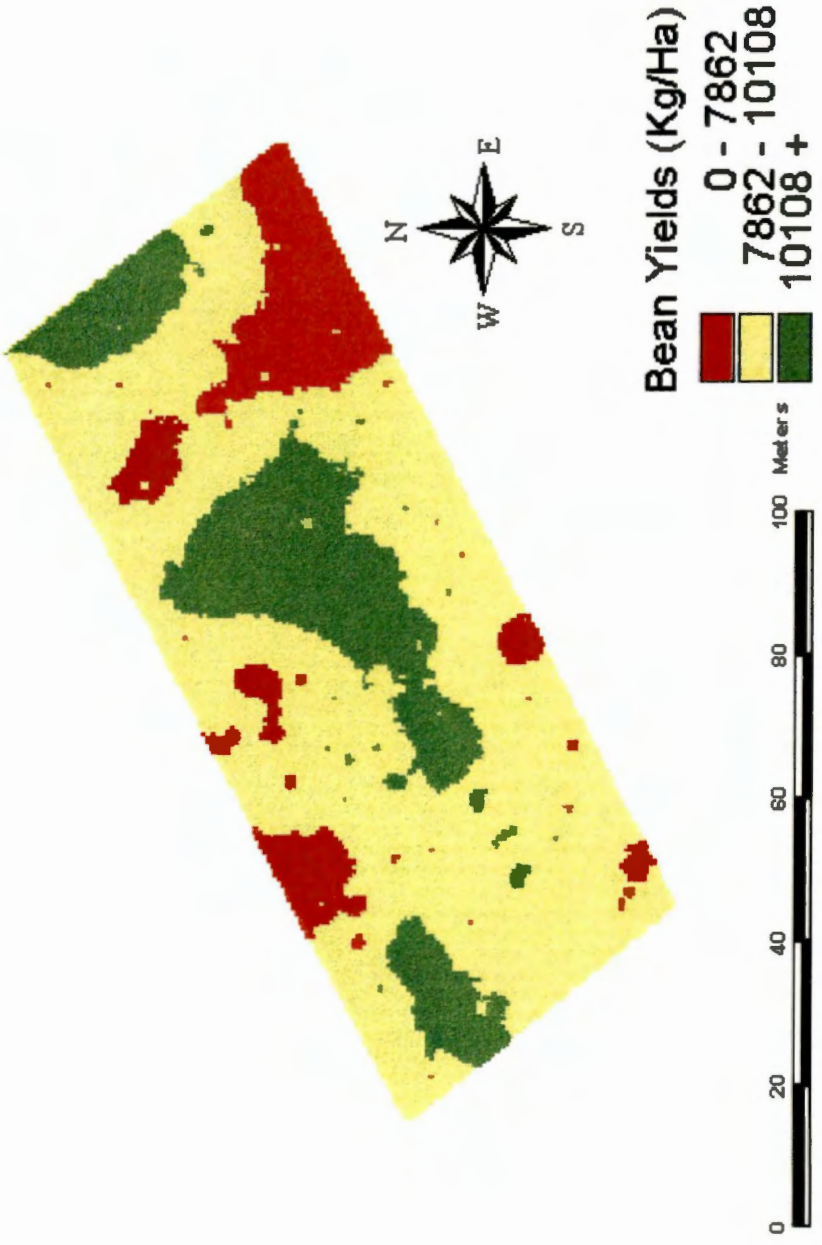


Figure 4.7: Snap bean yield trends observed in plot 2 at the Plateau Experiment Station.

Statistical Comparison of GPR Interpretations to Crop Yields

Though the images generated in the ArcView™ GIS software revealed trends in the GPR interpretations that were similar to crop yield data, statistical comparisons were needed to validate those trends. Before statistical analyses were conducted on these data, each data set was first examined for any discrepancies in the data. These discrepancies included incorrect positioning data, and false yield values generated during yield collection.

Plateau Experiment Station

Plot 1

Results of the comparison between the soil data and crop yield values obtained in plot 1 revealed a Pearson Correlation Coefficient of 0.49. According to the Experiment Station statistician, this was "fair" for biological data that was taking into account only one variable (i.e., soil depth) for comparisons (Saxton, 1998). Perhaps the most significant data rendered from the statistical analysis were the Least Squares Means (i.e., mean yield per soil code). The Least Squares Means and the Coefficient of Variance values for each soil code from plot 1 are listed in Table 4.6. The SAS® output from these data files are also listed in Appendix D1.

Plot 2

Statistical analysis of the data obtained in plot 2 revealed a trend much like that found in plot 1. The Pearson Correlation Coefficient of plot 2 was found to be 0.30,

which was slightly lower than the coefficient found in plot 1. Observations of the Least Squares Means revealed a similar trend as well. The Least Squares Means and Coefficient of Variance values for each soil code in plot 2 are also listed in Table 4.6.

Milan Experiment Station

Plot 1

Figure 4.8 shows the GPR interpretation grid and Figure 4.9 illustrates the yield trends observed in plot 1 at the Milan Experiment Station. Statistical analyses of these data revealed a Pearson Correlation Coefficient of 0.74. Observations of the Least Squares Means for each soil code also revealed a correlative pattern in the data. Table 4.7 lists the Least Squares Means and Coefficient of Variance values for each interpreted soil code found in plot 1. The SAS^{R} output from these data files can be found in Appendix D2.

Plot 2

Results of the statistical analysis of the data in plot 2, which contained seven different identified soil codes, revealed slightly less correlation to yield trends than was found in the plot 1 data. Figure 4.10 shows the GPR interpretation grid and Figure 4.11 illustrates the yield trends observed in plot 2. Statistical analyses of these data revealed a Pearson Correlation Coefficient of 0.60. Table 4.8 lists the Least Squares Means and Coefficient of Variance values obtained for each of the seven soil codes that were identified in plot 2.

TABLE 4.6: Statistical significance of Least Squares Means data obtained in plots 1 and 2 at the Plateau Experiment Station Site.

Statistical Data Per Soil Depth Code			
Plot #	**Soil Code**	**Average Yield**	**CV%**
1			
	1 (0.00 – 0.90 m)	**a** 5346 kg/ha	44.51
	2 (0.90 – 1.35 m)	**b** 8356 kg/ha	29.95
	3 (1.35 m +)	**c** 10557 kg/ha	19.98
2			
	1 (0.00 – 0.90 m)	**a** 7682 kg/ha	21.64
	2 (0.90 – 1.35 m)	**b** 9120 kg/ha	18.79
	3 (1.35 m +)	**c** 9749 kg/ha	15.80

* Soil codes with same letters are not statistically different (P>0.05).

TABLE 4.7: Statistical significance of Least Squares Means data obtained on plot 1 at the Milan Experiment Station Site.

Statistical Data Per Soil Code			
Plot #	**Soil Code**	**Average Yield**	**CV%**
1			
	1	***a** 6025 kg/ha	34.83
	2	***a** 5146 kg/ha	66.24
	3	***b** 8598 kg/ha	19.77
	4	***b** 8284 kg/ha	28.14
	5	**c** 11987 kg/ha	8.68

* Soil codes with same letters are not statistically different (P>0.05).

TABLE 4.8: Statistical significance of Least Squares Means data obtained on plot 2 at the Milan Experiment Station Site.

Statistical Data Per Soil Code			
Plot #	**Soil Code**	**Average Yield**	**CV%**
2			
	1	****a** 7468 kg/ha	22.35
	2	****b** 6213 kg/ha	35.29
	3	**c** 2008 kg/ha	101.86
	4	***d** 9665 kg/ha	12.78
	5	****ab** 7280 kg/ha	26.71
	6	***d** 9916 kg/ha	15.85
	7	**e** 12803 kg/ ha	8.76

* Soil codes with same letters are not statistically different (P>0.05).
** Soil codes 1 and 2 are not statistically different from soil code 5 (P>0.05), but soil codes 1 and 2 are statistically different (P<0.05).

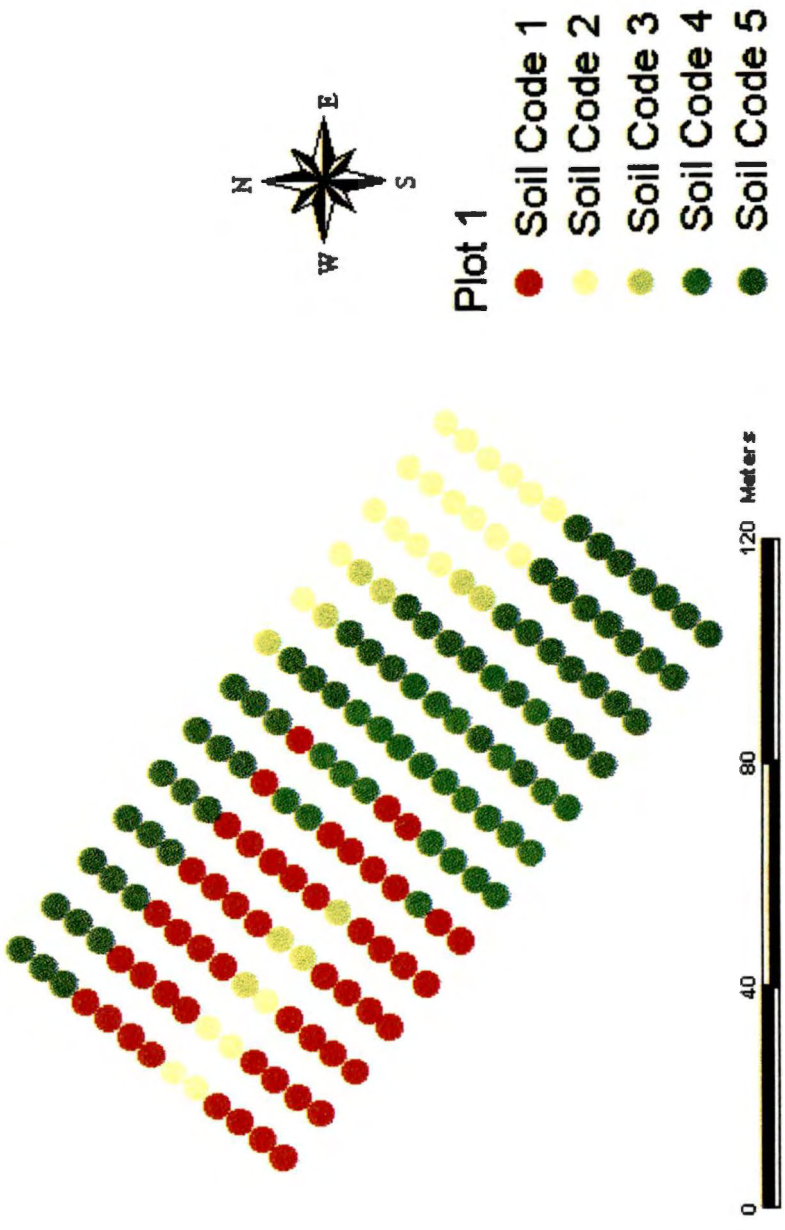


Figure 4.8: GPR grid from plot 1 (Milan Experiment Station) illustrating the interpretations of each data point.

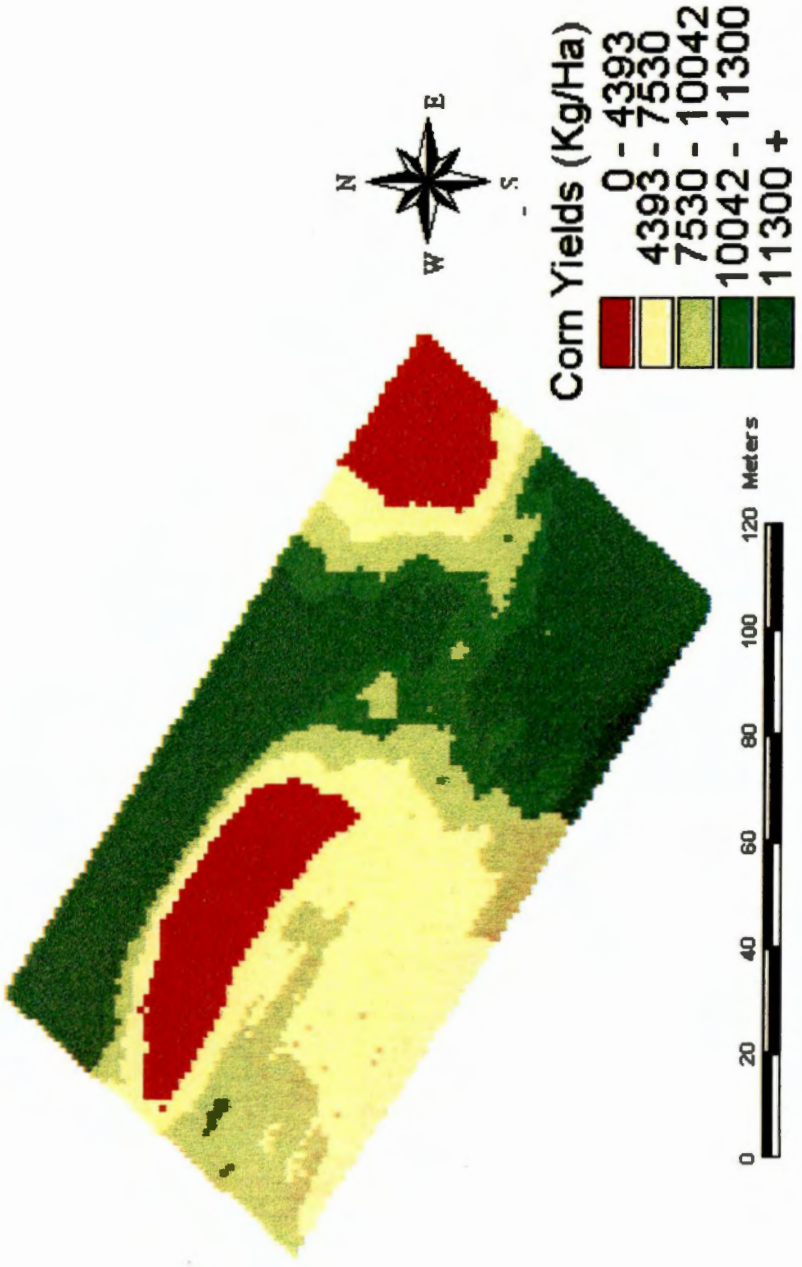


Figure 4.9: Corn yield trends observed in plot 1 at the Milan Experiment Station.

Figure 4.10: GPR grid from plot 2 (Milan Experiment Station) illustrating the interpretations of each data point.

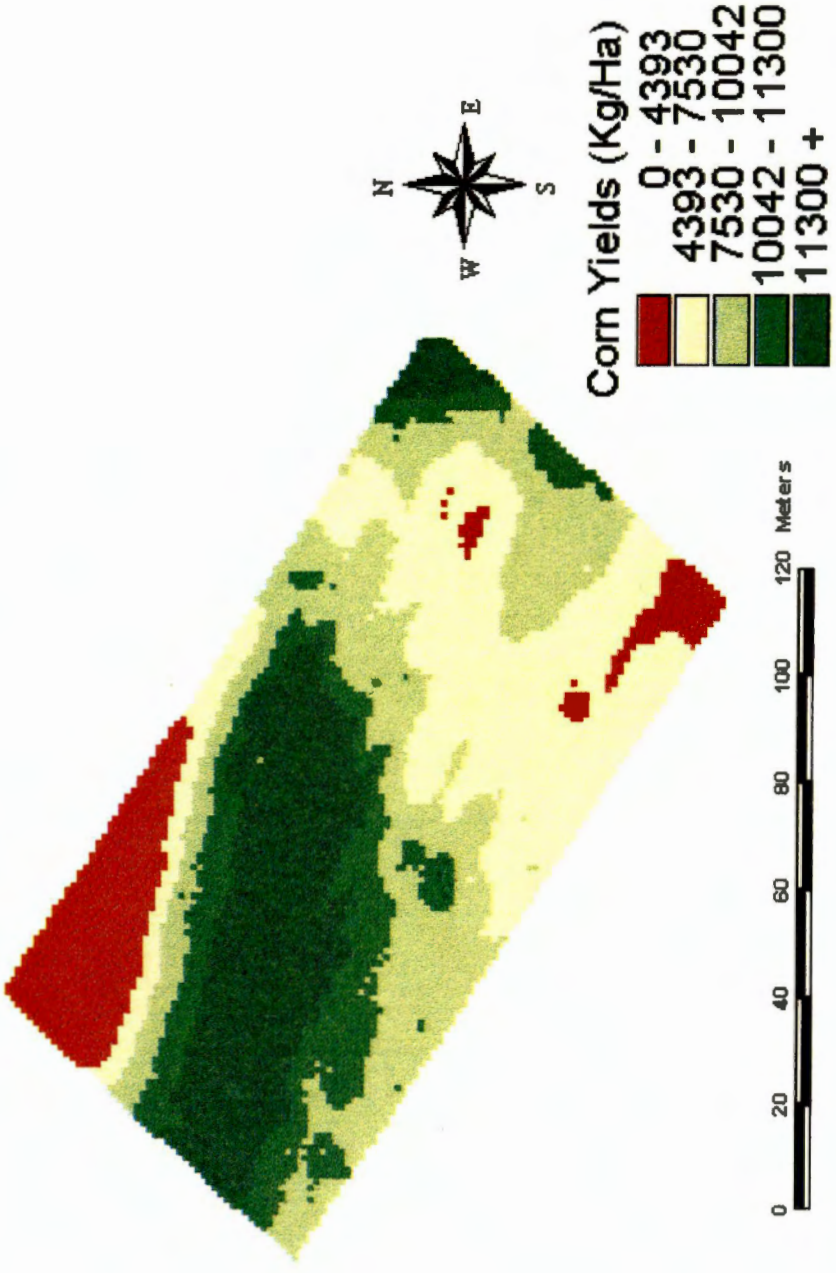


Figure 4.11: Corn yield trends observed in plot 2 at the Milan Experiment Station.

Discussion

Plateau Experiment Station

Statistical analysis of the crop yield values and GPR depth interpretations obtained at the Plateau Experiment Station yielded soil information that may be valuable to both producers and researchers. From the limited amount of data obtained during this project, it appears that the average yields per soil depth code obtained from the Least Squares Means analysis might also be viewed as the yield potential of soils meeting the specified depth criteria. For example, soils of 0.00 – 0.90-m depth could be considered low, soils of 0.90 – 1.35-m depth could be considered medium, and soils of 1.35 m and deeper could be considered high yield potential areas.

This subsurface information obtained from GPR could greatly benefit vegetable crop producers of the Cumberland Plateau by allowing them to quickly and nondestructively determine the soil depth of production fields. Large areas found to be less than 1 m deep could be identified using GPR and taken out of production. By taking these areas of low yield potential out of production, producers could greatly increase the yield potential of the fields they are farming, thus maximizing outputs while reducing the costs of seed, fertilizer, and pesticides.

This information might also benefit research conducted at the Plateau Experiment Station. For example, vegetable crop variety tests could be greatly improved by implementing GPR mapping to determine the yield potential of research tracts based on the depth of the soil above bedrock. Non biased yield trials could then be conducted in soils of homogeneous yield potentials. Thus the variations found between the different varieties would be more realistic and beneficial.

Milan Experiment Station

Though the GPR images collected at the Milan Experiment Station exhibited characteristics that allowed them to be classified into separate codes, future research is needed to determine what soil characteristics the images represent. From the limited amount of data collected in fields A6 and A7, it appears that the characteristics used as criteria to classify the GPR imagery may directly represent characteristics found within the soil as well. Those soil characteristics appear to be specific soil series and/or areas within a soil series classified into subcategories due to differences in the depth of fragipan horizons.

For example, the soil codes that represented the lowest average yield values were soil code 2 in plot 1 and soil code 3 in plot 2. Though the GPR characteristics were different, when the locations of these codes were compared to soil classification maps (Barbosa, 1996), both codes 2 and 3 coincided very closely with soils classified as Collins soil series. Least Squares Means analysis revealed the average yield for soil code 2 in plot 1 to be 5146 kg/ha. The average yield observed for code 3 in plot2 was 2008 kg/ha.

Observations of the soil classification map also revealed a pattern within a specific soil series. For example, the yields associated with soil code 1 in both plots coincided with soils classified as Loring series with a relatively shallow fragipan (30 – 76 cm). The GPR characteristics of soil code 1 were very similar in both plots 1 and 2. The Least Squares Means analysis revealed an average yield of 6025 kg/ha in the code 1 soils of plot 1, and 7468 kg/ha in the code 1 soils of plot 2.

Soil code 5 in plot 1 and code 7 in plot 2 had extremely similar GPR characteristics. When compared to the soil classification maps, these codes coincided very closely with soils classified as Loring series. However, codes 5 and 7 fell in areas classified as having no fragipan present above 92-cm depth. Least Squares Means analysis revealed the average yield for code 5 to be 11987 kg/ha and the average yield for code 7 to be 12803 kg/ha.

These data were also tested to determine if the differences of the Least Squares Means were statistically different ($P>0.05$). This analysis revealed that the average yield found in soil codes 1 and 2 in plot 1 were not statistically different ($P=0.0946$). This test also determined that soil codes 3 and 4 in plot 1 were not statistically different ($P=0.7207$).

Results of the data from plot 2 were different. Soil codes 4 and 6 were not statistically different ($P=0.6538$). Furthermore, soil code 1 was not significantly different from soil code 5 ($P=0.7305$), and soil code 2 was not significantly different from soil code 5 ($P=0.0632$). However, soil codes 1 and 2 were significantly different ($P=0.0328$). Each of these soil codes, average yields, and the probable soil series for each soil code are listed in Table 4.9.

TABLE 4.9: Probable soil series (Barbosa, 1996) and yield potentials of selected soil codes interpreted from GPR data obtained at the Milan Experiment Station.

Probable Soil Series Per Soil Code			
Plot #	**Soil Code**	**Avg. Yield**	**Probable Soil Series**
1			
	1	***a** 6025 kg/ha	Loring, 5-8% slope (fragipan 30 – 50 cm)
	2	***a** 5146 kg/ha	Collins/Falaya/Waverly, 0-2% slope
	3	***b** 8598 kg/ha	Transition Zone
	4	***b** 8284 kg/ha	Loring, 2-5% slope (fragipan 50 – 76 cm)
	5	**c** 11987 kg/ha	Loring, 2-5% slope (no pan above 92 cm)
2			
	1	****a** 7468 kg/ha	Loring, 2-5% slope (fragipan 50 – 76 cm)
	2	****b** 6213 kg/ha	Loring, 5-8% slope (fragipan 50 – 76 cm)
	3	**c** 2008 kg/ha	Collins/Falaya/Waverly, 0-2% slope
	4	***d** 9665 kg/ha	Transition Zone
	5	****ab** 7280 kg/ha	Loring, 2-5% slope (fragipan 0 – 30 cm)
	6	***d** 9916 kg/ha	Grenada, 0-2% slope (fragipan 76 – 92 cm)
	7	**e** 12803 kg/ha	Loring, 2-5% slope (no pan above 92 cm)

* Soil codes with same letters are not statistically different ($P>0.05$).
** Soil codes 1 and 2 are not statistically different from soil code 5 ($P>0.05$), but soil codes 1 and 2 are statistically different ($P<0.05$).

Chapter 5

Recommendations

Data Collection

Environmental Conditions

Over the span of this project, several environmental conditions were encountered that temporarily prohibited the use of the GSSI SIR-10A radar mainframe. Extreme hot or cold conditions had the potential to cause the internal tape drive to drag or stop working completely, thus halting data collection for extended periods of time. Wet weather was also a primary factor that contributed to down time and extended overnight stays in the research areas.

Reduction of this down time would not only increase the amount of data obtained, but could also reduce the costs of research, by limiting time in the field. To overcome these limitations, a new method of transport for the mainframe and power source should be developed that would protect the GPR unit from the environment, while still providing mobility within the field. One approach would be to enclose the rear section of a four or six wheel all terrain vehicle (ATV) and install the GPR equipment within the enclosure. Several commercial models are presently available that possess the room and field mobility to accommodate the GPR mainframe and power source with minimal alterations to the structure of the vehicle.

Survey Techniques

One of the most substantial benefits of using GPR is the ability of the system to collect large amounts of continuous subsurface data. Theoretically, the entire subsurface of a large production field could be mapped using GPR in less than one day, thus greatly reducing the time and costs of manual subsurface data acquisition.

Implementing the above mentioned ATV with a DGPS receiver could effectively reduce time in the field while increasing GPR's ability to collect large amounts of data. Furthermore, research time could be reduced in the area of data processing through implementation of the DGPS. Much lab time was spent processing the positional data acquired for the GPR grids with the Pentax Total Station survey instrument. DGPS positional data could replace the total station data and would require little or no processing at all.

By programming the DGPS and GPR to simultaneously log data points at preset distance increments, much of the processing required to join crop yield data to GPR interpretations would be eliminated. Furthermore, a design of this nature would reduce time in the field by eliminating the need to survey precise grids with the Total Station survey instrument. Elimination of the survey grid's preset boundaries would also be beneficial by allowing for expansion of the research area if data from other areas of the field are needed.

GPR Data Interpretation

The data obtained during the blind test gave much insight into the subjective nature of GPR interpretations. The data obtained at the Plateau Experiment Station were interpreted at discreet points in the GPR imagery that represented the surface of sandstone bedrock. Analyses of the interpretations made by the primary interpreter and the secondary interpreter revealed that discreet depth interpretations were not always repeatable (82.5% repeatability).

The blind test data obtained at the Milan Experiment Station did not take into account discreet depth interpretations. These data were interpreted as image classifications (1, 2, or 3), which took into account the laterally occurring trends in the GPR data files. Analyses of the interpretations made by the primary interpreter and the secondary interpreter revealed the interpretations to be more repeatable than discreet measurements (97% repeatability).

Image classification might be more beneficial than discreet depth measurements in terms of correlating GPR imagery to crop yield trends as well. Though soil depth is a primary factor affecting the yields of most crops, this is the case only if the shallow soil represents an area large enough that the plant root system could not overcome stresses by migrating into areas of deeper soils.

This trend was observed in plot 1 on the Plateau Experiment Station. The largest area represented by soils of less than 0.90-m depth generated the lowest yields of either plot. However, there were discreet measurements of soils that were shallower, but that revealed higher yields because those areas of the plot were surrounded by deeper soils that the root systems had the potential to reach.

Using point source sampling (i.e., discreet depth measurements) to correlate GPR data and crop yield trends may never be statistically proven to a high degree. To determine the true correlative trends of these data, the GPR data should be interpreted by classifications that represent a specific soil type or soil condition that is known to affect crop yields.

Crop Yield Data Collection

In conducting research that compares GPR imagery to crop yield trends, accurate yield and positional data are a necessity. Though the yield data collected for this project fit those criteria at both research locales, a more automated method is needed for future data collection at the Plateau Experiment Station.

The design used to collect yield data at the Plateau Experiment Station required a minimum of eight people and two days to collect data from a plot of approximately one-acre. Implementation of technologies similar to those used at the Milan Experiment Station may be one approach to solving this problem. However, that approach would require new equipment and a great deal of capital investment. A simple and cost effective method of reducing data collection time would be to implement the Pixall bean picker with a DGPS receiver. Positional data and yield data could then be acquired for the flag locations simultaneously, thus reducing time in the field to one day.

Future Research

The initial groundwork phase of correlating GPR imagery with crop yields has been accomplished through the results observed in this research project. Future research is now needed in the area of automation in data collection and processing stages. The first phase of future research should be to conduct a study involving the most prevalent soil units encountered in a specific test area. An in depth study of the soil units and the characteristics of the GPR imagery produced by these units should be conducted. Results of this research might lead to documented image characteristics that are known to represent a specific soil unit or soil condition. These images could then be catalogued to compare with future GPR data.

The next phase of future research could then turn to automating the data processing through pattern recognition programs. Using the catalogued images, programs could be written that would allow a computer to interpret much larger quantities of GPR data than researchers are presently capable of handling.

This type of research would be very beneficial to future GPR use in site-specific agricultural applications. With the capacity to interpret large amounts of data, entire production fields could be mapped and correlated to yield trends while expending a minimum of man-hours and cost to the research institute.

Chapter 6

Summary and Conclusions

The primary objective of this project was to evaluate the ability of GPR to nonintrusively detect subsurface features that affect the productive capacities of agricultural production fields. Completion of this goal was based on the following secondary objectives:

1. Identify soil morphological features within GPR imagery that are known to effect crop yields.
2. Systematically interpret the characteristics of GPR images obtained from primary research plots, and
3. Statistically compare the interpreted characteristics of GPR images with georeferenced yield data.

The first objective was to identify soil features in the respective research areas that were known to effect crop yields. This objective was accomplished at the Ames Plantation, the Milan Experiment Station, and the Plateau Experiment Station during the calibration data collection phase. At these research sites, GPR was used to successfully identify coastal plains sediments, a loess/alluvium interface, a fragipan, and sandstone bedrock.

Calibration and system settings obtained during calibration stages of data collection were later used at both the Plateau Experiment Station and the Milan Experiment Station research sites during data collection from the primary research plots.

The calibration data were used for visual comparison with plot data and the system settings were used to decrease time spent calibrating the instrumentation before data collection in each physiographic region.

The second objective included systematically interpreting the characteristics of the GPR data collected from the primary research plots. This objective was accomplished at both research sites. Interpretations made at the Plateau Experiment Station consisted of discreet depths of the interface that represented sandstone bedrock. These discreet depth interpretations were then separated into depth classes (1 = 0.00 – 0.90 m, 2 = 0.90 – 1.35 m, and 3 = 1.35 m and deeper).

The data collected from the research plots located at the Milan Experiment Station were systematically classified into soil codes based on the laterally occurring characteristics present in the GPR imagery. Plot 1 consisted of five classified soil codes, while seven different soil codes were identified from the data collected in plot 2.

When the GPR interpretations were statistically compared to the georeferenced yield data, results indicated a fair degree of correlation between the data. However, analyses of the Least Squares Means (average yield per interpreted soil code) generated perhaps the most significant statistical data. These statistical comparisons may represent a new method of determining the soil factors that influence the usage of SSF practices. They also represent a foundation for future research in these areas.

Throughout the study GPR was used to effectively and nonintrusively identify soil features that correlated with crop yield trends. Future GPR research in the area of SSF applications should now focus on greater automation. Greater automation in the areas of data collection and data processing would not only decrease time and money

spent in research, but might also allow GPR to be used in other agricultural applications. Those applications could include countywide soil surveys, or the mapping of potential production lands before an area is cleared for production.

Bibliography

Bibliography

Auernhammer, H., M. Demmel, T. Muhr, J. Rottmeier and K. Wild. 1994. GPS for yield mapping on combines. Computers and Electronics in Agriculture. Vol. 11, pp 53-68.

Barbosa, R.N. 1996. Site-Specific Applications of Nitrogen In Corn Based On Yield Potential. Master's Thesis, The University of Tennessee, Knoxville.

Benson, R.C. and R.A. Glaccum. 1979. Radar surveys for geotechnical site assesment. American Convention and Exposition, Atlanta, GA. 164.

Brady, N.C. 1990. The Nature and Property of Soils. Tenth Edition. MacMillan Publishing Co. New York, NY.

Bouldin, J.D. 1997. Use of Ground Penetrating Radar To Map Soil Features That Influence Water Content. Master's Thesis, The University of Tennessee, Knoxville.

Collins, M.E., and J.A. Doolittle. 1987. Using ground penetrating radar to study soil microvariability. Soil Science Society America Journal. Vol 51, pp 491-493.

Collins, M.E.,J.A. Doolittle, and R.V. Rourke. 1989. Mapping depth to bedrock on a glaciated landscape with ground-penetrating radar. Soil Science Society of America Journal. Vol. 53: pp. 1806-1812.

Doolittle, J.A. 1982. Characterizing soil map units with the ground-penetrating. Soil Survey Horizons, pp. 3-10.

Doolittle, J.A. 1987. Using ground penetrating radar to increase the quality and efficiency of soil surveys. *Soil Surveys Techniques*. Special Publication. No. 20.

Doolittle, J.A. and M.E. Collins. 1995. Use of soil information to determine application of ground penetrating radar. Journal of Applied Geophysics. Vol. 33: pp. 102-106.

Evans, R.G., S. Han, and S.L. Rawlins. 1995. GIS capabilities and limitations for precision farming. ASAE Paper No. 95-3236. St. Joseph, MI.

ESRI. 1995. Understanding GIS: The ARC/INFO Method. Environmental Systems Research Institute, Inc. Redlands, CA.

Franzen, D.W. and T.R. Peck. 1995. Field soil sampling density for variable rate fertilization. Journal of Production Agriculture. Vol. 8, No. 4. pp 568-574.

Hamlett, J.C. 1995. Nonintrusive Reconnaissance of Cumberland Plateau Soils with Ground-Penetrating Radar. Master's Thesis, The University of Tennessee, Knoxville.

Harrison, J.D., S.J. Birrell, K.A. Suddeth, and S.C. Borgelt. 1992. Global positioning applications for site-specific farming research. ASAE Paper No. 92-3615. St. Joseph, MI.

Hurn, Jeff. 1989. GPS a Guide to the Next Utility. Trimble Navigation, Ltd. 645 North May Ave., Sunnyvale, CA 94086

Johnson A.I., C.B. Pettersson, and J.L. Fulton, editors. 1992. Geographic information systems (GIS) and mapping-practices and standards. ASTM Special Technical Publication; 1126

Miller R.W. and R.L. Donahue. 1990. Soils: An Introduction to Soils and Plant Growth. Sixth Edition. Prentice-Hall, Inc. Englewood Cliffs, NJ.

National Research Council (U.S.) Committee on Assessing Crop Yield: Site-Specific Farming, Information Systems, and Research Opportunities. 1997. Precision Agriculture in the 21st Century. National Academy Press, Washington, D.C.

Palmer, M.S. 1997. The design and implementation of a field-scale monitoring system to evaluate spatial variability within production cotton fields. Master's Thesis, The University of Tennessee, Knoxville.

Rhoton, F.E., D.D. Tyler, and D.L. Lindbo. 1996. Fragipan soils in the Lower Mississippi River Valley: their distribution, characteristics, erodibility, production, and management. U.S. Department of Agriculture, ARS-137.

Rupert, C. and R.L. Clark. 1994. Accuracy of DGPS position information point data with a C/A code receiver. ASAE Paper No. 94-3546. St. Joseph, MI.

Saxton, A.M. 1998. Personal Communication. Professor. Statistics, The University of Tennessee, Knoxville.

Schellentrager, G.W., J.A. Doolittle, T.E. Calhoun, and C.A. Wettstein. 1988. Using ground penetrating radar to update soil survey information. Soil Science Society of America Journal. Vol 52, pp. 746-752.

Schueller, J.K. and M.W. Wang. 1994. Spatially-variable fertilizer and pesticide application with GPS and DGPS. Computers and Electronics in Agriculture. No. 11 (1994) pp. 69-83.

Schumann, H.W. 1984. Potential for moisture stress on vegetation on the Cumberland Plateau of Tennessee. Master's Thesis. The University of Tennessee, Knoxville.

Stafford, J.V. and B. Ambler. 1994. In-field location using GPS for spatially variable field operations. Computers and Electronics in Agriculture. No. 11 (1994) pp. 23-36.

Star, J. and J. Estes. 1990. Geographic Information Systems: An Introduction. Prentice-Hall, Inc.

The Finnish Geotechnical Society. 1992. Ground Penetrating Radar: Geophysical Research Methods. Tampere: Tammer-Paino Oy.

Truman, C.C., H.F. Perkins, L.E. Asmussen, and H.D. Allison. 1988. Using ground penetrating radar to investigate variability in selected soil properties. Journal of Soil and Water Conservation. July-August 1988, pp. 341-345.

Tyler, D.D., J.G. Graveel, and J.R. Jones. 1991. Sourthern Loess Belt. In J.W.Gilliam and G.D. Bubenzer (ed.) Soil Erosion and Productivity. The University of Wisconsin, Madison, WI. Southern Regional Series Bulletin 360.

Ulrikson, C.P. F. 1982. Application of Impulse Radar To Civil Engineering. Ph.D. Thesis, Lund University of Technology, Lund, Sweden, Published in U.S. by GSSI.

Appendices

Appendix A

Appendix A1:

Crossville Blind Test Comparison

GPR File #	Flag #	Ground Truth	Primary Interpretation	Secondary Interpretation
File 1	F1	**0.74**	0.38	0.35
	F2	0.72	0.70	0.69
	F3	0.60	0.59	0.58
	F4	0.70	0.68	0.67
	F5	0.53	0.52	0.52
	F6	**0.84**	0.70	0.69
	F7	0.55	0.52	0.52
	F8	0.43	0.45	0.45
	F9	**0.78**	0.61	0.60
	F10	0.66	0.65	0.64
File 2	F1	**0.50**	0.40	0.41
	F2	0.50	**0.48**	**0.23**
	F3	0.53	0.50	0.49
	F4	0.55	0.55	0.56
	F5	0.65	0.64	0.64
	F6	**0.29**	0.48	0.47
	F7	0.48	0.49	0.49
	F8	0.32	**0.31**	**0.74**
	F9	0.44	0.40	0.38
	F10	0.55	0.50	0.50
File 3	F1	0.32	0.30	0.28
	F2	0.36	0.38	0.39
	F3	**0.26**	**0.32**	**0.26**
	F4	0.55	0.55	0.55
	F5	0.61	0.62	0.63
	F6	0.80	0.83	0.83
	F7	**0.80**	0.98	0.96
	F8	0.87	0.81	0.81
	F9	0.63	0.65	0.65
	F10	0.31	0.33	0.31
File 4	F1	0.14	0.14	0.15
	F2	0.23	**0.22**	**0.38**
	F3	0.19	**0.15**	**0.47**
	F4	0.35	**0.34**	**0.56**
	F5	0.44	0.43	0.43
	F6	0.84	**0.80**	**0.64**
	F7	0.86	0.81	0.81
	F8	0.79	0.80	0.80
	F9	0.65	0.72	0.73
	F10	0.30	0.38	0.38

Appendix A2:

Milan Blind Test Comparisons

File #	Flag #	Ground Truth	GPR Image	Primary Interpretation	Secondary Interpretation
File 1	1	n/p memphis	memphis	memphis	memphis
	2	charact. @ 1.06	transition	transition	transition
	3	charact. @ 1.06	greneda	greneda	greneda
	4	charact. @ 1.20	greneda	greneda	greneda
	5	transition	greneda	greneda	greneda
File 2	1	n/p memphis	memphis	memphis	memphis
	2	transition	transition	transition	transition
	3	pan @ 1.06	Greneda	greneda	greneda
	4	pan @ 0.74	Greneda	greneda	greneda
	5	pan @ 0.64	Greneda	greneda	greneda
File 3	1	n/p memphis	memphis	memphis	memphis
	2	n/p memphis	memphis	memphis	memphis
	3	n/p greneda	transition	transition	transition
	4	n/p greneda	greneda	greneda	greneda
	5	n/p greneda	greneda	greneda	greneda
File 4	1	pan @ 0.50 greneda	greneda	**transition**	**grenada**
	2	pan @ 0.50 greneda	greneda	greneda	greneda
	3	pan @ 0.61 greneda	greneda	greneda	greneda
	4	pan @ 0.71 greneda	greneda	greneda	greneda
	5	pan @ 1.01 greneda	greneda	greneda	greneda
File 5	1	pan @ 1.01 greneda	greneda	greneda	greneda
	2	pan @ 0.71 greneda	greneda	greneda	greneda
	3	pan @ 0.61 greneda	greneda	greneda	greneda
	4	pan @ 0.50 greneda	greneda	greneda	greneda
	5	pan @ 0.50 greneda	greneda	greneda	greneda
File 6	1	n/p memphis	memphis	memphis	memphis
	2	n/p memphis	memphis	memphis	memphis
	3	n/p memphis	memphis	memphis	memphis
	4	n/p memphis	memphis	memphis	memphis
	5	charact. @ 1.06	memphis	memphis	memphis
File 7	1	n/p memphis	memphis	memphis	memphis
	2	n/p memphis	Transition	transition	transition
	3	n/p greneda	greneda	greneda	greneda
	4	n/p greneda	greneda	greneda	greneda
	5	n/p greneda	greneda	greneda	greneda
File 8	1	n/p greneda	greneda	greneda	greneda
	2	n/p greneda	greneda	greneda	greneda
	3	n/p greneda	greneda	greneda	greneda
	4	n/p memphis	Transition	transition	transition
	5	n/p memphis	memphis	memphis	memphis
File 9	1	pan @ 0.50 greneda	greneda	greneda	greneda
	2	pan @ 0.61 greneda	greneda	greneda	greneda

	3	pan @ 0.71 greneda	greneda	greneda	greneda
	4	pan @ 1.01 greneda	greneda	greneda	greneda
	5	pan @ 1.06 greneda	greneda	greneda	greneda
File 10	1	n/p memphis	memphis	memphis	memphis
	2	n/p memphis	memphis	memphis	memphis
	3	n/p memphis	memphis	memphis	memphis
	4	n/p memphis	memphis	memphis	memphis
	5	n/p memphis	memphis	memphis	memphis
File 11	1	pan @ 0.71	greneda	greneda	greneda
	2	pan @ 0.96	greneda	greneda	greneda
	3	transition	greneda	greneda	greneda
	4	charact. @ 1.20	greneda	greneda	greneda
	5	charact. @ 1.06	greneda	greneda	greneda
File 12	1	n/p memphis	memphis	memphis	memphis
	2	n/p memphis	memphis	memphis	memphis
	3	n/p memphis	memphis	memphis	memphis
	4	n/p memphis	memphis	memphis	memphis
	5	n/p memphis	memphis	memphis	memphis
File 13	1	transition	transition	greneda	greneda
	2	pan @ 1.06 greneda	greneda	greneda	greneda
	3	pan @ 1.01 greneda	greneda	greneda	greneda
	4	pan @ 0.71 greneda	greneda	greneda	greneda
	5	pan @ 0.61 greneda	greneda	greneda	greneda
File 14	1	disturbed soil	Greneda	greneda	greneda
	2	pan @ 0.64	Greneda	greneda	greneda
	3	pan @ 0.74	Greneda	greneda	greneda
	4	pan @ 1.06	Greneda	greneda	greneda
	5	transition	transition	**transition**	**greneda**
File 15	1	n/p memphis	memphis	memphis	memphis
	2	n/p memphis	memphis	memphis	memphis
	3	n/p memphis	memphis	memphis	memphis
	4	**transition**	**transition**	memphis	memphis
	5	**pan @ 1.06**	**Greneda**	transition	transition
File 16	1	transition	greneda	greneda	greneda
	2	charact. @ 1.20	greneda	greneda	greneda
	3	charact. @ 1.06	greneda	greneda	greneda
	4	charact. @ 1.06	transition	transition	transition
	5	n/p memphis	memphis	memphis	memphis
File 17	1	pan @ 1.01 greneda	greneda	greneda	greneda
	2	pan @ 0.71 greneda	greneda	greneda	greneda
	3	pan @ 0.61 greneda	greneda	greneda	greneda
	4	pan @ 0.50 greneda	greneda	greneda	greneda
	5	pan @ 0.50 greneda	greneda	**transition**	**greneda**
File 18	1	n/p memphis	memphis	memphis	memphis
	2	n/p memphis	memphis	memphis	memphis
	3	n/p memphis	memphis	memphis	memphis
	4	n/p memphis	memphis	memphis	memphis
	5	n/p memphis	memphis	memphis	memphis
File 19	1	n/p memphis	memphis	memphis	memphis
	2	n/p memphis	Transition	transition	transition
	3	n/p greneda	greneda	greneda	greneda

	4	n/p greneda	greneda	greneda	greneda
	5	n/p greneda	greneda	greneda	greneda
File 20	1	transition	transition	transition	transition
	2	pan @ 1.06	Greneda	greneda	greneda
	3	pan @ 0.74	Greneda	greneda	greneda
	4	pan @ 0.64	Greneda	greneda	greneda
	5	disturbed soil	Greneda	greneda	greneda

Appendix B

Appendix B:

SAS Program

```
data one;
 input lat long soilcode yield;
cards;


;
proc corr;
 var yield soilcode;
run;
proc plot;
 plot yield*soilcode;
run;
proc mixed covtest;
 class soilcode;
 model yield=soilcode;
 repeated /type=sp(sph)(lat long);
 lsmeans soilcode/ pdiff;
run;
proc sort; by soilcode;
proc univariate plot normal; by soilcode;
 var yield;
run;
proc freq data=one;
 tables yldcode*soilcode/measures chisq;
run;
```

Appendix C

Appendix C:

Raw Data File Names

Date	File Name
4/98	Dump
4/98	Potato
6/98	Plt1_60ns
6/98	Plt2_60ns

Figures

Figure	Raw File	ProcessedFile Name
2.1	Corel 8 Drawing	Fig2_1.CDR
2.2	Photograph	Fig2_2.BMP
2.3	Photograph	Fig2_3.BMP
3.1	Photograph	Fig3_1.BMP
3.2	a6_a7.APR	Fig3_2.BMP
3.3	Corel 8 Drawing	Fig3_3.CDR
3.4	pot_2.APR	Fig3_4.BMP
3.5	dmp_2.APR	Fig3_5.BMP
3.6	plot 1\A01.DZT	Fig3_6.BMP
3.7	plot 1\A12.DZT	Fig3_7.BMP
3.8	plot 2\A01.DZT	Fig3_8.BMP
3.9	plot 2\A10.DZT	Fig3_9.BMP
3.10	Photograph	Fig3_10.BMP
4.1	CentStack\A4.DZT	Fig4_1.BMP
4.2	CentStack.DZT	Fig4_2.BMP
4.3	4-H Camp\P13.DZT	Fig4_3.BMP
4.4	PrelimPan.DZT	Fig4_4.BMP
4.5	BTData\D4r.DZT	Fig4_5.BMP
4.6	pot_2.APR	Fig4_6.BMP
4.7	dmp_2.APR	Fig4_7.BMP
4.8	plotylds.APR	Fig4_8.BMP
4.9	plotylds.APR	Fig4_9.BMP
4.10	plotylds.APR	Fig4_10.BMP
4.11	plotylds.APR	Fig4_11.BMP

Appendix D

Appendix D1:

Statistical Output from Plot 1, Plateau Experiment Station

Plot 1 20:07 Friday, March 12, 1999 1

Correlation Analysis

2 'VAR' Variables: SOILCODE YIELD

Simple Statistics

Variable	N	Mean	Std Dev	Sum	Minimum	Maximum
SOILCODE	409	2.40342	0.56973	983.00000	1.00000	3.00000
YIELD	409	205.76211	59.92216	84157	43.02907	333.21999

Pearson Correlation Coefficients / Prob > |R| under Ho: Rho=0 / N = 409

	SOILCODE	YIELD
SOILCODE	1.00000 0.0	0.49577 0.0001
YIELD	0.49577 0.0001	1.00000 0.0

Plot 1 20:07 Friday, March 12, 1999 2

The MIXED Procedure

Class Level Information

Class	Levels	Values
SOILCODE	3	1 2 3

REML Estimation Iteration History

Iteration	Evaluations	Objective	Criterion
0	1	3628.8708988	
1	1	3628.8708988	0.00000000

Convergence criteria met.

Covariance Parameter Estimates (REML)

Cov Parm	Estimate
SP(SPH)	2.00000000
Residual	2711.1802565

Model Fitting Information for YIELD

Description	Value
Observations	409.0000

Res Log Likelihood	-2187.52
Akaike's Information Criterion	-2189.52
Schwarz's Bayesian Criterion	-2193.53
-2 Res Log Likelihood	4375.049
Null Model LRT Chi-Square	0.0000
Null Model LRT DF	1.0000
Null Model LRT P-Value	1.0000

Tests of Fixed Effects

Source	NDF	DDF	Type III F	Pr > F
SOILCODE	2	406	67.18	0.0001

Least Squares Means

Effect	SOILCODE	LSMEAN	Std Error	DF	t	Pr > |t|
SOILCODE	1	119.42618788	12.62858628	406	9.46	0.0001
SOILCODE	2	186.85642456	3.59310203	406	52.00	0.0001
SOILCODE	3	235.64071182	3.85961071	406	61.05	0.0001

Differences of Least Squares Means

Effect	SOILCODE	_SOILCOD	Difference	Std Error	DF	t	Pr > |t|
SOILCODE	1	2	-67.43023667	13.12979717	406	-5.14	0.0001
SOILCODE	1	3	-116.2145239	13.20521815	406	-8.80	0.0001
SOILCODE	2	3	-48.78428727	5.27323212	406	-9.25	0.0001

---------- SOILCODE=1 ----------

Univariate Procedure

Variable=YIELD

Moments

N	17	Sum Wgts	17
Mean	119.4262	Sum	2030.245
Std Dev	53.15303	Variance	2825.244
Skewness	1.229735	Kurtosis	1.894934
USS	287668.3	CSS	45203.91
CV	44.50701	Std Mean	12.8915
T:Mean=0	9.263947	Pr>|T|	0.0001
Num ^= 0	17	Num > 0	17
M(Sign)	8.5	Pr>=|M|	0.0001
Sgn Rank	76.5	Pr>=|S|	0.0001
W:Normal	0.882359	Pr<W	0.0344

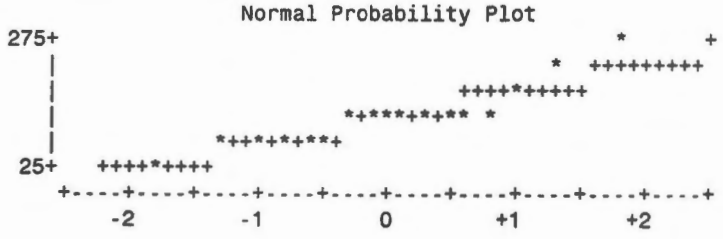
Quantiles(Def=5)

100% Max	255.0895	99%	255.0895
75% Q3	123.8679	95%	255.0895
50% Med	109.8269	90%	214.509
25% Q1	95.28121	10%	54.32732
0% Min	43.02907	5%	43.02907
		1%	43.02907
Range	212.0604		
Q3-Q1	28.58672		
Mode	43.02907		

Extremes

Lowest	Obs	Highest	Obs
43.02907(	16)	123.8679(	6)
54.32732(	10)	124.4546(	2)
72.48056(	8)	171.6567(	15)
86.63793(	7)	214.509(	1)
95.28121(	9)	255.0895(	17)

```
Stem Leaf                     #             Boxplot
   2 6                        1                *
   2 1                        1                *
   1 7                        1                0
   1 0001122222              10               +--+--+
   0 579                      3                |
   0 4                        1                0
     ----+----+----+----+
 Multiply Stem.Leaf by 10**+2
```



---------- SOILCODE=2 ----------

Univariate Procedure

Variable=YIELD

Moments

N	210	Sum Wgts	210
Mean	186.8564	Sum	39239.85
Std Dev	55.96169	Variance	3131.711
Skewness	-0.22283	Kurtosis	-0.92645
USS	7986746	CSS	654527.6
CV	29.94903	Std Mean	3.861724
T:Mean=0	48.38679	Pr>|T|	0.0001
Num ^= 0	210	Num > 0	210
M(Sign)	105	Pr>=|M|	0.0001
Sgn Rank	11077.5	Pr>=|S|	0.0001
W:Normal	0.950262	Pr<W	0.0001

Quantiles(Def=5)

100% Max	313.3469	99%	288.369
75% Q3	232.8727	95%	264.1575
50% Med	191.4257	90%	253.8339
25% Q1	138.0089	10%	108.6839
0% Min	58.91038	5%	96.81856
		1%	71.22251
Range	254.4365		
Q3-Q1	94.86379		
Mode	58.91038		

Extremes

Lowest	Obs	Highest	Obs
58.91038(	19)	277.8088(	140)
69.50962(	69)	287.2835(	100)
71.22251(	64)	288.369(	121)
73.28518(	4)	304.0207(	207)
81.96845(	**195)**	**313.3469(**	**104)**

Statistical Output from Plot 2, Plateau Experiment Station

Plot 2 20:15 Friday, March 12, 1999 1

Correlation Analysis

2 'VAR' Variables: YIELD SOILCODE

Simple Statistics

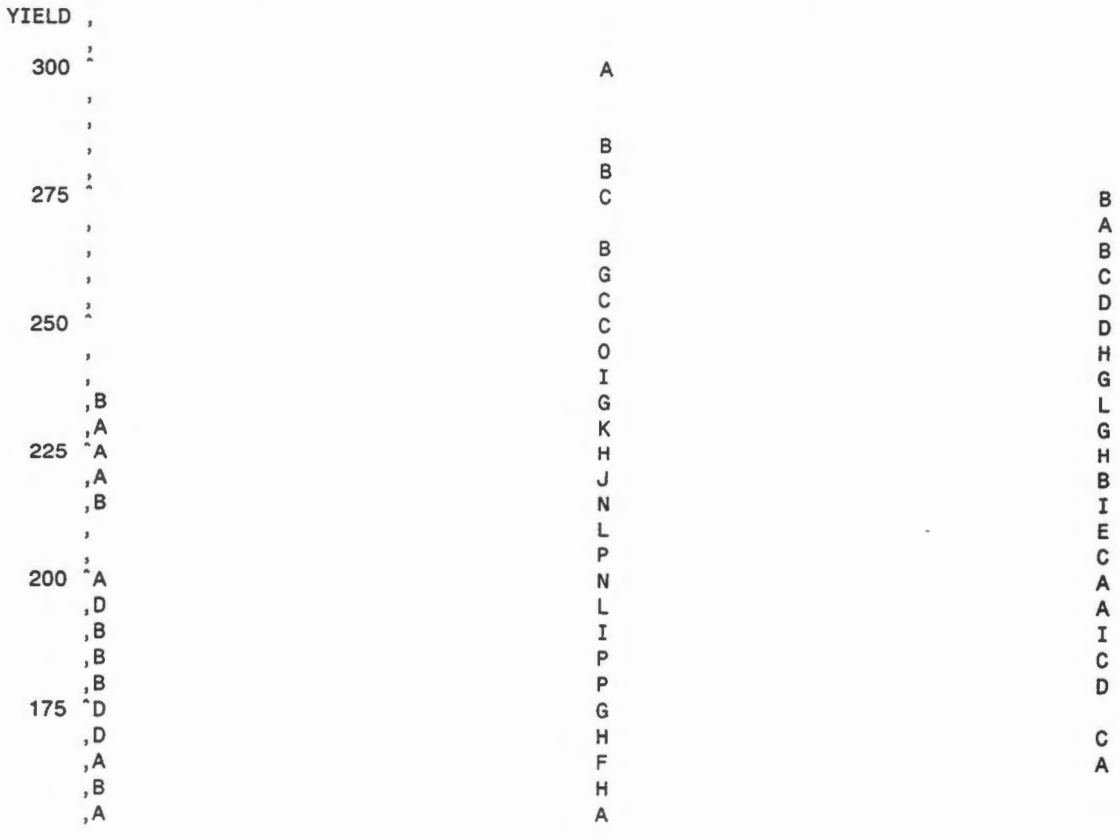
Variable	N	Mean	Std Dev	Sum	Minimum	Maximum
YIELD	387	204.01995	39.04396	78956	54.26687	299.24186
SOILCODE	387	2.17313	0.59227	841.00000	1.00000	3.00000

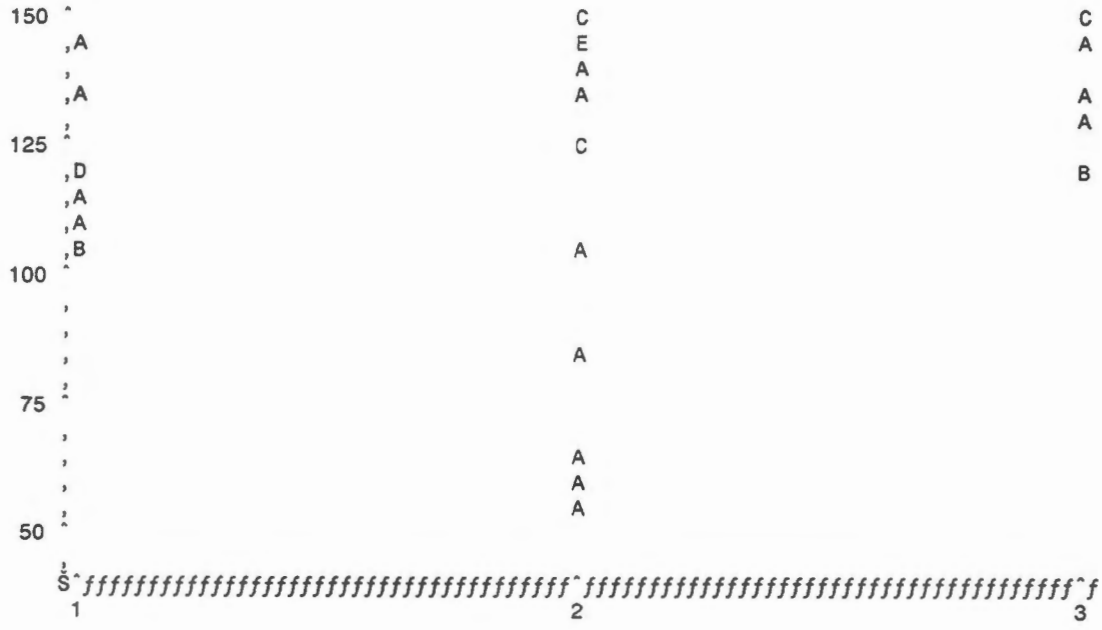
Pearson Correlation Coefficients / Prob > |R| under Ho: Rho=0 / N = 387

	YIELD	SOILCODE
YIELD	1.00000 0.0	0.30087 0.0001
SOILCODE	0.30087 0.0001	1.00000 0.0

Plot 2 20:15 Friday, March 12, 1999 2

Plot of YIELD*SOILCODE. Legend: A = 1 obs, B = 2 obs, etc.





Plot 2 20:15 Friday, March 12, 1999 3

The MIXED Procedure

Class Level Information

Class	Levels	Values
SOILCODE	3	1 2 3

REML Estimation Iteration History

Iteration	Evaluations	Objective	Criterion
0	1	3173.2402493	
1	1	3173.2402493	0.00000000

Convergence criteria met.

Covariance Parameter Estimates (REML)

Cov Parm	Estimate
SP(SPH)	2.00000000
Residual	1376.9121565

Model Fitting Information for YIELD

Description	Value
Observations	387.0000
Res Log Likelihood	-1939.49
Akaike's Information Criterion	-1941.49

Schwarz's Bayesian Criterion	-1945.44
-2 Res Log Likelihood	3878.985
Null Model LRT Chi-Square	0.0000
Null Model LRT DF	1.0000
Null Model LRT P-Value	1.0000

Tests of Fixed Effects

Source	NDF	DDF	Type III F	Pr > F
SOILCODE	2	384	21.68	0.0001

Least Squares Means

Effect	SOILCODE	LSMEAN	Std Error	DF	t	Pr > |t|
SOILCODE	1	171.87600142	5.86709501	384	29.29	0.0001
SOILCODE	2	203.54479284	2.39523151	384	84.98	0.0001
SOILCODE	3	217.10215763	3.58724656	384	60.52	0.0001

Differences of Least Squares Means

Effect	SOILCODE	_SOILCOD	Difference	Std Error	DF	t	Pr > |t|
SOILCODE	1	2	-31.66879142	6.33718691	384	-5.00	0.0001
SOILCODE	1	3	-45.22615621	6.87685552	384	-6.58	0.0001
SOILCODE	2	3	-13.55736479	4.31340607	384	-3.14	0.0018

---------- SOILCODE=1 ----------

Univariate Procedure

Variable=YIELD

Moments

N	40	Sum Wgts	40
Mean	171.876	Sum	6875.04
Std Dev	37.18814	Variance	1382.958
Skewness	-0.28342	Kurtosis	-0.71704
USS	1235590	CSS	53935.35
CV	21.63661	Std Mean	5.879961
T:Mean=0	29.23081	Pr>|T|	0.0001
Num ^= 0	40	Num > 0	40
M(Sign)	20	Pr>=|M|	0.0001
Sgn Rank	410	Pr>=|S|	0.0001
W:Normal	0.943374	Pr<W	0.0628

Quantiles(Def=5)

100% Max	234.7058	99%	234.7058
75% Q3	195.5364	95%	231.2991
50% Med	174.5013	90%	220.7351
25% Q1	149.7873	10%	115.9859
0% Min	103.27	5%	106.5846
		1%	103.27
Range	131.4358		
Q3-Q1	45.7491		
Mode	103.27		

Extremes

Lowest	Obs	Highest	Obs
103.27(	36)	218.779(	15)
105.2369(	40)	222.6912(	23)
107.9322(	39)	229.4748(	10)
114.3551(	1)	233.1234(	21)
117.6167(	30)	234.7058(	17)

Stem	Leaf	#	Boxplot
23	35	2	
22	39	2	
21	459	3	
20	2	1	
19	223477	6	+-----+
18	0157	4	| |
17	13456	5	*--+--*
16	17889	5	| |
15	79	2	+-----+
14	3	1	
13	3	1	
12	122	3	
11	48	2	
10	358	3	

----+----+----+----+

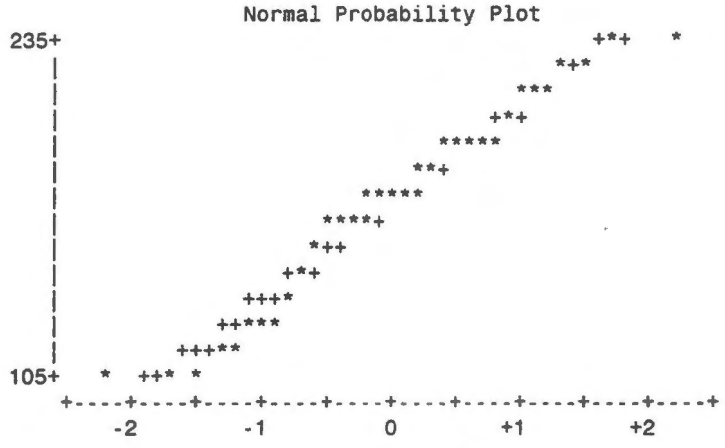
Multiply Stem.Leaf by 10**+1

---------- SOILCODE=1 ----------

Univariate Procedure

Variable=YIELD

Normal Probability Plot



---------- SOILCODE=2 ----------

Univariate Procedure

Variable=YIELD

Moments

N	240	Sum Wgts	240	100% Max	299.2419	99%	285.7258
Mean	203.5448	Sum	48850.75	75% Q3	230.3548	95%	259.7461
Std Dev	38.26462	Variance	1464.181	50% Med	204.2674	90%	246.6516
Skewness	-0.63904	Kurtosis	1.789413	25% Q1	181.1064	10%	161.0117
USS	10293255	CSS	349939.4	0% Min	54.26687	5%	145.7749
CV	18.79912	Std Mean	2.469971			1%	64.96534
T:Mean=0	82.40777	Pr>|T|	0.0001	Range	244.975		
Num ^= 0	240	Num > 0	240	Q3-Q1	49.2484		
M(Sign)	120	Pr>=|M|	0.0001	Mode	54.26687		
Sgn Rank	14460	Pr>=|S|	0.0001				
W:Normal	0.965819	Pr<W	0.0010				

Extremes

Lowest	Obs	Highest	Obs
54.26687(	195)	280.2436(	65)
58.95575(	167)	281.3283(	127)
64.96534(	174)	285.7258(	137)
86.92463(	232)	285.9554(	138)
105.7994(	21)	299.2419(	67)

Stem	Leaf	#	Boxplot
29	9	1	|
28	0166	4	|
27	466	3	|
26	0235	4	|

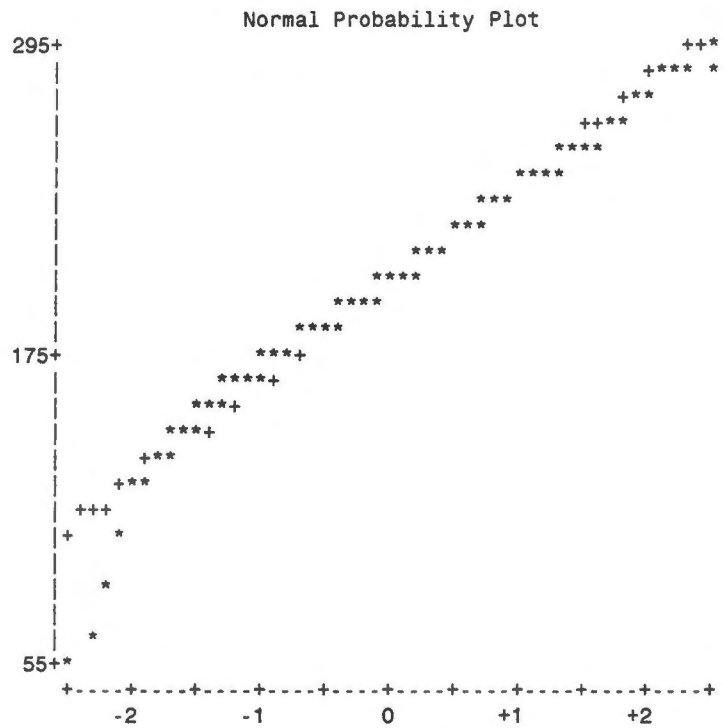
```
 25 0145788999                                10
 24 1123333335556667778                       19
 23 00002223356777888899                      20
 22 001112333346668899                        18
 21 000111222233334445555678999               28
 20 00012222234444455556666789                27
 19 0012244556667777789999                    22
 18 00111111223333445556666778899             30
 17 111223567777888999                        18
 16 000222445677889                           15
 15 0689                                       4
 14 3577788                                    7
 13 78                                         2
 12 347                                        3
 11
 10 6                                          1
  9
  8 7                                          1
  7
  6 5                                          1
  5 49                                         2
    ----+----+----+----+----+----+
Multiply Stem.Leaf by 10**+1
```



---------- SOILCODE=2 ----------

Univariate Procedure

Variable=YIELD



Plot 2 20:15 Friday, March 12, 1999 8

---------- SOILCODE=3 ----------

Univariate Procedure

Variable=YIELD

Moments

N	107	Sum Wgts	107
Mean	217.1022	Sum	23229.93
Std Dev	34.32084	Variance	1177.92
Skewness	-0.87344	Kurtosis	0.484155
USS	5168128	CSS	124859.5
CV	15.80861	Std Mean	3.317921
T:Mean=0	65.43319	Pr>|T|	0.0001
Num ^= 0	107	Num > 0	107
M(Sign)	53.5	Pr>=|M|	0.0001
Sgn Rank	2889	Pr>=|S|	0.0001
W:Normal	0.930796	Pr<W	0.0001

Quantiles(Def=5)

100% Max	276.3574	99%	272.7683
75% Q3	241.5035	95%	262.3917
50% Med	226.3796	90%	254.6598
25% Q1	192.1436	10%	171.1226
0% Min	117.9187	5%	149.8264
		1%	118.4293
Range	158.4387		
Q3-Q1	49.35995		
Mode	117.9187		

Extremes

Lowest	Obs	Highest	Obs
117.9187(	2)	266.0533(	71)
118.4293(	12)	266.3237(	77)
129.6645(	10)	269.8248(	91)

133.6215(13) 272.7683(48)
145.8249(22) 276.3574(50)

Appendix D2:

Statistical Output from Plot 1, Milan Experiment Station

The SAS System 20:20 Friday, March 12, 1999 1

Correlation Analysis

2 'VAR' Variables: YIELD SOILCODE

Simple Statistics

Variable	N	Mean	Std Dev	Sum	Minimum	Maximum
YIELD	169	135.79763	54.80628	22950	9.20000	237.60000
SOILCODE	169	3.11243	1.70235	526.00000	1.00000	5.00000

Pearson Correlation Coefficients / Prob > |R| under Ho: Rho=0 / N = 169

	YIELD	SOILCODE
YIELD	1.00000 0.0	0.74416 0.0001
SOILCODE	0.74416 0.0001	1.00000 0.0

The SAS System 20:20 Friday, March 12, 1999 3

The MIXED Procedure

Class Level Information

Class	Levels	Values
SOILCODE	5	1 2 3 4 5

REML Estimation Iteration History

Iteration	Evaluations	Objective	Criterion
0	1	1329.2808921	
1	1	1329.2808921	0.00000000

Convergence criteria met.

Covariance Parameter Estimates (REML)

Cov Parm	Estimate	Std Error	Z	Pr > |Z|
SP(SPH)	2.00000000	.	.	.
Residual	1100.4871791	121.52847861	9.06	0.0001

Model Fitting Information for YIELD

Description	Value
Observations	169.0000
Res Log Likelihood	-815.346
Akaike's Information Criterion	-817.346
Schwarz's Bayesian Criterion	-820.446
-2 Res Log Likelihood	1630.693
Null Model LRT Chi-Square	0.0000
Null Model LRT DF	1.0000
Null Model LRT P-Value	1.0000

Tests of Fixed Effects

Source	NDF	DDF	Type III F	Pr > F
SOILCODE	4	164	73.64	0.0001

Least Squares Means

Effect	SOILCODE	LSMEAN	Std Error	DF	t	Pr > |t|
SOILCODE	1	96.81176471	4.64523196	164	20.84	0.0001
SOILCODE	2	82.80434783	6.91717201	164	11.97	0.0001
SOILCODE	3	137.11000000	10.49041076	164	13.07	0.0001
SOILCODE	4	132.68846154	6.50587657	164	20.40	0.0001
SOILCODE	5	191.30338983	4.31883376	164	44.30	0.0001

Differences of Least Squares Means

Effect	SOILCODE	_SOILCOD	Difference	Std Error	DF	t	Pr > |t|
SOILCODE	1	2	14.00741688	8.33219351	164	1.68	0.0946
SOILCODE	1	3	-40.29823529	11.47287662	164	-3.51	0.0006

Differences of Least Squares Means

Effect	SOILCODE	_SOILCOD	Difference	Std Error	DF	t	Pr > |t|
SOILCODE	1	4	-35.87669683	7.99403590	164	-4.49	0.0001
SOILCODE	1	5	-94.49162512	6.34275217	164	-14.90	0.0001
SOILCODE	2	3	-54.30565217	12.56566698	164	-4.32	0.0001
SOILCODE	2	4	-49.88411371	9.49598329	164	-5.25	0.0001
SOILCODE	2	5	-108.4990420	8.15472830	164	-13.31	0.0001
SOILCODE	3	4	4.42153846	12.34403289	164	0.36	0.7207
SOILCODE	3	5	-54.19338983	11.34464821	164	-4.78	0.0001
SOILCODE	4	5	-58.61492829	7.80888949	164	-7.51	0.0001

---------- SOILCODE=1 ----------

Univariate Procedure

Variable=YIELD

Moments

				Quantiles(Def=5)			
N	51	Sum Wgts	51	100% Max	172.4	99%	172.4
Mean	96.81176	Sum	4937.4	75% Q3	118.5	95%	149.8
Std Dev	33.71482	Variance	1136.689	50% Med	104.6	90%	129.9

Skewness	-0.1748	Kurtosis	-0.44387	25% Q1	72.2	10%	44.7
USS	534832.9	CSS	56834.45	0% Min	33	5%	39.7
CV	34.82513	Std Mean	4.721019			1%	33
T:Mean=0	20.50654	Pr>|T|	0.0001	Range	139.4		
Num ^= 0	51	Num > 0	51	Q3-Q1	46.3		
M(Sign)	25.5	Pr>=|M|	0.0001	Mode	67.2		
Sgn Rank	663	Pr>=|S|	0.0001				
W:Normal	0.950417	Pr<W	0.0569				

Extremes

Lowest	Obs	Highest	Obs
33(	42)	134.5(	22)
39.2(	37)	135.2(	17)
39.7(	41)	149.8(	23)
41(	40)	165.8(	45)
43.2(	36)	172.4(	51)

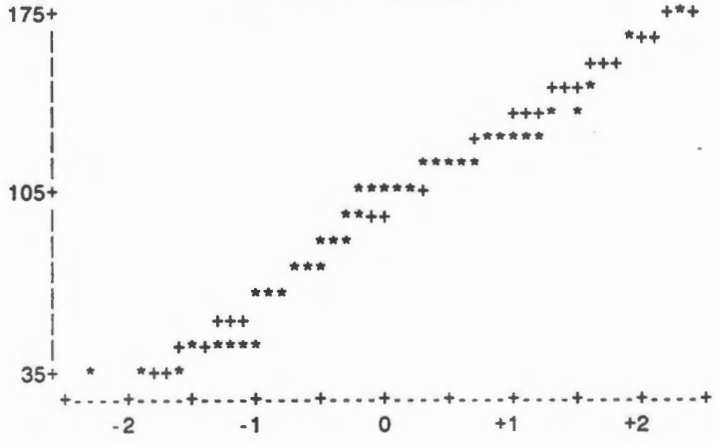
```
Stem Leaf                     #             Boxplot
  17 2                        1                |
  16 6                        1                |
  15 0                        1                |
  14                          0                |
  13 0045                     4                |
  12 2667                     4                |
  11 234556789                9             +-----+
  10 1344556668              10             *-----*
   9 56                       2             |  +  |
   8 0028                     4             |     |
   7 238                      3             +-----+
   6 0377                     4                |
   5                          0                |
   4 013555                   6                |
   3 39                       2                |
     ----+----+----+----+
Multiply Stem.Leaf by 10**+1
```


---------- SOILCODE=1 ----------

Univariate Procedure

Variable=YIELD

Normal Probability Plot



---------- SOILCODE=2 ----------

Univariate Procedure

Variable=YIELD

Moments

N	23	Sum Wgts	23
Mean	82.80435	Sum	1904.5
Std Dev	54.84681	Variance	3008.172
Skewness	0.021316	Kurtosis	-1.47533
USS	223880.7	CSS	66179.79
CV	66.23663	Std Mean	11.43635
T:Mean=0	7.240452	Pr>|T|	0.0001
Num ^= 0	23	Num > 0	23
M(Sign)	11.5	Pr>=|M|	0.0001
Sgn Rank	138	Pr>=|S|	0.0001
W:Normal	0.91288	Pr<W	0.0456

Quantiles(Def=5)

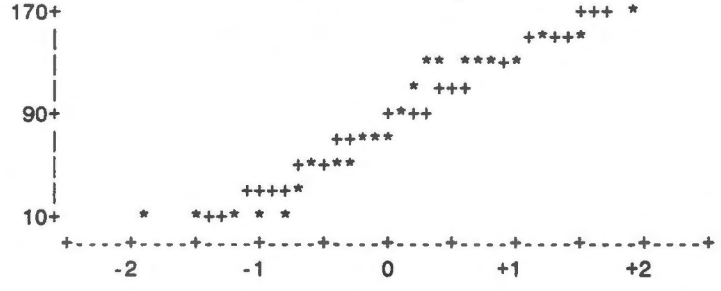
100% Max	171.7	99%	171.7
75% Q3	128.3	95%	158.9
50% Med	76.7	90%	155.9
25% Q1	22.9	10%	11.2
0% Min	9.2	5%	10.8
		1%	9.2
Range	162.5		
Q3-Q1	105.4		
Mode	9.2		

Extremes

Lowest	Obs	Highest	Obs
9.2(	19)	135.7(	2)
10.8(	16)	138.7(	7)
11.2(	20)	155.9(	3)
13(	14)	158.9(	6)
15.9(	17)	171.7(	23)

```
Stem Leaf                     #             Boxplot
  16 2                        1                |
  14 69                       2                |
  12 367869                   6             +-----+
  10 8                        1             |     |
   8 8                        1             |  +  |
   6 287                      3             *-----*
   4 880                      3             |     |
   2 3                        1             +-----+
   0 91136                    5                |
     ----+----+----+----+
Multiply Stem.Leaf by 10**+1
```

Normal Probability Plot



---------- SOILCODE=3 ----------

Univariate Procedure

Variable=YIELD

Moments

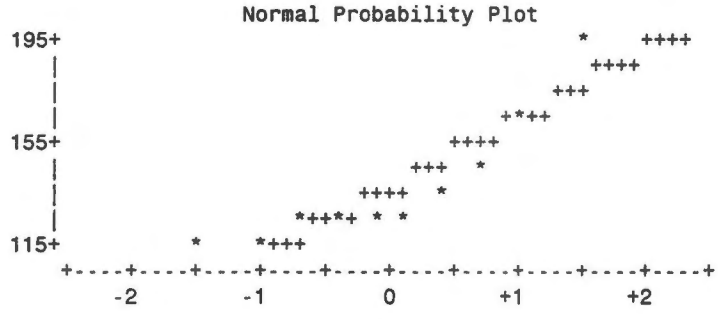
				Quantiles(Def=5)			
N	10	Sum Wgts	10	100% Max	198.7	99%	198.7
Mean	137.11	Sum	1371.1	75% Q3	147.4	95%	198.7
Std Dev	27.11168	Variance	735.0432	50% Med	124.2	90%	183.7
Skewness	1.644178	Kurtosis	2.105179	25% Q1	121.4	10%	116.3
USS	194606.9	CSS	6615.389	0% Min	116.2	5%	116.2
CV	19.77367	Std Mean	8.573466			1%	116.2
T:Mean=0	15.99236	Pr>|T|	0.0001	Range	82.5		
Num ^= 0	10	Num > 0	10	Q3-Q1	26		
M(Sign)	5	Pr>=|M|	0.0020	Mode	121.4		
Sgn Rank	27.5	Pr>=|S|	0.0020				
W:Normal	0.774218	Pr<W	0.0074				

Extremes

Lowest	Obs	Highest	Obs
116.2(	8)	125.6(	6)

```
      116.4(       3)    132.5(       7)
      121.4(       4)    147.4(       5)
      121.4(       1)    168.7(       9)
      122.8(       2)    198.7(      10)
```

```
Stem Leaf                     #            Boxplot
  19 9                        1               0
  18
  17
  16 9                        1               |
  15                                          |
  14 7                        1            +-----+
  13 2                        1            |  +  |
  12 1136                     4            *-----*
  11 66                       2               |
     ----+----+----+----+
 Multiply Stem.Leaf by 10**+1
```



---------- SOILCODE=4 ----------

Univariate Procedure

Variable=YIELD

Moments

N	26	Sum Wgts	26
Mean	132.6885	Sum	3449.9
Std Dev	37.33307	Variance	1393.758
Skewness	-0.96756	Kurtosis	0.530573
USS	492605.9	CSS	34843.95
CV	28.13588	Std Mean	7.321617
T:Mean=0	18.12284	Pr>|T|	0.0001
Num ^= 0	26	Num > 0	26
M(Sign)	13	Pr>=|M|	0.0001
Sgn Rank	175.5	Pr>=|S|	0.0001
W:Normal	0.909545	Pr<W	0.0264

Quantiles(Def=5)

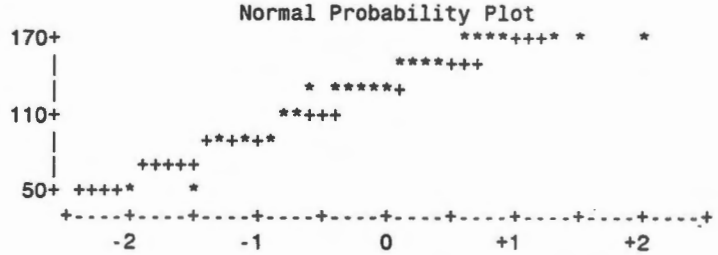
100% Max	178.8	99%	178.8
75% Q3	164.6	95%	177.5
50% Med	136.3	90%	175.3
25% Q1	109.9	10%	82.2
0% Min	41.9	5%	47.4
		1%	41.9
Range	136.9		
Q3-Q1	54.7		
Mode	166.4		

Extremes

Lowest	Obs	Highest	Obs
41.9(	26)	166.4(	1)
47.4(	23)	166.4(	10)
82.2(	19)	175.3(	4)
94.9(	12)	177.5(	17)
99.8(	8)	178.8(	20)

```
Stem Leaf                     #             Boxplot
  16 45666589                 8             +-----+
  14 0837                     4             |     |
  12 1001158                  7             *--+--*
  10 020                      3             +-----+
   8 25                       2                |
   6                                           |
   4 27                       2                |
     ----+----+----+----+
Multiply Stem.Leaf by 10**+1
```

Normal Probability Plot



---------- SOILCODE=5 ----------

Univariate Procedure

Variable=YIELD

Moments

Quantiles(Def=5)

N	59	Sum Wgts	59	100% Max	237.6	99%	237.6
Mean	191.3034	Sum	11286.9	75% Q3	199.3	95%	214.3
Std Dev	16.61238	Variance	275.971	50% Med	193.2	90%	208.6
Skewness	-0.62433	Kurtosis	1.529013	25% Q1	187.2	10%	165.6
USS	2175229	CSS	16006.32	0% Min	146.3	5%	154.4
CV	8.683785	Std Mean	2.162747			1%	146.3
T:Mean=0	88.45389	Pr>|T|	0.0001	Range	91.3		
Num ^= 0	59	Num > 0	59	Q3-Q1	12.1		
M(Sign)	29.5	Pr>=|M|	0.0001	Mode	193.4		
Sgn Rank	885	Pr>=|S|	0.0001				
W:Normal	0.936259	Pr<W	0.0058				

Extremes

Lowest	Obs	Highest	Obs
146.3(	42)	209.4(	19)
148.7(	41)	212.7(	11)
154.4(	27)	214.3(	44)
155.3(	28)	217(	17)
162.9(	**25)**	**237.6(**	**21)**

Statistical Output from Plot 2, Milan Experiment Station

The SAS System 20:27 Friday, March 12, 1999 1

Correlation Analysis

2 'VAR' Variables: YIELD SOILCODE

Simple Statistics

Variable	N	Mean	Std Dev	Sum	Minimum	Maximum
YIELD	169	138.75385	53.16391	23449	0	239.40000
SOILCODE	169	4.48521	2.16879	758.00000	1.00000	7.00000

Pearson Correlation Coefficients / Prob > |R| under Ho: Rho=0 / N = 169

	YIELD	SOILCODE
YIELD	1.00000 0.0	0.60460 0.0001
SOILCODE	0.60460 0.0001	1.00000 0.0

The SAS System 20:27 Friday, March 12, 1999 3

The MIXED Procedure

Class Level Information

Class	Levels	Values
SOILCODE	7	1 2 3 4 5 6 7

REML Estimation Iteration History

Iteration	Evaluations	Objective	Criterion
0	1	1245.1305708	
1	1	1245.1305708	0.00000000

Convergence criteria met.

Covariance Parameter Estimates (REML)

Cov Parm	Estimate	Std Error	Z	Pr > |Z|
SP(SPH)	2.00000000	.	.	.
Residual	702.23166700	78.02574078	9.00	0.0001

Model Fitting Information for YIELD

Description	Value
Observations	169.0000
Res Log Likelihood	-771.433

Akaike's Information Criterion	-773.433
Schwarz's Bayesian Criterion	-776.521
-2 Res Log Likelihood	1542.867
Null Model LRT Chi-Square	0.0000
Null Model LRT DF	1.0000
Null Model LRT P-Value	1.0000

Tests of Fixed Effects

Source	NDF	DDF	Type III F	Pr > F
SOILCODE	6	162	85.70	0.0001

Least Squares Means

Effect	SOILCODE	LSMEAN	Std Error	DF	t	Pr > |t|
SOILCODE	1	119.15161290	4.75947838	162	25.03	0.0001
SOILCODE	2	99.12727273	7.98994634	162	12.41	0.0001
SOILCODE	3	32.65714286	7.08233046	162	4.61	0.0001
SOILCODE	4	154.18000000	8.37992641	162	18.40	0.0001
SOILCODE	5	116.76785714	5.00796390	162	23.32	0.0001
SOILCODE	6	158.36904762	4.08898540	162	38.73	0.0001
SOILCODE	7	204.40303030	4.61299767	162	44.31	0.0001

Differences of Least Squares Means

Effect	SOILCODE	_SOILCOD	Difference	Std Error	DF	t	Pr > |t|
SOILCODE	1	2	20.02434018	9.30010091	162	2.15	0.0328
SOILCODE	1	3	86.49447005	8.53299708	162	10.14	0.0001
SOILCODE	1	4	-35.02838710	9.63720920	162	-3.63	0.0004
SOILCODE	1	5	2.38375576	6.90885930	162	0.35	0.7305
SOILCODE	1	6	-39.21743472	6.27474589	162	-6.25	0.0001
SOILCODE	1	7	-85.25141740	6.62815072	162	-12.86	0.0001
SOILCODE	2	3	66.47012987	10.67701490	162	6.23	0.0001
SOILCODE	2	4	-55.05272727	11.57853225	162	-4.75	0.0001
SOILCODE	2	5	-17.64058442	9.42968424	162	-1.87	0.0632
SOILCODE	2	6	-59.24177489	8.97546902	162	-6.60	0.0001
SOILCODE	2	7	-105.2757576	9.22599534	162	-11.41	0.0001
SOILCODE	3	4	-121.5228571	10.97189917	162	-11.08	0.0001
SOILCODE	3	5	-84.11071429	8.67404791	162	-9.70	0.0001
SOILCODE	3	6	-125.7119048	8.17797080	162	-15.37	0.0001
SOILCODE	3	7	-171.7458874	8.45216850	162	-20.32	0.0001
SOILCODE	4	5	37.41214286	9.76231884	162	3.83	0.0002
SOILCODE	4	6	-4.18904762	9.32432133	162	-0.45	0.6538
SOILCODE	4	7	-50.22303030	9.56571556	162	-5.25	0.0001
SOILCODE	5	6	-41.60119048	6.46525359	162	-6.43	0.0001
SOILCODE	5	7	-87.63517316	6.80877741	162	-12.87	0.0001
SOILCODE	6	7	-46.03398268	6.16437743	162	-7.47	0.0001

---------- SOILCODE=1 ----------

Univariate Procedure

Variable=YIELD

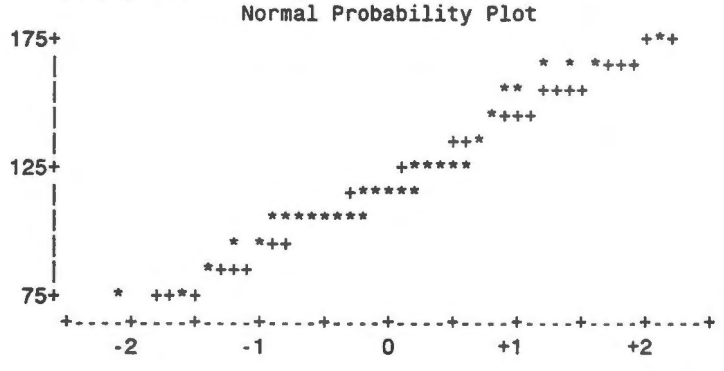
Moments Quantiles(Def=5)

N	31	Sum Wgts	31	100% Max	171.6	99%	171.6
Mean	119.1516	Sum	3693.7	75% Q3	138.6	95%	166.3
Std Dev	26.63275	Variance	709.3032	50% Med	110.8	90%	160.2
Skewness	0.448442	Kurtosis	-0.42833	25% Q1	104.1	10%	92.7
USS	461389.4	CSS	21279.1	0% Min	70.2	5%	76.2
CV	22.35198	Std Mean	4.783383			1%	70.2
T:Mean=0	24.90949	Pr>|T|	0.0001	Range	101.4		
Num ^= 0	31	Num > 0	31	Q3-Q1	34.5		
M(Sign)	15.5	Pr>=|M|	0.0001	Mode	70.2		
Sgn Rank	248	Pr>=|S|	0.0001				
W:Normal	0.941281	Pr<W	0.1074				

Extremes

Lowest	Obs	Highest	Obs
70.2(	13)	158.2(	30)
76.2(	18)	160.2(	27)
84.7(	10)	166(	16)
92.7(	12)	166.3(	21)
95.9(	11)	171.6(	28)

```
Stem Leaf                     #             Boxplot
  17 2                        1                |
  16 066                      3                |
  15 18                       2                |
  14 3                        1                |
  13 09                       2               +-----+
  12 2356                     4               |     |
  11 01114                    5               *--+--*
  10 01456679                 8               +-----+
   9 36                       2                  |
   8 5                        1                  |
   7 06                       2                  |
     ----+----+----+----+
  Multiply Stem.Leaf by 10**+1
```



---------- SOILCODE=2 ----------

Univariate Procedure

Variable=YIELD

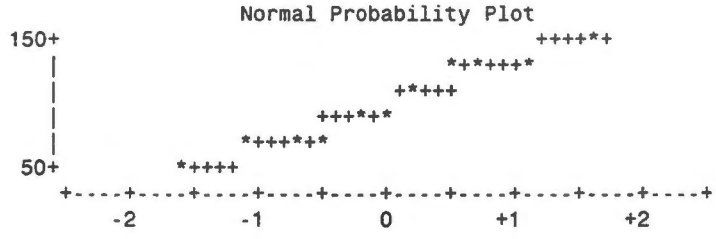
Moments				Quantiles(Def=5)			
N	11	Sum Wgts	11	100% Max	153.1	99%	153.1

Mean	99.12727	Sum	1090.4	75% Q3	127.3	95%	153.1
Std Dev	34.97745	Variance	1223.422	50% Med	93.8	90%	135.4
Skewness	-0.06769	Kurtosis	-1.16368	25% Q1	66.6	10%	61.2
USS	120322.6	CSS	12234.22	0% Min	43.3	5%	43.3
CV	35.2854	Std Mean	10.5461			1%	43.3
T:Mean=0	9.399426	Pr>|T|	0.0001	Range	109.8		
Num ^= 0	11	Num > 0	11	Q3-Q1	60.7		
M(Sign)	5.5	Pr>=|M|	0.0010	Mode	43.3		
Sgn Rank	33	Pr>=|S|	0.0010				
W:Normal	0.965711	Pr<W	0.8231				

Extremes

Lowest	Obs	Highest	Obs
43.3(	1)	118.6(	8)
61.2(	3)	124.2(	7)
66.6(	4)	127.3(	11)
77.5(	2)	135.4(	10)
89.4(	5)	153.1(	9)

```
Stem Leaf                     #             Boxplot
  14 3                        1                |
  12 475                      3               +-----+
  10 9                        1               |     |
   8 94                       2               *--+--*
   6 178                      3               +-----+
   4 3                        1                  |
     ----+----+----+----+
 Multiply Stem.Leaf by 10**+1
```



---------- SOILCODE=3 ----------

Univariate Procedure

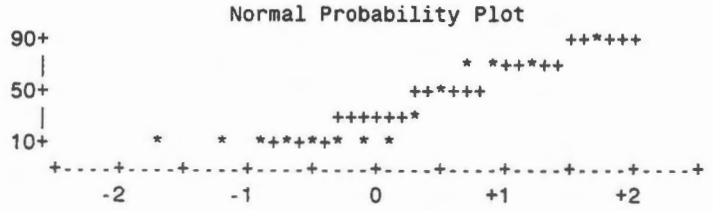
Variable=YIELD

Moments				Quantiles(Def=5)			
N	14	Sum Wgts	14	100% Max	93.5	99%	93.5
Mean	32.65714	Sum	457.2	75% Q3	62.7	95%	93.5
Std Dev	33.2655	Variance	1106.593	50% Med	15.95	90%	76.3
Skewness	0.657699	Kurtosis	-1.20875	25% Q1	4.7	10%	0
USS	29316.56	CSS	14385.71	0% Min	0	5%	0
CV	101.8629	Std Mean	8.890579			1%	0
T:Mean=0	3.67323	Pr>|T|	0.0028	Range	93.5		
Num ^= 0	12	Num > 0	12	Q3-Q1	58		
M(Sign)	6	Pr>=|M|	0.0005	Mode	0		
Sgn Rank	39	Pr>=|S|	0.0005				
W:Normal	0.856675	Pr<W	0.0269				

Extremes

Lowest	Obs	Highest	Obs
0(	13)	55.7(	2)
0(	12)	62.7(	10)
1.3(	8)	75.4(	6)
4.7(	7)	76.3(	3)
9.8(	5)	93.5(	1)

```
Stem Leaf                     #             Boxplot
   8 4                        1                |
   6 356                      3               +-----+
   4 6                        1               |     |
   2 6                        1               |  +  |
   0 00150039                 8               *-----*
     ----+----+----+----+
 Multiply Stem.Leaf by 10**+1
```



SOILCODE=4

Univariate Procedure

Variable=YIELD

Moments

N	10	Sum Wgts	10
Mean	154.18	Sum	1541.8
Std Dev	19.69911	Variance	388.0551
Skewness	-1.02824	Kurtosis	-0.05063
USS	241207.2	CSS	3492.496
CV	12.7767	Std Mean	6.229407
T:Mean=0	24.75035	Pr>|T|	0.0001
Num ^= 0	10	Num > 0	10
M(Sign)	5	Pr>=|M|	0.0020
Sgn Rank	27.5	Pr>=|S|	0.0020
W:Normal	0.872222	Pr<W	0.1014

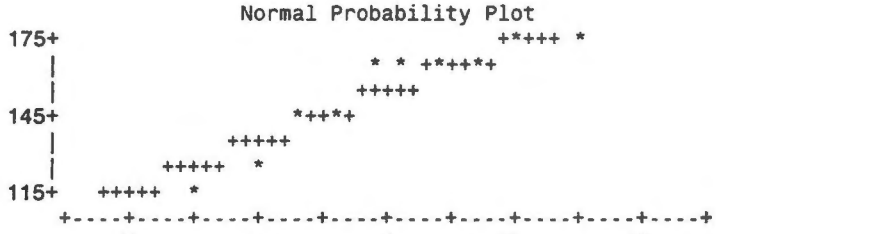
Quantiles(Def=5)

100% Max	176	99%	176
75% Q3	166.8	95%	176
50% Med	161.95	90%	173.75
25% Q1	148.1	10%	120.75
0% Min	118.1	5%	118.1
		1%	118.1
Range	57.9		
Q3-Q1	18.7		
Mode	118.1		

Extremes

Lowest	Obs	Highest	Obs
118.1(	6)	163.2(	9)
123.4(	10)	165.1(	7)
148.1(	8)	166.8(	4)
148.9(	5)	171.5(	2)
160.7(	3)	176(	1)

```
Stem Leaf                     #             Boxplot
  17 26                       2                |
  16 1357                     4            +-----+
  15                                       |  +  |
  14 89                       2            +-----+
  13                                          |
  12 3                        1              |
  11 8                        1              0
     ----+----+----+----+
 Multiply Stem.Leaf by 10**+1
```



---------- SOILCODE=5 ----------

Univariate Procedure

Variable=YIELD

Moments				Quantiles(Def=5)			
N	28	Sum Wgts	28	100% Max	192.8	99%	192.8
Mean	116.7679	Sum	3269.5	75% Q3	141.6	95%	171.2
Std Dev	31.18928	Variance	972.7712	50% Med	106.5	90%	155.1
Skewness	0.578859	Kurtosis	-0.19223	25% Q1	95.65	10%	75.9
USS	408037.3	CSS	26264.82	0% Min	67.2	5%	72.5
CV	26.7105	Std Mean	5.89422			1%	67.2
T:Mean=0	19.81057	Pr>|T|	0.0001	Range	125.6		
Num ^= 0	28	Num > 0	28	Q3-Q1	45.95		
M(Sign)	14	Pr>=|M|	0.0001	Mode	67.2		
Sgn Rank	203	Pr>=|S|	0.0001				
W:Normal	0.954797	Pr<W	0.2888				

Extremes

Lowest	Obs	Highest	Obs
67.2(	5)	150.4(	16)
72.5(	6)	154.9(	21)
75.9(	13)	155.1(	22)
84.8(	1)	171.2(	23)
88.6(	12)	192.8(	26)

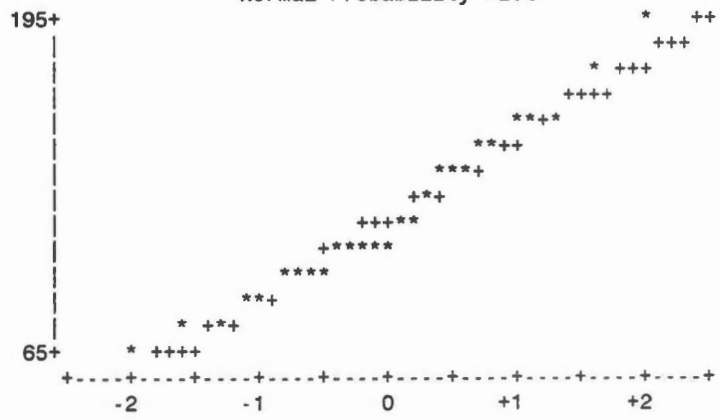
```
Stem Leaf                     #          Boxplot
  19 3                        1             |
  18                                        |
  17 1                        1             |
  16                                        |
  15 055                      3             |
  14 47                       2          +-----+
  13 459                      3          |     |
  12 0                        1          |     |
  11 17                       2          |  +  |
  10 033567                   6          *-----*
   9 5569                     4          +-----+
   8 59                       2             |
   7 26                       2             |
   6 7                        1             |
     ----+----+----+----+
 Multiply Stem.Leaf by 10**+1
```


---------- SOILCODE=5 ----------

Univariate Procedure

Variable=YIELD

Normal Probability Plot



---------- SOILCODE=6 ----------

Univariate Procedure

Variable=YIELD

Moments

N	42	Sum Wgts	42	100% Max	238.4	99%	238.4
Mean	158.369	Sum	6651.5	75% Q3	171	95%	187.5
Std Dev	25.10292	Variance	630.1568	50% Med	157.4	90%	179.7
Skewness	0.827768	Kurtosis	2.218024	25% Q1	146.8	10%	124.7
USS	1079228	CSS	25836.43	0% Min	108.7	5%	124.2
CV	15.8509	Std Mean	3.873465			1%	108.7
T:Mean=0	40.88562	Pr>|T|	0.0001	Range	129.7		
Num ^= 0	42	Num > 0	42	Q3-Q1	24.2		
M(Sign)	21	Pr>=|M|	0.0001	Mode	163.2		
Sgn Rank	451.5	Pr>=|S|	0.0001				
W:Normal	0.93559	Pr<W	0.0271				

Extremes

Lowest	Obs	Highest	Obs
108.7(	1)	179.7(	21)
122.7(	36)	182.4(	37)
124.2(	30)	187.5(	33)
124.4(	18)	224.9(	34)
124.7(	42)	238.4(	40)

Stem	Leaf	#	Boxplot
23	8	1	0
22	5	1	0
21			
20			
19			
18	028	3	|
17	1125788	7	+-----+
16	23333556	8	| |
15	14666678	8	*--+--*
14	27788	5	+-----+
13	136	3	|
12	34456	5	|
11			
10	9	1	0

----+----+----+----+

Multiply Stem.Leaf by 10**+1

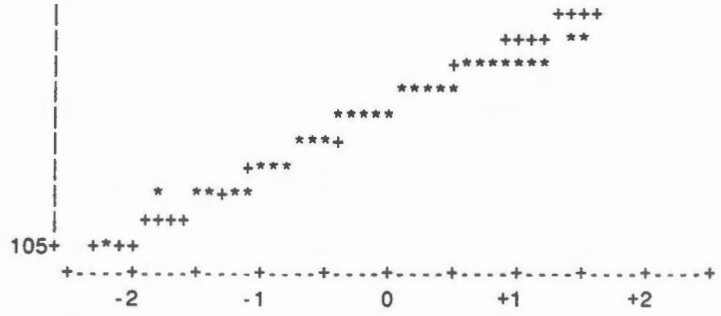
---------- SOILCODE=6 ----------

Univariate Procedure

Variable=YIELD

Normal Probability Plot





SOILCODE=7

Univariate Procedure

Variable=YIELD

Moments

N	33	Sum Wgts	33	100% Max	239.4	99%	239.4
Mean	204.403	Sum	6745.3	75% Q3	214.6	95%	234.5
Std Dev	17.91364	Variance	320.8984	50% Med	204.3	90%	230.2
Skewness	-0.15529	Kurtosis	0.043607	25% Q1	195.3	10%	184.7
USS	1389029	CSS	10268.75	0% Min	164.8	5%	168.9
CV	8.763881	Std Mean	3.118364			1%	164.8
T:Mean=0	65.54816	Pr>|T|	0.0001	Range	74.6		
Num ^= 0	33	Num > 0	33	Q3-Q1	19.3		
M(Sign)	16.5	Pr>=|M|	0.0001	Mode	164.8		
Sgn Rank	280.5	Pr>=|S|	0.0001				
W:Normal	0.975659	Pr<W	0.7088				

Extremes

Lowest	Obs	Highest	Obs
164.8(	23)	228.8(	28)
168.9(	1)	230.2(	8)
173.6(	2)	232.2(	21)
184.7(	13)	234.5(	10)
185.5(	**27)**	**239.4(**	**20)**

Vita

Jonathan Troy Adamson was born on December 30, 1973 in Nashville, Tennessee. He attended Portland High School and was graduated in May 1992. In August of 1992 he entered Columbia State Community College and received an Associates of Science degree in Agricultural Science in May 1995. The following August he transferred to Tennessee Technological University. There he received a Bachelor of Science degree in Agriculture with a concentration in Environmental Soil Science in December of 1996. He was employed as a Graduate Research Assistant at The University of Tennessee at Knoxville in January 1997 and began study toward the Master of Science degree in Biosystems Engineering Technology. Upon completion of his course work and research, he entered employment with John Deere Corporation.

8233 3339 43
10•21•99 MAB